11-21-2003

Studies on Antibacterial Activities of *N*-Thiolated β-Lactams and Their Polymeric Nanoparticles Against MRSA

Jeung-Yeop Shim
University of South Florida

Studies on Antibacterial Activities of *N*-Thiolated β-Lactams and Their Polymeric Nanoparticles Against MRSA

by

Jeung-Yeop Shim

A dissertation submitted in partial fulfillment
of the requirements for the degree of
Doctor of Philosophy
Department of Chemistry
College of Arts and Science
University of South Florida

Major Professor: Edward Turos, Ph.D
Julie P. Harmon, Ph..D.
Bill J. Baker, Ph.D.
Kirpal S. Bisht, Ph.D.
Michael W. Fountain, Ph.D.

Date of Approval:
November 21, 2003

Keywords: Antibiotics, Biopolymers, MRSA, β-Lactams, Drug-Resistance

ACKNOWLEDGEMENT

I would like to thank with all my heart Professor Edward Turos, my major professor for all of his help, guidance, and knowledge. He has given me numerous opportunities in order to experience a wonderful career in multi-science areas. He has provided a tremendous learning environment to thrive over the years. I am also grateful for his warm heart and his patience. He is my teacher as well as my best friend. With my sincerest respect, I would like to express my deepest thanks to my teacher, Dr. Edward Turos for sharing of all.

I would also like to thank my committee members, Professor Julie Harmon, Professor Bill J. Baker, and Professor Kirpal Bisht for their guidance while at USF. Also I would like to acknowledge Dr. Michael Fountain for opening my eyes to the world of drug delivery and business.

Also, I would like to express my appreciation to Dr. ChangKiu Lee for encouraging my breakable mind to further pursue in science. His inspiration, guidance, and encouragement are beyond my ability to describe.

While in Dr. Turos lab, I met and worked with a wonderful group of individuals: Dr. Seyoung Jang, Dr. Suresh Reddy, Bart Heldreth, Cristina Coates, Timothy Long, J. Michelle Leslie, Sampath Abeylath, Helen Wang, Marci Culbreath, Kerriann Greenhalgh, Casey Cosner. They all gave me warm heart and good friendship.

Last, I want to express my sincerest appreciation to my wife. Without her invested and scarified time, efforts, love, patience, I would not have completed this goal. Her continued encouragement led me to complete this success. I want to say to my wife " I love you forever". Also, I want to say my two sons, David and Daniel, "I love you".

TABLE OF CONTENTS

LIST OF TABLES

LIST OF FIGURES

LIST OF SCHEMES

ABBREVIATIONS

MRSA	Methicillin-resistant *Staphylococcus aureus*
NAG	*N*-Acetylglucosamine
NAM	*N*-Acetylmuramic acid
DAP	Diaminopimelate
GTPase	Glycopeptide transpeptidase
MIC	Minimum inhibitory concentration
VISA	Vancomycin-intermediate *Staphylococcus aureus*
VRSA	Vancomycin-resistant *Staphylococcus aureus*
DCC	Dicyclohexyl carbodiimide
DMAP	4-Dimethylaminopyridine
ATCC	American type culture collection
PEG	Polyethylene glycol
CMC	Critical micelle concentration
SEM	Scanning Electron Microscopy
EDC	1-ethyl-3-(3-dimethylaminopropyl) carbodimide
DIPEA	Diisopropylethylamine

Studies on Antibacterial Activities of *N*-Thiolated β-Lactams and Their Polymeric Nanoparticles Against MRSA

Jeung-Yeop Shim

Abstract

Methicillin-resistant *Staphylococcus Aureus* (MRSA) is now the most challenging bacterial pathogen affecting patients in hospitals and in care centers, and has brought on the need to develop new drugs for MRSA. This thesis centers on studies of *N*-thiolated β-lactams, a new family of potent antibacterial compounds that selectively inhibit the growth of methicillin-resistant *Staphylococcus aureus* (MRSA).

Chapter 1 describes MRSA in more detail. Chapter 2 outlines experiments on the effect of a fatty ester group (CO_2R) on the C_4-phenyl ring of *N*-methylthio β-lactams, expecting that attachment of long chain ester moieties might increase the hydrophobicity, and thus enhance the drug's ability to penetrate through the cell membrane. However, the results indicate that antibacterial activity drops off rapidly when more than seven carbon atoms are in the chain. These results led to the idea about examining a β-lactam conjugated polymer as a possible pro-drug delivery method, which is the focus of Chapter 3.

To synthesize the initial drug-polymer candidate, microemulsion polymerization of an acrylate-substituted lactam was done in aqueous solution to form hydrophilic

polymeric nanoparticles containing the highly water-insoluble solid antibiotic, *N*-methylthio β-lactam. This method has advantages over the conventional emulsion polymerization methods because a solid co-monomer (β-lactam drug) can be utilized.

SEM studies show that these polymeric nanoparticles have a microspherical morphology with nano-sizes of 40-150 nm. The *N*-thiolated β-lactam containing nanoparticles display potent anti-MRSA activity at much lower drug amounts compared with free lactam drug, penicillin G or vancomycin. Although at this time the relationship between particle size and activity is not clear and the mode of action is unknown, the *N*-thiolated β-lactam containing nanoparticles dramatically enhance bioactivity, possibly due to increased bioavailability of the antibiotic via endocytosis.

In chapter 4, Fluorescence-active emulsified nanoparticles containing naphthyl or anthracenyl side chains were also successfully prepared by microemulsion polymerization for possible use in fluorescence studies to determine if the drug enters the cell of MRSA through endocytosis, and where possible bioaccumulation site are located.

Chapter One

Methicillin-resistant *Staphylococcus aureus* (MRSA)

1.1 Introduction[1,2,3,4]

Penicillin was the first antibiotic chemotherapeutic agent discovered and it was proven to be effective against specific bacteria when administered in the human body without destroying the body's own cells.

In 1928, Sir Alexander Fleming, professor of bacteriology at St. Mary's Hospital in London, was culturing *Staphylococcus aureus.* He noticed zones of growth inhibition where mold spores were growing. He named the mold *Penicillium rubrum.* It was determined that a secretion of the mold was effective against Gram-positive bacteria. In 1940 Lord Howard Florey and Sir Ernst Chain successfully isolated the antimicrobial agent. It was determined to be an inhibitor of cell wall synthesis in gram-positive bacterial. Amidst the need for antibacterial agents in WW II, penicillin was isolated, purified and injected into experimental animals, where it was found to not only cure infections but also to possess low toxicity. This opened the age of antibiotic chemotherapy and promoted an intense search for similar antimicrobial agents of low toxicity that might prove useful in the treatment of infectious disease. Some time later, another mold was found which produced a bacteria-killing chemical, and the structure of the molecule was determined to be very similar to the penicillin molecule; this chemical

and its cousins were called "cephalosporins" after the Cephalous mold from which they were derived (Fig. 1-1). Chemical changes have been made to the molecules over the years to improve their bacteria-fighting abilities and to help them overcome biochemical breakdown and "immunity" of resistant bacteria.

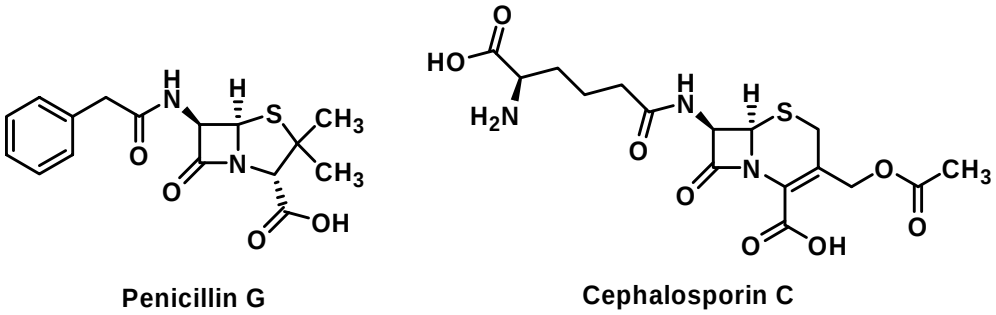

Fig. 1-1 Chemical structure of penicillin G and cephalosporin C

The isolation of streptomycin, chloramphenicol and tetracycline soon followed, and by the 1950's, these and several other antibiotics were in clinical usage.

The bacterial cell has a cell wall similar to the outer layer of plant cells, but which is missing in human and animal cells. This wall must grow along with the cell, or the growing cell will eventually become too big for the wall and burst and die. Penicillins and cephalosporins kill bacteria by messing up the wall-building system. Since human cell do not have cell walls, and plants have a different wall-building system, neither human, nor animals, nor plants are affected by the penicillins. Some bacteria have changed the structure of their walls to prevent penicillin from entering, or have come up with ways to break down the penicillin structure. In the 1940's and 1950's, most bacteria could be killed by penicillin. Now, because no longer penicillins and cephalosporins have

been used so often there are many bacteria that no longer are killed by penicillin. Antibiotic resistance is a growing problem.

1.2 Cell Wall Biosynthesis and Its Inhibition by Penicillins in Gram-positive Bacteria

The Gram-positive bacteria possess a thick cell wall composed of a cellulose-like polymer covalently interbound via short peptide units into layers (Fig. 1-2). This peptidoglycan substance is also found in Gram-negative cells, but is thinner and less fortified. Gram negative organisms also possess an outer membrane composed of lipoproteins, lipopolysaccharides, and phospholipids, which provide a natural barrier to the antimicrobial effects of penicillin.[5]

The polysaccharide portion of the peptidoglycan structure (fig. 1-5) is made of repeating units of *N*-acetylglucosamine (NAG) linked to *N*-acetylmuramic acid (NAG-NAM) (Fig. 1-3). The peptide varies, but begins with L-Ala and ends with D-Ala. In the middle is a dibasic amino acid, diaminopimelate (DAP). The terminal Ala residues are used for glycan linkage; the DAP for interpeptide linkages. Different species of Gram-positive bacteria possess different peptide units in the peptidoglycan cell wall.[4,5]

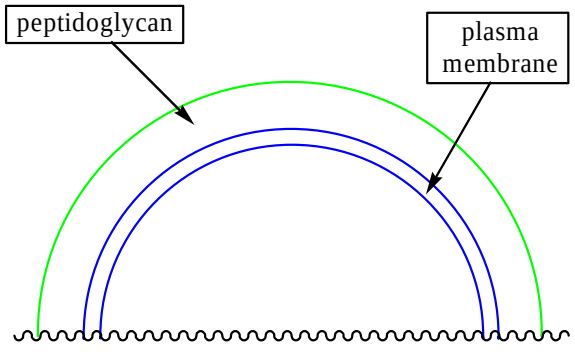

Fig. 1-2 Gram-positive bacteria cell wall[5]

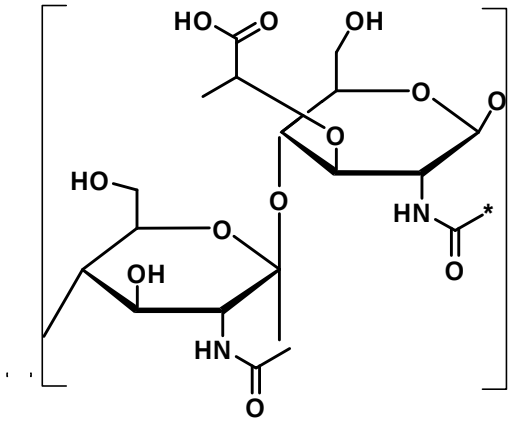

Fig. 1-3 Chemical structure of NAG-NAM[1,2,5]

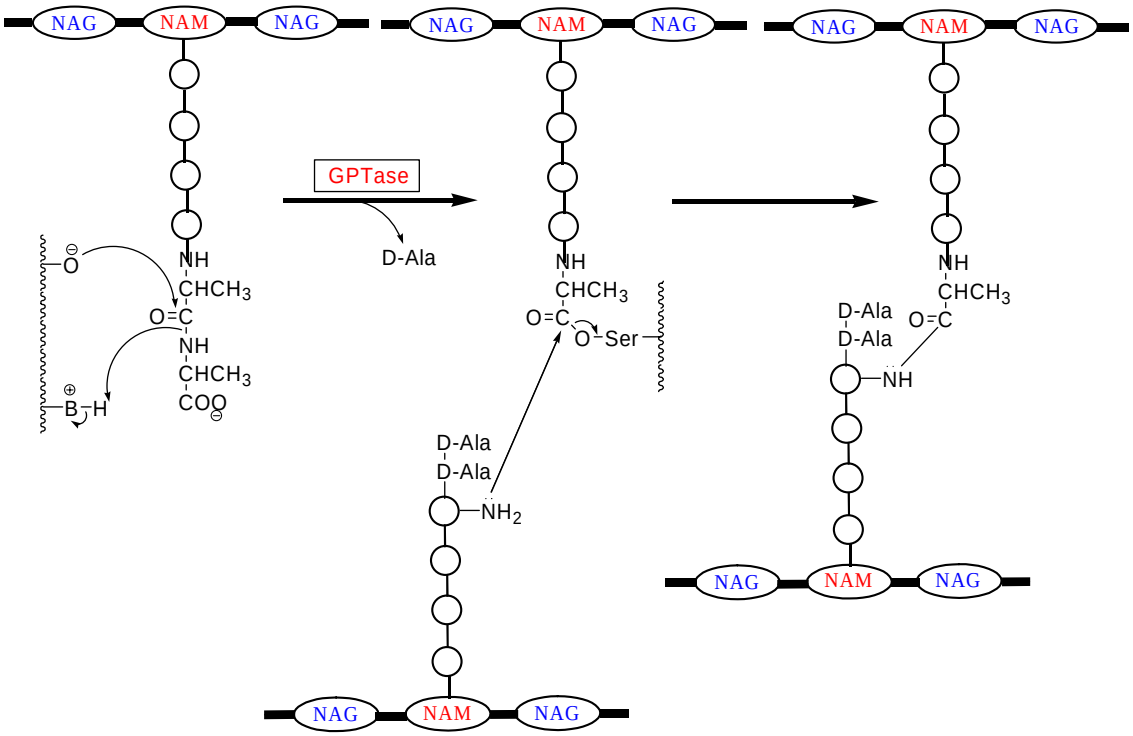

Fig. 1-4 Cell wall biosynthesis of gram-positive bacteria[1]

The NAM part of the NAG-NAM monomer group provides the point of attachment for the peptide. The L-Ala residue is attached to the NAM. DAP provides a linkage to the

D-Ala residue on an adjacent peptide, which continues to link distally with another layer of NAG-NAM (Fig. 1-4).

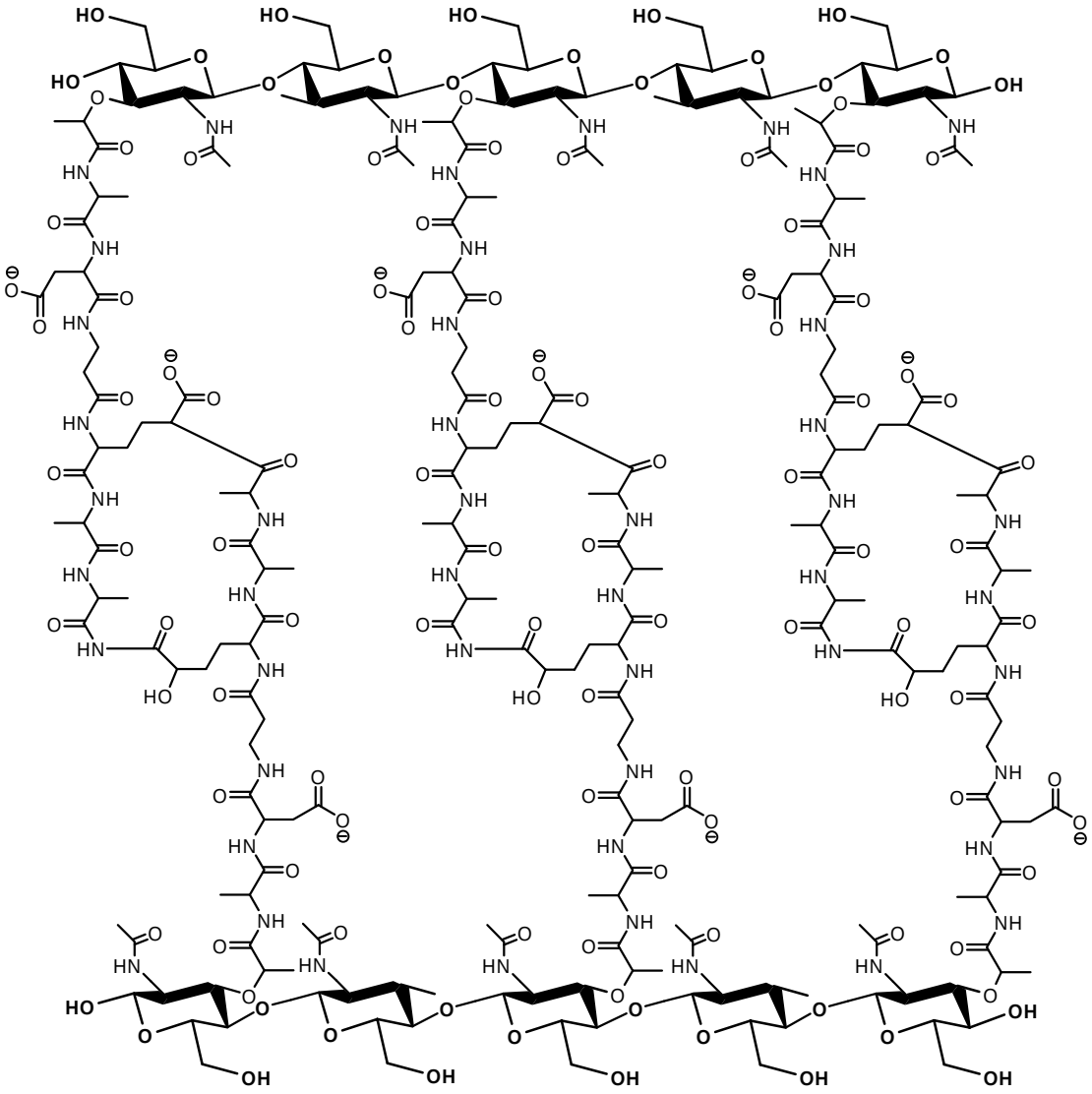

Fig. 1-5 Structure of peptidoglycan

The transpeptide linkages are catalyzed by the enzyme glycopeptide transpeptidase (GPTase). A ser residue in the active site of GPTase is the target of penicillin attack. The anionic Ser residue attacks the carbonyl carbon of the β-lactam ring since the

conformation resembles the transition state of the normal GPTase substrate. This forms an indefinitely stable structure; thereby rendering the enzyme inactive. Without an active site, glycoprotein transpeptidation can not occur. Without transpeptidation, Gram-positive cell walls can not be crosslinked. Therefore, those bacteria are easily killed (Fig. 1-6).[4,5]

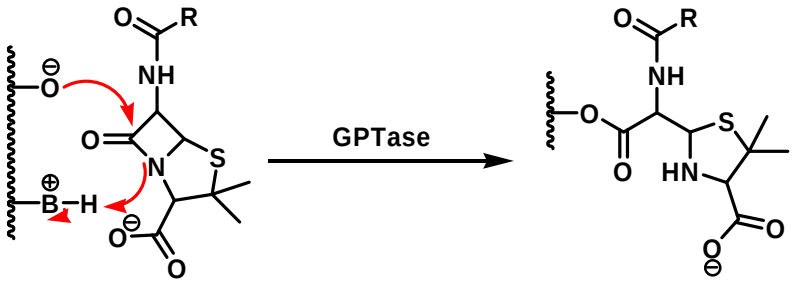

Fig. 1-6 Inhibition of GTPase by penicillin

1.3 Methicillin-Resistance

As early as the 1940s, bacteria began to develop resistance to penicillin. β-Lactamases (or penicillinases) are enzymes produced by a bacterium which render penicillin useless by hydrolyzing the β-lactam ring. The β-lactamases catalytically disrupt the amide bond of penicillin, and other β-lactams, via the formation of a serine-ester-linked acyl enzyme derivative. β-Lactams are structural analogs of the peptidyl-D-alanyl-D-alanine terminal moiety of peptidoglycan cell wall precursors. Following β-lactam binding, the β-lactam ring is opened by nucleophilic attack by the hydroxyl group of a serine residue. Acylation of the enzyme generates an acyl enzyme intermediate,

which undergoes subsequent hydrolysis to release the penicilloyl moiety and regenerating the active enzyme (Fig. 1-7).[6,7,8,9]

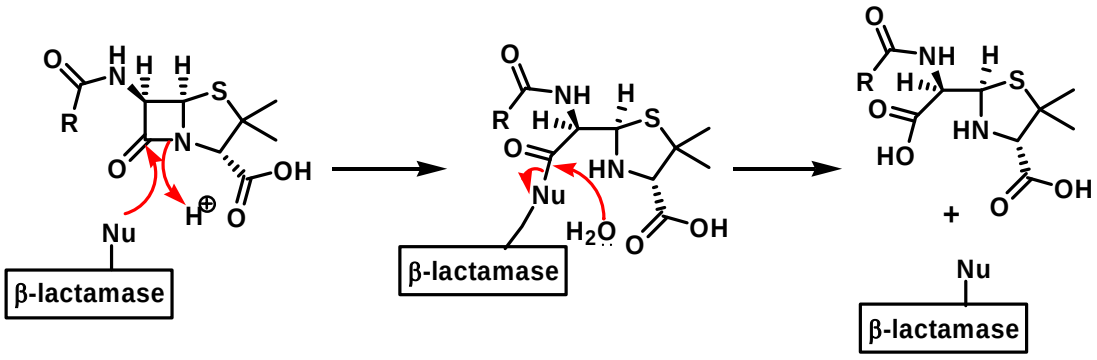

Fig. 1-7 Hydrolysis of penicillin by β-lactamase

Strains of *Staphylococcus aureus* are resistant to methicillin, cloxacillin, flucloxacillin and to all the other β-lactam antibiotics, including all penicillins and cephalosporins. because of a change in the cell wall proteins. MRSA also has the ability to pick up other resistance mechanisms and may become resistant to all other anti-staphylococcal drugs. With the widespread emergence of MRSA, glycopeptide antibiotics such as vancomycin or teicoplanin have been more frequently used in the clinical practice. Popular use of these agents has led to the onset of glycopeptide resistance at the end of the 20th century. In 1997, an isolate of *S. aureus* with reduced susceptibility to vancomycin (MIC $\geq$ 8 μg/mL) was first reported from Japan.[10] Until 2002, a total of 24 cases of Vancomycin-Intermediate *Staphylococcus aureus* (VISA) infections were reported from 11 countries in the world. In 2002, two strains of VRSA with high-level resistance to vancomycin (MIC $\geq$ 32 μg/mL) with van A gene from

enterococci were reported in the U.S.[11,12] It is anticipated that glycopeptide resistance will only continue to get worse within a few years.

1.4 Trends in Resistance and Prospect for New Therapies

Natural selection is the driving force for the appearance of drug resistant strains. Once one strain of bacteria has become resistant, the resistance can be transferred between strains by several mechanisms involving exchange of genetic material. These mechanisms include conjugation, transduction, and transformation. The more an antibiotic is used, the greater the selective pressure of bacteria to become resistant, and the faster resistance spreads. The most evident example is penicillin. When penicillin was first discovered, it was believed to be a miracle drug and was used at any sign of infection. The emergence of resistant strains was almost immediate. MRSA is now the most challenging bacterial pathogen that currently affects patients in hospital and in the community. Infection caused by this important nosocomial bacterium has become a serious national and global problem. Fig. 1-8[13] indicates the development of MRSA in the recent years. Therefore, by studying the mechanisms by which strains become resistant, a better understanding of how to stop or slow down the emergence of resistant strains is possible. For example, for strains that produce β-lactamases, a β-lactamase inhibitor can be added in addition to the β-lactam drug to render the bacteria sensitive to the antibiotic. Development of drugs with a new mechanism of action are needed. Alternatively, new ways to deliver the antibiotic to the cell may help overcome resistance and minimize further expose of bacteria to the drug.

In next chapter, studies on a new family of potent antibacterial compounds, N-thiolated β-lactams, that selectively inhibit the growth of *Staphylococcus* species are described.

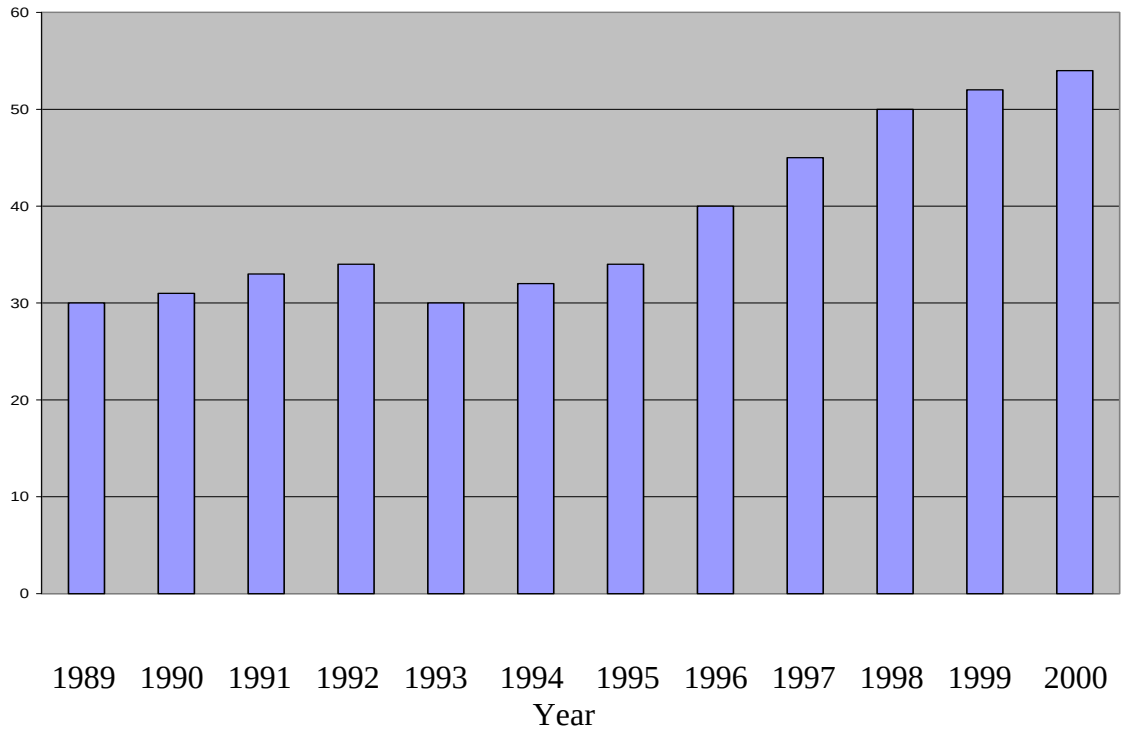

Fig. 1-8 Proportion of *S. aureus* Nosocomial Infections Resistant to Oxacillin
Source: National Nocosomial Infections Surveillance (NNIS)

References

1. Sweet, R. M., In Cephalosporins and Penicillins, Chemistry and Biology; Flynn, E. H., Ed.; **1972**.

2. Morin, R.B. and Gorman, M., Chemistry and Biology of β-Lactam Antibiotics; Academic Express: New York, **1982**, Volumes 1-3.

3. Kukacs, F. and Ohno, M., Recent Progress in the Chemical Synthesis of Antibiotics; Springer-Verlag: Berlin-Heidelberg, 1990.

4. Silverman, R.B. The Organic Chemistry of Drug Design and Drug Action; Academic Press: IL, 1st Ed., **1992**.

5. Lim, D., Microbiology; Kendall/Hunt Publishing Company: Iowa, 3rd Ed., **2003**.

6. Alkema, W.B.L. *et al*., Charecterisation of the ß-lactam binding site of penicillin acylase of *Escherichia coli* by structural and site-directed mutagenesis studies, *Protein Engineering* **2000**, *13*, 857.

7. Lamotte-Brasseur, J. *et al*., *Streptomyces albus G* serine ß-lactamase, *Biochem. J.* **1992,** *82*, 189.

8. Lamotte-Brasseur, J. *et al*., Mechanism of acyl transfer by the class A serine ß-lactamase of *Streptomyces albus G., Biochem. J.* **1991**, *279*, 213.

9. Zawadzke, L.E. *et al.,* An engineered *Staphylococcus aureus* PC1 serine ß-lactamase that hydrolyses third-generation cephalosporins, *Protein Engineering* **1995**, *12*, 1275.

10. Hiramatsu K, Hanaki H, Ino T, *et al*. Methicillin-resistant *Staphylococcus aureus* clinical strain with reduced vancomycin susceptibility. *J. Antimicrob. Chemother.* **1997**, *40*, 135.

11. Centers for Disease Control and Prevention. *Staphylococcus aureus* resistant to vancomycin-United States, 2002. *Morb Mort Weekly Report.* **2002**, *51*, 565.

12. Centers for Disease Control and Prevention. Public health dispatch : vancomycin-resistant *Staphylococcus aureus* - Pennsylvania, 2002. *Morb Mort Weekly Report.* **2002**, *51*, 902.

13. http://www.cdc.gov/ncidod/hip/ARESIST/mrsa.htm

Chapter Two

Influence of Fatty Ester Side Chains on the Antibacterial Activity of *N*-Methylthio β-Lactams

2.1 Introduction

N-Thiolated β-lactams are a new family of potent antibacterial compounds that selectively inhibit the growth of *Staphylococcus* species. Members of this family of antibiotics show enhanced activity towards *Staphylococcus* microbes, including methicillin-resistant *Staphylococcus aureus* (MRSA), over other common bacterial genera.[1] The initial lead compound **I-A** developed earlier in the Turos laboratory led to further investigations on the structure-activity studies patterns of these new antibacterial agents.[2] Previous work found that certain lipophilic and electron withdrawing functionalities on the ring may be preferred.

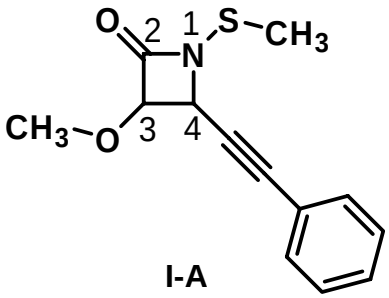

I-A

The analogs of *N*-methylthio β-lactams, **II-A, II-B, II-C, II-D,** show potent activities against MRSA.[3] These compounds are lipophilic and have the electron withdrawing functionality on the C_4-phenyl group.

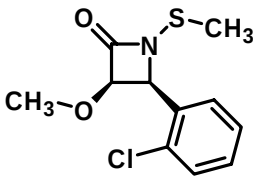

II-A

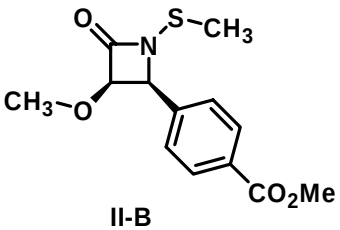

II-B

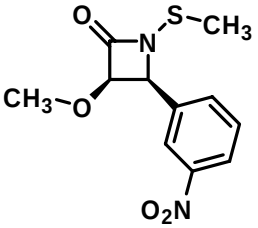

II-C

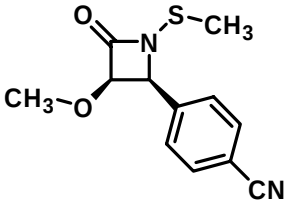

II-D

C_4-Saturated/unsaturated side chain aryl analogs, **III-A, III-B, III-C** also have moderate antibacterial activities against MRSA.[3] These compounds are lipophilic and even have no electron withdrawing substituent at C_4.

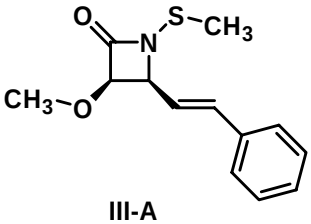

III-A

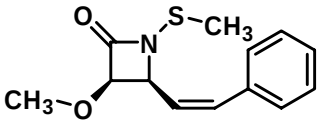

III-B

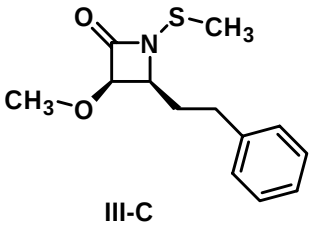

III-C

C_4-Fluoro aryl analogs, **IV-A, IV-B, IV-C, IV-D,** also have strong antibacterial activities against MRSA.[4]

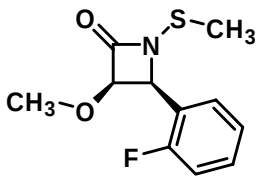

IV-A

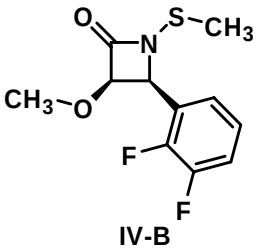

IV-B

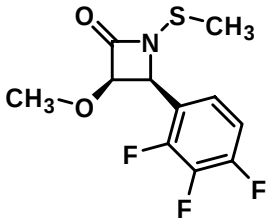

IV-C

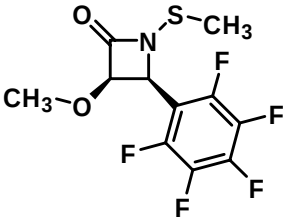

IV-D

One of these compounds, ester analog **II-B,** has an ester group (CO_2Me) on the C_4-phenyl ring of the lactam. This compound was found to be a reasonably potent analog among those we examined. The electron withdrawing ester group on the C_4-phenyl group as well as the long alkyl chain of the ester group can possibly increase the hydrophobicity of *N*-methylthio β-lactam and thus may increase bioavailability by enhancing penetration through the cell membrane. Therefore, it is a good candidate for systematic investigation of the structure-activity relationship for *N*-methylthio β-lactams.

In this study, the synthesis and evaluation of additional fatty ester analogs was carried out to address whether increasing the length or the degree of branching, and thus the hydrophobic character of the ester side chain, may alter the antibacterial properties.

2.2 Synthesis

A series of *N*-thiolated β-lactams **1,** having a C_4-fatty ester on the phenyl group was prepared.

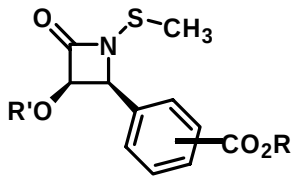

1

Scheme II-1 summarizes the synthesis of the first of these analogs, 3-methoxy-substituted C_4-benzoate alkyl esters **7**. 4-Carboxybenzaldehyde **2** was coupled with the appropriate alcohol using dicyclohexylcarbodiimide/dimethylaminopyridine (DCC/DMAP), followed by reaction with *p*-anisidine, to give alkyl ester imines **4**. Staudinger coupling[5-8] of methoxyacetyl chloride with the imine **4** gave *N*-aryl protected β-lactam alkyl ester **5**. Dearylation of β-lactam **5** with ceric ammonium nitrate and methylthiolation with N-(methylthio)phthalimide affords C_3-methoxy *N*-methylthio β-lactam ester analogs **7**.[2]

Ortho-substituted β-lactams **13** are also good candidates for the study of biological activity. These compounds were prepared as shown in Scheme II-2. Even though *ortho* substituted methyl, ethyl, propyl and pentyl ester analogs were tried under the usual Staudinger coupling conditions, only *ortho* ethyl ester, gave results. In this case, cis and trans adducts were obtained. These adducts were taken on to the N-methylthio β-lactams **13**, which independently were tested for antibacterial activity by the Kirby-Bauer method of disc diffusion on agar plates.

Scheme II-3 summarizes the synthesis of C_3-acetoxy N-methylthio β-lactams **15**. Staudinger coupling of acetoxyacetyl chloride with imine **4** gave C_3-acetoxy *N*-aryl protected β-lactam **14**. In some cases, both ***cis*** and ***trans*** adducts could be obtained from the Staudinger reaction. Dearylation of β-lactam **14** with ceric ammonium nitrate, followed by methylthiolation with N-(methylthio)phthalimide affords C_3-acetoxy *N*-methylthio β-lactams **15**.

C_3-Alkyl carbonate and methyl dithiocarbonate moieties also could be introduced to examine the effect of different functionalities and chain branching on bioactivity of the β-lactam. Scheme II-4 summarizes the synthesis of C_3-alkylcarbonate N-methylthio β-lactam analogs **20.** The C_3-hydroxy β-lactam **17** could be easily obtained by cleavage of C_3-acetoxy β-lactam **16** with methanolic KOH. The resulting free hydroxyl compound **17** was reacted with alkyl orthochloroformate to give the C_3-alkyl carbonate β-lactams **18**. Dearylation and methylthiolation provided N-methylthio β-lactams **20**.

Scheme II-1

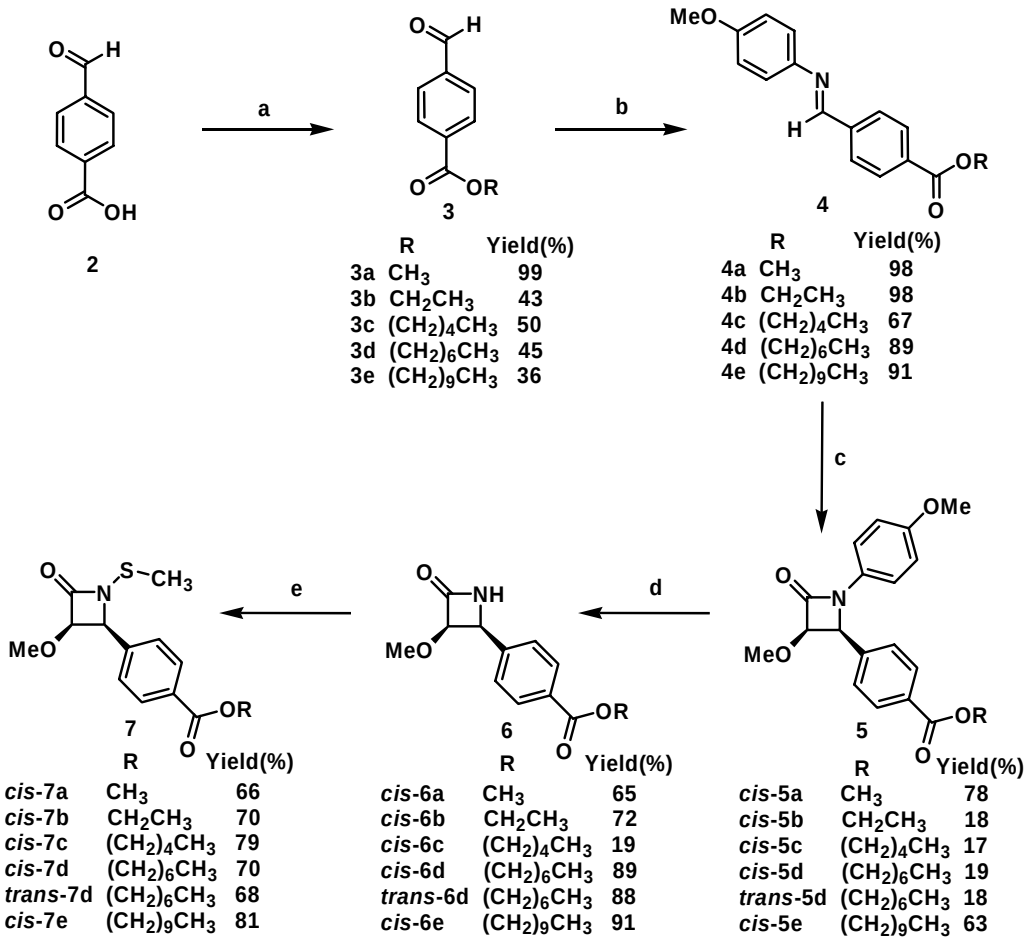

	R	Yield(%)
3a	CH_3	99
3b	CH_2CH_3	43
3c	$(CH_2)_4CH_3$	50
3d	$(CH_2)_6CH_3$	45
3e	$(CH_2)_9CH_3$	36

	R	Yield(%)
4a	CH_3	98
4b	CH_2CH_3	98
4c	$(CH_2)_4CH_3$	67
4d	$(CH_2)_6CH_3$	89
4e	$(CH_2)_9CH_3$	91

	R	Yield(%)
cis-5a	CH_3	78
cis-5b	CH_2CH_3	18
cis-5c	$(CH_2)_4CH_3$	17
cis-5d	$(CH_2)_6CH_3$	19
trans-5d	$(CH_2)_6CH_3$	18
cis-5e	$(CH_2)_9CH_3$	63

	R	Yield(%)
cis-6a	CH_3	65
cis-6b	CH_2CH_3	72
cis-6c	$(CH_2)_4CH_3$	19
cis-6d	$(CH_2)_6CH_3$	89
trans-6d	$(CH_2)_6CH_3$	88
cis-6e	$(CH_2)_9CH_3$	91

	R	Yield(%)
cis-7a	CH_3	66
cis-7b	CH_2CH_3	70
cis-7c	$(CH_2)_4CH_3$	79
cis-7d	$(CH_2)_6CH_3$	70
trans-7d	$(CH_2)_6CH_3$	68
cis-7e	$(CH_2)_9CH_3$	81

Conditions: (a) ROH, DCC, DMAP, dry acetone, reflux; in case of 3a: MeOH, $SOCl_2$, 0°C to rt. (b) *p*-anisidine, Et_3N, CH_2Cl_2. (c) $MeOCH_2COCl$, Et_3N, CH_2Cl_2. (d) $(NH_4)_2Ce(NO_3)_6$, MeCN-H_2O. (e) N-(methylthio)phthalimide, Et_3N, CH_2Cl_2.

Scheme II-2

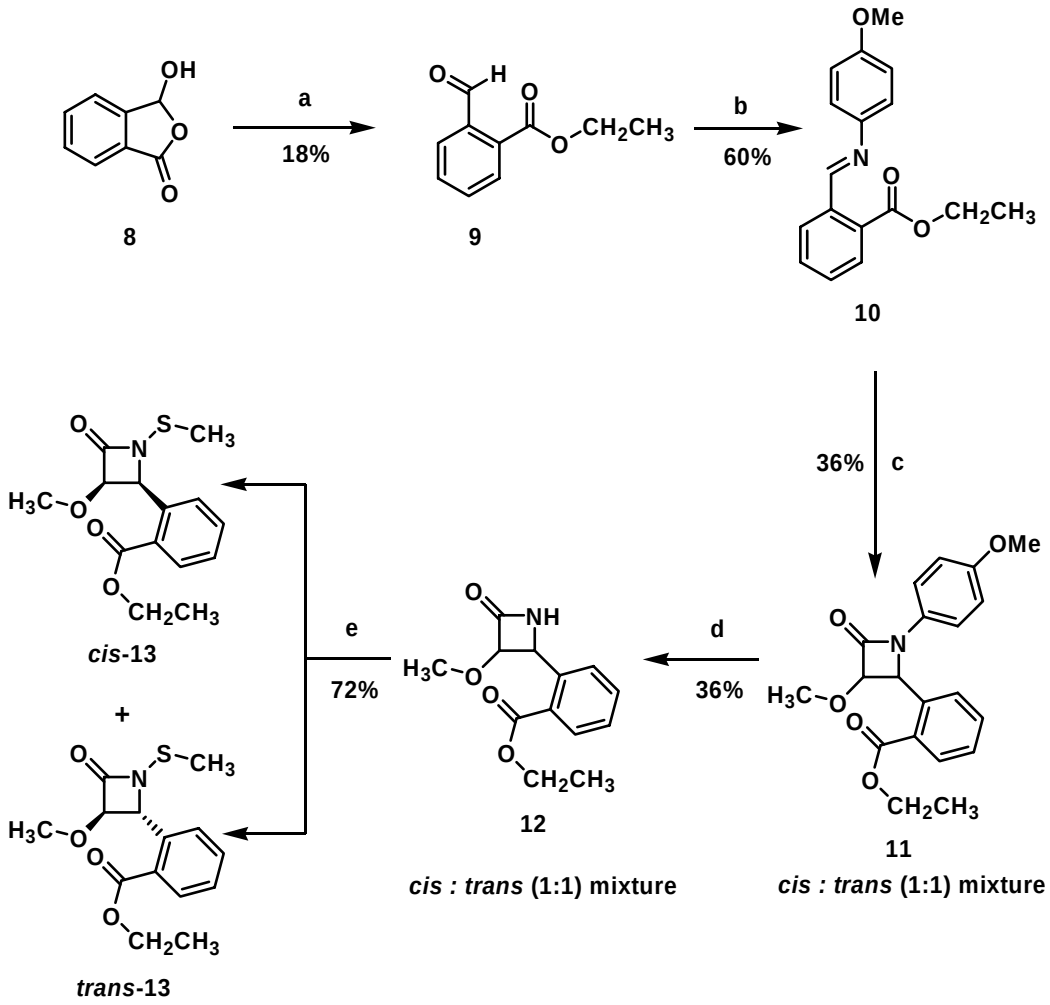

Conditions: (a) EtI, K_2CO_3,dry acetone, reflux. (b) *p*-anisidine, Et_3N, CH_2Cl_2. (c) $MeOCH_2COCl$, Et_3N, CH_2Cl_2. (d) $(NH_4)_2Ce(NO_3)_6$, MeCN-H_2O; (e) N-(methylthio)phthalimide, Et_3N, CH_2Cl_2.

Scheme II-3

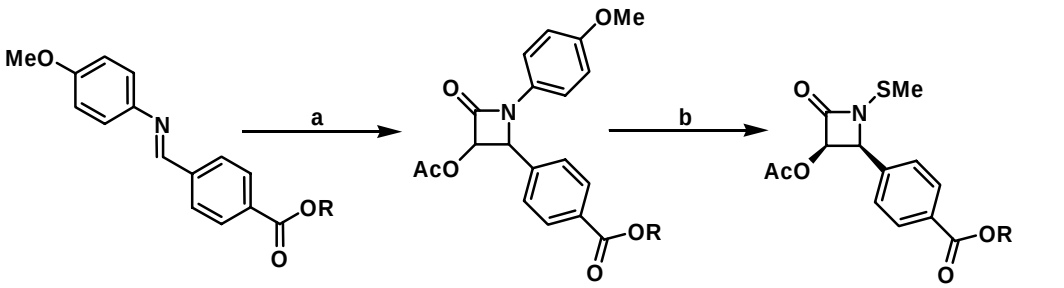

	R	Yield(%)
cis-14a	CH_3	25
trans-14a	CH_3	
cis-14b	CH_2CH_3	43
trans-14c	$(CH_2)_4CH_3$	12
trans-14d	$(CH_2)_6CH_3$	40
cis-14e	$(CH_2)_9CH_3$	57
trans-14e	$(CH_2)_9CH_3$	

	R	Yield(%)
cis-15a	CH_3	8
trans-15a	CH_3	10
cis-15b	CH_2CH_3	12
trans-15c	$(CH_2)_4CH_3$	5
trans-15d	$(CH_2)_6CH_3$	2
cis-15e	$(CH_2)_9CH_3$	9
trans-15e	$(CH_2)_9CH_3$	12

:Conditions: (a) $AcOCH_2COCl$, Et_3N, CH_2Cl_2. (b) (i) $(NH_4)_2Ce(NO_3)_6$, MeCN-H_2O; (ii) N-(methylthio)phthalimide, Et_3N, CH_2Cl_2.

Scheme II-4

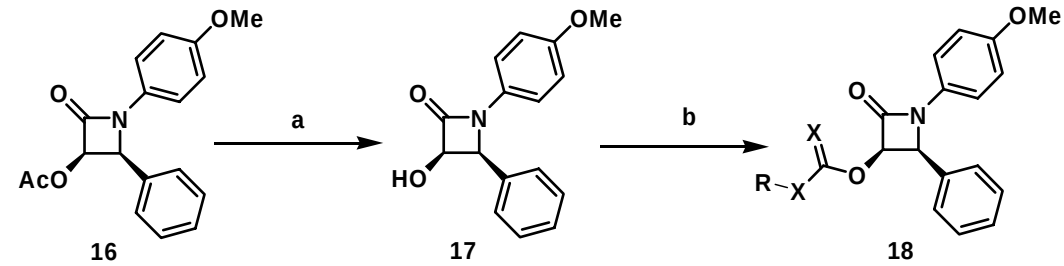

	R	Yield(%)
18a	Me, X=O	55
18b	Et, X=O	39
18c	CMe_3, X=O	98
18d	Ph, X=O	21
18e	Me, X=S	15

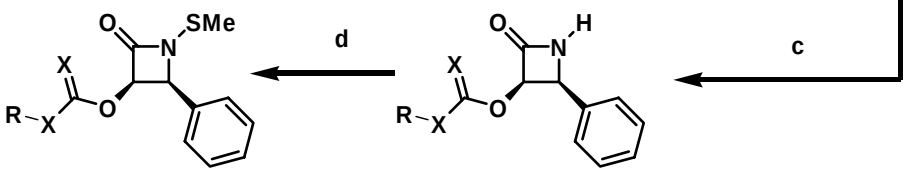

	R	Yield(%)
19a	Me, X=O	63
19b	Et, X=O	2
19c	CMe_3, X=O	72
19d	Ph, X=O	78
19e	Me, X=S	1

	R	Yield(%)
20a	Me, X=O	5
20b	Et, X=O	35
20c	CMe_3, X=O	1
20d	Ph, X=O	53
20e	Me, X=S	1

Conditions: (a) KOH, MeOH, 0°C. (b) NaH, CH_2Cl_2, RT then ROCOCl; in case of 14e: CS_2, NaH, THF, RT then MeI. (c) $(NH_4)_2Ce(NO_3)_6$, MeCN-H_2O.
(d) N-(methylthio)phthalimide, Et_3N, CH_2Cl_2.

2.3 Biological Activity

Fatty ester N-methylthio β-lactams **7, 13, 15** and **20** were tested for antibacterial activity by the Kirby-Bauer method of disc diffusion on agar plates. Mr. Timothy Long and Ms. Sonja Dickey performed these assays. Table 1, 2 and 3 displays a plot of the microbiological data for these 20 β-lactams.

Table II-1. Zones of inhibition obtained from agar well diffusion experiments using 20 μg of the test compound. The values correspond to the diameters in mm for the zone of growth inhibition appearing around the well after 24 hours. Penicillin G (Pen G) was used as a reference antibiotic. Staphylococcus aureus and β-lactamase-producing strains of methicillin-resistant Staphylococcus aureus were obtained from a clinical testing laboratory at Lakeland Regional Medical Center, Lakeland, FL (labeled MRSA USF652-659) or from ATCC sources. ("nt" indicates "not tested")

Microorganisms	***cis*-7a**	***cis*-7b**	***cis*-7c**	***cis*-7d**	***trans*-7d**	***cis*-7e**	***cis*-13**	***trans*-13**	**Pen G**
MRSA USF652	12	17	17	11	9	0	18	18	8
MRSA USF653	14	14	13	8	8	0	21	23	15
MRSA USF654	8	9	11	10	9	0	19	20	10
MRSA USF655	14	12	13	9	9	0	20	22	14
MRSA USF656	11	11	14	10	8	0	20	22	12
MRSA USF657	12	14	14	9	9	0	19	21	12
MRSA USF658	9	11	12	9	8	0	21	23	19
MRSA USF659	13	13	12	10	9	0	18	19	16
S. aureus ATCC 25923	13	13	13	11	10	0	16	18	33
S. epidermidis	12	16	12	9	8	0	nt	nt	50

Table II-2. Zones of inhibition obtained from agar well diffusion experiments using 20 μg of the test compound. The values correspond to the diameters in mm for the zone of growth inhibition appearing around the well after 24 hours. Penicillin G (Pen G) was used as a reference antibiotic. Staphylococcus aureus and β-lactamase-producing strains of methicillin-resistant Staphylococcus aureus were obtained from a clinical testing laboratory at Lakeland Regional Medical Center, Lakeland, FL (labeled MRSAUSF652-659) or from ATCC sources.

Microorganisms	***cis*-15a**	***trans*-15a**	***cis*-15b**	***trans*-15c**	***trans*-15d**	***cis*-15e**	***trans*-15e**	**Pen G**
MRSA USF652	15	18	14	15	9	0	0	8
MRSA USF653	12	15	12	11	8	0	0	15
MRSA USF654	12	16	11	11	9	0	0	10
MRSA USF655	13	16	12	13	8	0	0	14
MRSA USF656	14	17	14	14	9	0	0	12
MRSA USF657	11	15	11	12	8	0	0	12
MRSA USF658	14	15	13	11	8	0	0	19
MRSA USF659	13	18	13	13	9	0	0	16
S. aureus ATCC 25923	14	17	13	12	9	0	0	33
S. epidermidis	14	15	12	11	8	0	0	50

Table II-3 Zones of inhibition obtained from agar well diffusion experiments using 20 μg of the test compound. The values correspond to the diameters in mm for the zone of growth inhibition appearing around the well after 24 hours. Penicillin G (Pen G) was used as a reference antibiotic. Staphylococcus aureus and β-lactamase-producing strains of methicillin-resistant Staphylococcus aureus were obtained from a clinical testing laboratory at Lakeland Regional Medical Center, Lakeland, FL (labeled MRSAUSF652-659) or from ATCC sources.

Microorganisms	**20a**	**20b**	**20c**	**20d**	**20e**	**Pen G**
MRSA USF652	23	21	18	13	15	8
MRSA USF653	24	20	20	9	15	15
MRSA USF654	21	18	18	8	14	10
MRSA USF655	23	21	19	9	16	14
MRSA USF656	22	18	18	10	15	12
MRSA USF657	20	17	15	9	14	12
MRSA USF658	21	18	16	10	16	19
MRSA USF659	15	17	13	8	17	16
S. aureus ATCC 25923	23	20	20	9	13	33

2.4 Discussion

It is apparent that β-lactams ***cis*-7a**, ***cis*-7b**, and ***cis*-7c** are about equal in potency, suggesting that alkyl chain length of the benzoate ester moiety may not influence in vitro antimicrobial activity. However, activity drops dramatically for derivatives having seven carbons (***cis*-7d** and ***trans*-7d)** or more in the ester chain, as for the inactive decyl ester ***cis*-7e**. Fig. 1 displays the observed structure-activity relationship for β-lactams **7**.

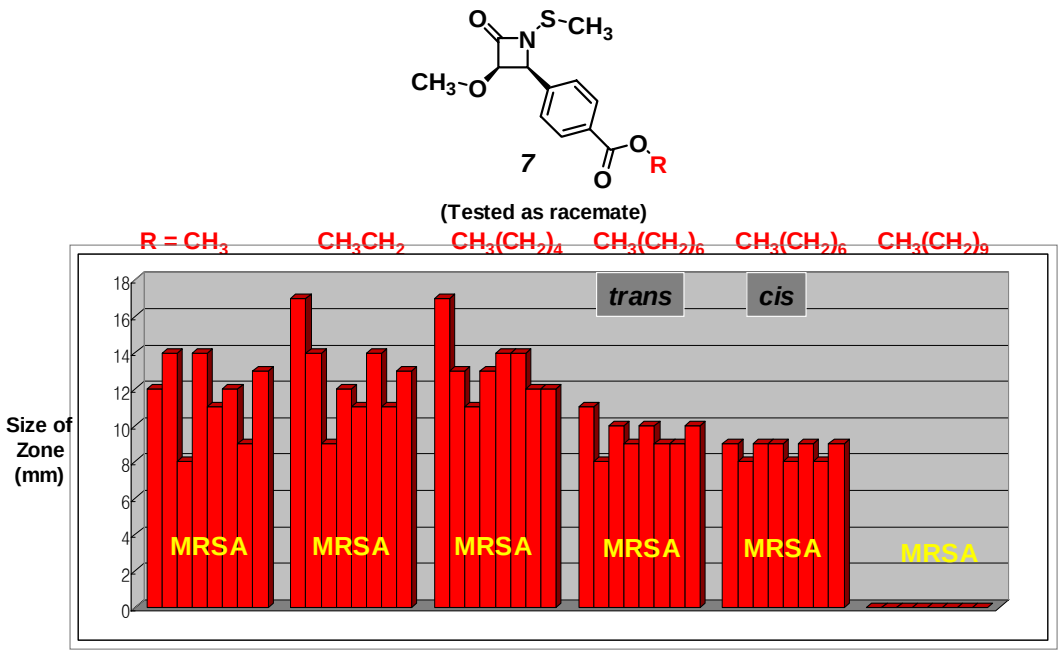

Fig. 2-1 Effect of increasing R chain length on antibacterial activity against MRSA for β-lactams 5.

In addition to the fatty ester residues on the C_4 aryl ring, as in the above series of compounds, the substitution of the C_3 methoxy group for an acetoxy group also can provides a good opportunity to study of two series of compounds for biological activity.

Fig. 2 displays the structure-activity relationship for β-lactams **7** and **15**. It is clear that β-lactams **7** and **15** have about equal biological activity, suggesting that C_3 methoxy and acetoxy moieties may exert equal influence over antimicrobial activity. However, for both β-lactams **7** and **15,** activity drops dramatically for derivatives having seven carbons or more in the ester chain, as for the inactive decyl ester analogs.

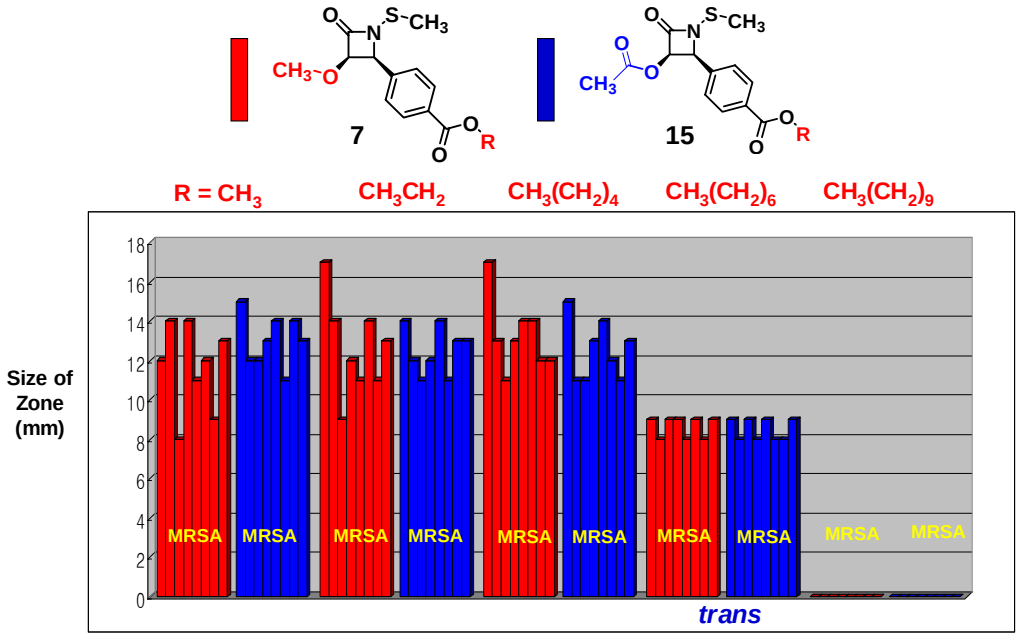

Fig. 2-2 Comparison of bioactivities for methoxy and acetoxy β-lactams 7 & 15.

It is also interesting to study side-by-side the *cis* and *trans* isomers of C_3-acetoxy N-methylthio -lactams **15**. Fig. 3 shows that there is not much difference between the *cis* and *trans* analogs, and once again, activity drops dramatically for derivatives having seven carbons or more in the ester chain. In the case of methyl ester analogs, the *trans* isomer was found to be about 10% more active than the *cis* analogs.

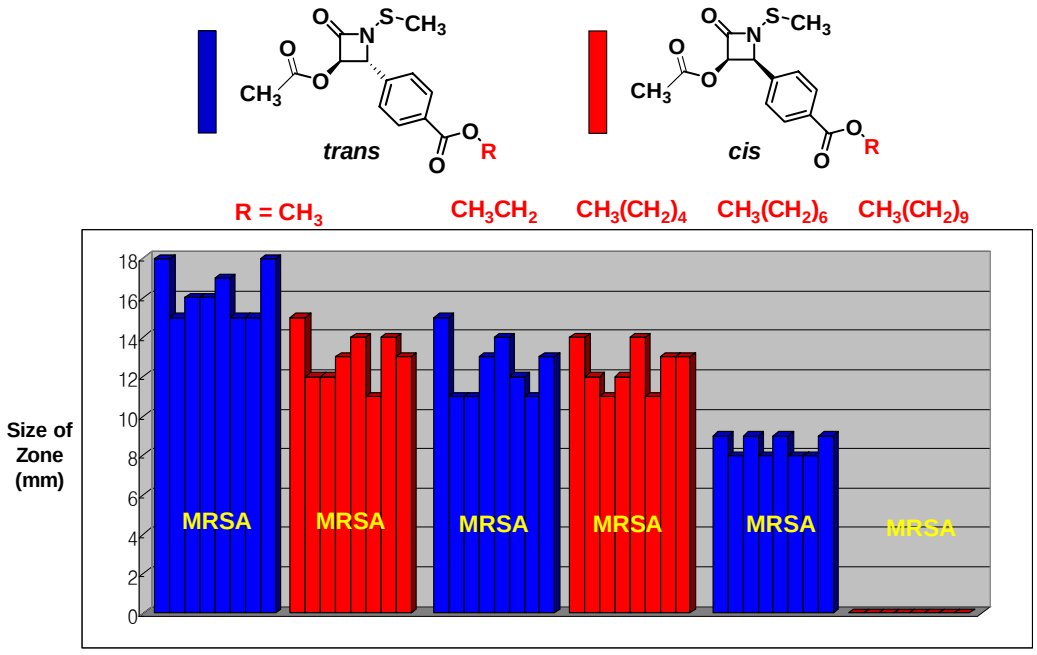

Fig. 2-3 Comparison of bioactivities for *trans* and *cis* β-lactams 15

Fig. 4 displays the comparison of bioactivities for *ortho* and *para* ethyl ester analogs. It is apparent that *ortho* analogs have about 40% more potent activity than that of the *para* analogs, so bioactivities depend on the position of the ester substituent on the phenyl ring. The reason for more potent activity of the *ortho* analogs is not clear yet.

The other hand, C_3-alkyl carbonate and methyl dithiocarbonate analogs **20** are good candidates for examining the effect of different functionalities and chain branching on bioactivity at C_3. Fig 5. shows the comparison of activities as increasing the bulkiness of the alkyl group. Upon increasing the size of alkyl group, the activity gradually drops up to 50% compared to the methyl and phenyl analogs. It is also apparent that the methyl carbonate analog has about 25% more activity than that of methyl dithiocarbonate.

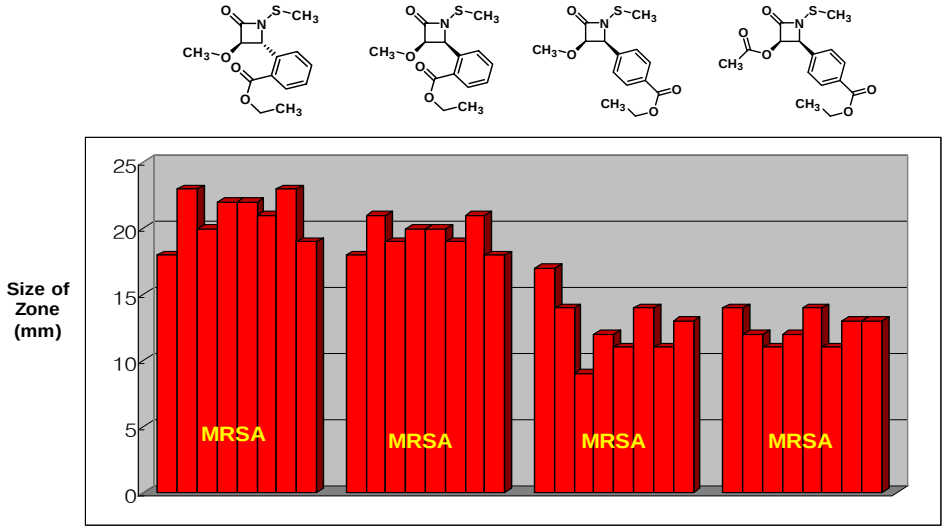

Fig. 2-4 Comparison of bioactivities for *ortho* and *para* isomers

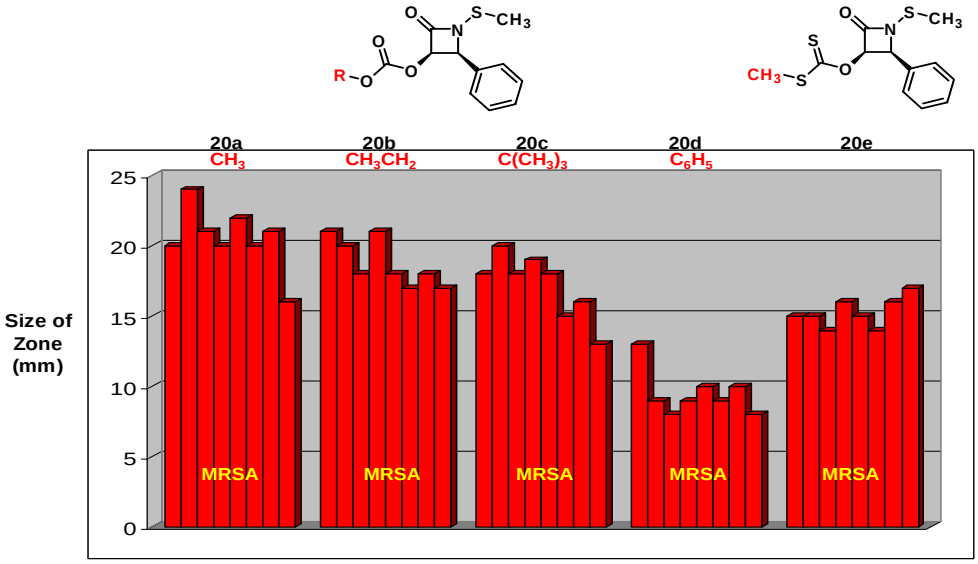

Fig. 2-5 Comparison of bioactivities for MRSA

2.5 Conclusion

In general, the antibacterial properties of the fatty ester N-methylthio β-lactams is loosely associated with lipophilicity within the C_4 side chain. Activity drops off rapidly when more than seven carbon atoms are in the ester. However, the *cis* and *trans* stereochemistry and methoxy/acetoxy substitution at C_3 seem to exert no significant effect. *Ortho*-substituted C_4-aryl analogs have more potent activity than that of the *para* analogs.

Therefore, as these studies show, there is an optimal chain length for the fatty ester groups, with activity dropping off rapidly when more than seven carbon atoms are in the chain. These results gave us the idea about developing a β-lactam prodrug system and a β-lactam conjugated polymer drug delivery system. The inactive form of β-lactam conjugated in the long cacrbon chain like the polymer can be changed to the active form after biological or enzymatical cleavage from polymer. In the next chaper, β-lactam conjugated polymeric nanoparticles are going to be described as a possible new drug delivery system.

2.6 Experimental

All reagents were purchased from Sigma-Aldrich Chemical Company and used without further purification. Solvents were obtained from Fisher Scientific Company. Thin layer chromatography (TLC) was carried out using EM Reagent plates with a fluorescence indicator (SiO_2-60, F-254). Products were purified by flash chromatography using J.T. Baker flash chromatography silica gel (40 μm). NMR spectra were recorded in $CDCl_3$ unless otherwise noted. ^{13}C NMR spectra were proton broad-band decoupled.

Procedure for the Synthesis of 4-(Methoxycarbonyl)benzaldehyde (3a)

To a stirred milky solution of 4-carboxybenzaldehyde (1.00 g, 6.7 mmol) in dry methanol (20 ml) in an ice-water bath was added dropwise thionyl chloride (0.54 ml, 7.3 mmol). After 30 min, the mixture was allowed to warm to room temperature and stirred for an additional 8 h. The mixture was diluted with CH_2Cl_2 (20 ml), followed by evaporation under reduced pressure to 1.08 g (99%) of aldehyde **3a** as an off-white solid. mp 44-45 ^oC. ^1H NMR (250 MHz) δ10.11 (s, 1H), 8.21 (d, J = 8.4 Hz, 2H), 7.96 (d, J = 8.4 Hz, 2H), 3.97 (s, 3H). ^{13}C NMR (63 MHz) δ191.6, 165.4, 139.0, 135.3, 130.0, 129.4, 61.5.

Procedure for the Synthesis of 4-(Alkyloxycarbonyl)benzaldehydes 3b-3e

To a stirred milky solution of 4-carboxybenzaldehyde (1g, 6.66 mmol) and DCC (1.51g, 7.33 mmol) in dry CH_2Cl_2 (20 ml) at rt was added dry ethanol (1 ml). The resultant mixture was refluxed for 8 h. The solvent was removed under reduced pressure to yield a white solid. The crude material was purified by flash column chromatography on silica gel (1:9 EtOAc:hexanes) to afford 0.51 g (43%) of aldehyde **3b** as a colorless semi-solid. ^{1}H NMR (250 MHz) δ9.97 (s, 1H), 8.06 (d, *J* = 8.3 Hz, 2H), 7.82 (d, *J* = 8.3 Hz, 2H), 4.29 (q, *J* = 7.1 Hz, 2H), 1.30 (t, *J* = 7.1 Hz, 3H). ^{13}C NMR (63 MHz) δ191.6, 165.3, 139.0, 135.2, 130.0, 129.3, 61.4, 14.1.

4-(Pentoxycarbonyl)benzaldehyde (3c)

Colorless semi-solid, 50%. ^{1}H NMR (250 MHz) δ10.06 (s, 1H), 8.16 (d, *J* = 8.4 Hz, 2H), 7.92 (d, *J* = 8.4 Hz, 2H), 4.31 (t, *J* = 6.7 Hz, 2H), 1.73 (m, 2H), 1.36 (m, 6H), 0.90 (m, 3H) ^{13}C NMR (63 MHz) δ191.6, 165.5, 139.0, 135.4, 130.1, 129.4, 65.7, 28.3, 28.1, 22.3, 13.9.

4-(Heptyloxycarbonyl)benzaldehyde (3d)

Colorless semi-solid, 45%. ^{1}H NMR (250 MHz) δ10.05 (s, 1H), 8.14 (d, *J* = 8.3 Hz, 2H), 7.90 (d, *J* = 8.3 Hz, 2H), 4.30 (t, *J* = 6.7 Hz, 2H), 1.74 (m, 2H), 1.26-1.38 (m, 8H), 0.84 (m, 3H). ^{13}C NMR (63 MHz) δ191.6, 165.5, 139.0, 135.4, 130.0, 129.4, 65.7, 31.6, 28.9, 28.6, 25.9, 22.5, 14.0.

4-(Decyloxycarbonyl)benzaldehyde (3e)

Colorless semi-solid, 36%. ^{1}H NMR (250 MHz) δ10.08 (s, 1H), 8.17 (d, *J* = 8.3 Hz, 2H), 7.93 (d, *J* = 8.3 Hz, 2H), 4.33 (t, *J* = 6.7 Hz, 2H), 1.76 (m, 2H), 1.24-1.41 (m, 14H), 0.84

(m, 3H). ^{13}C NMR (63 MHz) δ191.6, 165.5, 139.0, 135.4, 130.1, 129.4, 65.7, 31.8, 29.5 (double), 29.2 (double), 26.0, 22.6, 14.1.

Procedure for the Synthesis of *N*-(4-Methoxyphenyl)-Substituted Imines 4.

To a solution of *p*-anisidine (9.45 g, 77.0 mmol) in 50 ml of CH_2Cl_2 was added benzaldehyde (10.50 g, 64.0 mmol) and a catalytic amount of camphorsulfonic acid. The resultant mixture was stirred until TLC indicated the disappearance of starting materials. The solvent was removed under reduced pressure, and the crude material was purified by recrystallization from methanol to yield 17.02 g (98%) of **4a** as a yellow solid. mp 157-159 °C. ^{1}H NMR (250 MHz) δ 8.54 (s, 1H), 8.14 (d, *J* = 7.9 Hz, 2H), 7.97 (d, *J* = 7.9 Hz, 2H), 7.29 (d, *J* = 8.4 Hz, 1H), 6.96 (d, *J* = 8.4 Hz, 1H), 3.96 (s, 3H), 3.85 (s, 3H). ^{13}C NMR (63 MHz) δ 166.3, 158.7, 156.9, 144.2, 140.2, 132.3, 129.9, 128.4, 122.4, 114.4, 55.4, 52.3.

An analogous procedure was used to prepare lactams **4b-e**.

4-(Ethoxycarbonyl)benzaldehyde *N*-(4-methoxyphenyl)imine (**4b**).

Yellow solid, mp 104-107 °C, 98%. ^{1}H NMR (250 MHz) δ 8.51 (s, 1H), 8.11 (d, *J* = 8.1 Hz, 2H), 7.93 (d, *J* = 8.1 Hz, 2H), 7.26 (d, *J* = 8.6 Hz, 1H), 6.92 (d, *J* = 8.6 Hz, 1H), 4.39 (q, *J* = 7.1 Hz, 2H), 3.82 (s, 3H), 1.40 (t, *J* = 7.1 Hz, 3H). ^{13}C NMR (63 MHz) δ 166.2, 158.7, 156.9, 144.2, 140.2, 132.3, 129.9, 128.3, 122.4, 114.4, 61.2, 55.5, 14.3.

4-(Pentoxycarbonyl)benzaldehyde *N*-(4-methoxyphenyl)imine (**4c**).

Yellow solid, mp 68-70°C, 67%. ^{1}H NMR (250 MHz) δ 8.54 (s, 1H), 8.13 (d, *J* = 8.2 Hz, 2H), 7.95 (d, *J* = 8.2 Hz, 2H), 7.28 (d, *J* = 8.8 Hz, 1H), 6.95 (d, *J* = 8.8 Hz, 1H), 4.34 (t, *J* = 6.7 Hz, 2H), 3.84 (s, 3H), 1.80 (m, 2H), 1.42 (m, 4H), 0.94 (m, 3H). ^{13}C NMR (63

MHz) δ 166.2, 158.7, 156.9, 144.2, 140.2, 132.3, 129.9, 128.3, 122.4, 114.4, 65.4, 55.5, 28.4, 28.2, 22.4, 14.0.

4-(Heptyloxycarbonyl)benzaldehyde *N*-(4-methoxyphenyl)imine (**4d**).

Yellow solid, mp 59-60 °C, 89%. ^{1}H NMR (250 MHz) δ 8.54 (s, 1H), 8.13 (d, *J* = 8.3 Hz, 2H), 7.95 (d, *J* = 8.3 Hz, 2H), 7.28 (d, *J* = 8.9 Hz, 1H), 6.95 (d, *J* = 8.9 Hz, 1H), 4.34 (t, *J* = 6.7 Hz, 2H), 3.84 (s, 3H), 1.80 (m, 2H), 1.32-1.44 (m, 8H), 0.90 (m, 3H), ^{13}C NMR (63 MHz) δ 166.2, 158.7, 156.8, 144.2, 140.2, 132.3, 129.9, 128.3, 122.4, 114.4, 65.4, 55.5, 31.7, 28.9, 28.7, 26.0, 22.6, 14.1.

4-(Decyloxycarbonyl)benzaldehyde *N*-(4-methoxyphenyl)imine (**4e**).

Yellow solid, mp 40-41°C, 91%. ^{1}H NMR (250 MHz) δ 8.54 (s, 1H), 8.13 (d, *J* = 8.2 Hz, 2H), 7.95 (d, *J* = 8.2 Hz, 2H), 7.28 (d, *J* = 8.7 Hz, 1H), 6.94 (d, *J* = 8.7 Hz, 1H), 4.34 (t, *J* = 6.7 Hz, 2H), 3.85 (s, 3H), 1.79 (m, 2H), 1.27-1.44 (m, 14H), 0.88 (m, 3H), ^{13}C NMR (63 MHz) δ 166.2, 158.7, 156.9, 144.2, 140.2, 132.3, 129.9, 128.3, 122.4, 114.4, 82.6, 65.4, 63.7, 60.8, 55.3, 52.3, 28.4, 28.1, 22.3, 20.4, 13.9.

Procedure for the Formation of *N*-(4-Methoxyphenyl)-substituted β-Lactams 5.

To a stirred solution of imine **4** (6.94 g, 25.8 mmol) and triethylamine (10.8 ml, 77.4 mmol) was added dropwise over 10 minutes a solution of methoxyacetyl chloride (2.83 ml, 37.7 mmol) in CH_2Cl_2. The resultant mixture was stirred at rt until TLC indicated the disappearance of starting material. The solvent was removed under reduced pressure, and the crude material was purified by washing with ice-cold methanol to afford 6.89 g (78%) of lactam ***cis*-5a** as a white solid. mp 157-159 °C. ^{1}H NMR (250 MHz) δ 8.05 (d, *J* = 8.1 Hz, 2H), 7.47 (d, *J* = 8.1 Hz, 2H), 7.23 (d, *J* = 8.9 Hz, 2H), 6.78 (d, *J* = 8.9 Hz, 2H), 5.22

(d, *J* = 4.7 Hz, 1H), 4.84 (d, *J* = 4.7 Hz, 1H), 3.91 (s, 3H), 3.74 (s, 3H), 3.20 (s, 3H). ^{13}C NMR (63 MHz) δ 166.7, 163.4, 156.5, 138.7, 130.4, 130.3, 129.8, 128.0, 118.7, 114.4, 84.9, 61.4, 58.5, 55.4, 52.2.

An analogous procedure was used to prepare lactams **5b-e**.

***cis*-4-(4-Ethoxycarbonylphenyl)-3-methoxy-*N*-(4-methoxyphenyl)-2-azetidinone (*cis*-5b)**.

White solid, mp 104-107 °C, 18%. ^{1}H NMR (250 MHz) δ 8.05 (d, *J* = 8.2 Hz, 2H). 7.46 (d, *J* = 8.2 Hz, 2H), 7.23 (d, *J* = 8.9 Hz, 2H), 6.77 (d, *J* = 8.9 Hz, 2H), 5.22 (d, *J* = 4.8 Hz, 1H), 4.85 (d, *J* = 4.8 Hz, 1H), 4.37 (q, *J* = 7.1 Hz, 2H), 3.73 (s, 3H), 3.19 (s, 3H), 1.38 (t, *J* = 7.1 Hz, 3H), ^{13}C NMR (63 MHz) δ 166.1, 163.4, 156.4, 138.6, 130.8, 130.3, 129.7, 127.9, 118.6, 114.3, 84.9, 61.4, 61.1, 58.5, 55.4, 14.3.

***cis*-3-Methoxy-*N*-(4-methoxyphenyl)-4-(4-pentoxycarbonylphenyl)-2-azetidinone (*cis*-5c)**.

White solid, mp 68-70 °C, 17%. ^{1}H NMR (250 MHz) δ 8.08 (d, *J* = 8.3 Hz, 2H). 7.49 (d, *J* = 8.3 Hz, 2H), 7.26 (d, *J* = 9.0 Hz, 2H), 6.81 (d, *J* = 9.0 Hz, 2H), 5.22 (d, *J* = 4.7 Hz, 1H), 4.88 (d, *J* = 4.7 Hz, 1H), 4.34 (t, *J* = 6.4 Hz, 2H), 3.78 (s, 3H), 3.52 (s, 3H), 1.79 (quintet, *J* = 6.9 Hz, 2H), 1.43 (m, 4H), 0.94 (t, *J* = 6.9 Hz, 3H), ^{13}C NMR (63 MHz) δ 166.2, 163.4, 156.4, 138.6, 130.8, 130.3, 129.8, 127.9, 118.7, 114.4, 85.0, 65.2, 61.4, 58.6, 55.4, 28.4, 28.2, 22.3, 14.0.

***cis*-4-(4-Heptyloxycarbonylphenyl)-3-methoxy-*N*-(4-methoxyphenyl)-2-azetidinone (*cis*-5d)**.

White solid, mp 51-53°C, 19%. ^{1}H NMR (250 MHz) δ 8.06 (d, *J* = 8.1 Hz, 2H), 7.47 (d, *J* = 8.1 Hz, 2H), 7.24 (d, *J* = 8.9 Hz, 2H), 6.79 (d, *J* = 8.9 Hz, 2H), 5.23 (d, *J* = 4.7 Hz, 1H), 4.85 (d, *J* = 4.7 Hz, 1H), 4.31 (t, *J* = 6.5 Hz, 2H), 3.74 (s, 3H), 3.21 (s, 3H), 1.75 (m, 2H), 1.30-1.38 (m, 8H), 0.89 (m, 3H). ^{13}C NMR (63 MHz) δ 166.2, 163.4, 156.4, 138.6, 130.8, 130.3, 129.8, 127.9, 118.7, 114.4, 85.0, 65.2, 61.4, 58.5, 55.4, 31.7, 28.9, 28.7, 26.0, 22.6, 14.0.

***trans*-4-(4-Heptyloxycarbonylphenyl)-3-methoxy-*N*-(4-methoxyphenyl)-2-azetidinone (*trans*-5d)**.

White solid, mp 55-57°C, 18%. ^{1}H NMR (250 MHz) δ 8.09 (d, *J* = 8.1 Hz, 2H), 7.42 (d, *J* = 8.1 Hz, 2H), 7.23 (d, *J* = 8.9 Hz, 2H), 6.80 (d, *J* = 8.9 Hz, 2H), 4.97 (app s, 1H), 4.43 (app s, 1H), 4.34 (t, *J* = 6.4 Hz, 2H), 3.75 (s, 3H), 3.60 (s, 3H), 1.78 (quintet, *J* = 6.5 Hz, 2H), 1.22-1.38 (m, 8H), 0.90 (m, 3H). ^{13}C NMR (63 MHz) δ 166.0, 163.1, 156.5, 141.3, 131.0, 130.5, 130.2, 126.0, 118.8, 114.4, 91.2, 65.3, 62.8, 58.2, 55.4, 31.7, 29.0, 28.7, 26.0, 22.6, 14.1.

***cis*-4-(4-Decyloxycarbonylphenyl)-3-methoxy-*N*-(4-methoxyphenyl)-2-azetidinone (*cis*-5e)**.

White solid, mp 95-96°C, 63%. ^{1}H NMR (250 MHz) δ 8.05 (d, *J* = 8.2 Hz, 2H), 7.46 (d, *J* = 8.2 Hz, 2H), 7.23 (d, *J* = 9.0 Hz, 2H), 6.78 (d, *J* = 9.0 Hz, 2H), 5.22 (d, *J* = 4.7 Hz, 1H), 4.85 (d, *J* = 4.7 Hz, 1H), 4.30 (t, *J* = 6.4 Hz, 2H), 3.74 (s, 3H), 3.21 (s, 3H), 1.75 (m, 2H), 1.26-1.42 (m, 14H), 0.89 (m, 3H). ^{13}C NMR (63 MHz) δ 166.2, 163.4, 156.5, 138.6, 130.9, 130.3, 129.8, 127.9, 118.7, 114.4, 85.0, 65.3, 61.4, 58.6, 55.4, 31.8, 29.5 (double), 29.3 (double), 28.7, 26.0, 22.6, 14.1.

Procedure for the *N*-Dearylation of *N*-(4-Methoxylphenyl)-substituted β-Lactams 6.

To a solution of ***cis*-5a** (1.00 g, 2.93 mmol) in 15 ml of acetonitrile in ice-water bath, was added ceric ammonium nitrate (4.82 g, 8.79 mmol) in 15 ml of water. The resultant mixture was stirred for 5 minutes, and 20 ml of water was added. The solution was extracted (3 x 25 ml) with EtOAc. The combined organic layers were washed with 75 ml of 5% $NaHSO_3$, 5% $NaCO_3$, and dried over anhydrous $MgSO_4$. The solvent was removed under reduced pressure to yield a brown oil, which after purification by flash column chromatography on silica gel (1:2 EtOAc:hexanes) afforded 0.45 g (65% yield) of lactam ***cis*-6a** as a brown oil. ^{1}H NMR (250 MHz) δ 8.03 (d, *J* = 8.3 Hz, 2H), 7.43 (d, *J* = 8.3 Hz, 2H), 6.40 (bs, 1H), 4.89 (d, *J* = 4.5 Hz, 1H), 4.77 (dd, *J* = 4.5, 2.7 Hz, 1H), 3.90 (s, 3H), 3.15 (s, 3H).

An analogous procedure was used to prepare lactams **6b-e**.

***cis*-4-(4-Ethoxycarbonylphenyl)-3-methoxy-2-azetidinone (*cis*-6b)**.

Brown oil, 72%. ^{1}H NMR (250 MHz) δ 8.08 (d, *J* = 8.2 Hz, 2H). 7.47 (d, *J* = 8.2 Hz, 2H), 6.70 (bs, 1H), 4.93 (d, *J* = 4.5 Hz, 1H), 4.81 (dd, *J* = 4.5, 2.9 Hz, 1H), 4.40 (q, *J* = 7.1 Hz, 2H), 3.19 (s, 3H), 1.42 (t, *J* = 7.1 Hz, 3H).

cis*-3-Methoxy-4-(4-pentoxycarbonylphenyl)-2-azetidinone** (cis*-6c**).

Brown oil, 19%. ^{1}H NMR (250 MHz) δ 8.09 (d, *J* = 8.2 Hz, 2H). 7.48 (d, *J* = 8.2 Hz, 2H), 6.36 (bs, 1H), 4.95 (d, *J* = 4.7 Hz, 1H), 4.83 (dd, *J* = 4.7, 2.8 Hz, 1H), 4.35 (t, *J* = 6.7 Hz, 2H), 3.22 (s, 3H), 1.79 (quintet, *J* = 6.7 Hz, 2H), 1.43 (m, 4H), 0.94 (t, *J* = 6.9 Hz, 3H).

cis*-4-(4-Heptyloxycarbonylphenyl)-3-methoxy-2-azetidinone** (cis*-6d**)

Brown oil, 89%. ^{1}H NMR (250 MHz) δ 8.06 (d, *J* = 8.3 Hz, 2H), 7.45 (d, *J* = 8.3 Hz, 2H), 6.38 (bs, 1H), 4.92 (d, *J* = 4.5 Hz, 1H), 4.80 (dd, *J* = 4.5, 2.8 Hz, 1H), 4.31 (t, *J* = 6.7 Hz, 2H), 3.18 (s, 3H), 1.78 (quintet, *J* = 6.5 Hz, 2H), 1.22-1.38 (m, 8H), 0.89 (m, 3H).

trans*-4-(4-Heptyloxycarbonylphenyl)-3-methoxy-2-azetidinone** (trans*-6d**).

Brown oil, 88%. ^{1}H NMR (250 MHz) δ 8.11 (d, *J* = 8.3 Hz, 2H), 7.49 (d, *J* = 8.3 Hz, 2H), 6.35 (bs, 1H), 4.64 (app s, 1H), 4.43 (app s, 1H), 4.34 (t, *J* = 6.4 Hz, 2H), 3.60 (s, 3H), 1.78 (quintet, *J* = 6.5 Hz, 2H), 1.22-1.38 (m, 8H), 0.90 (m, 3H).

cis*-4-(4-Decyloxycarbonylphenyl)-3-methoxy-2-azetidinone** (cis*-6e**).

Brown oil, 91%. ^{1}H NMR (250 MHz) δ 8.02 (d, *J* = 8.1 Hz, 2H), 7.42 (d, *J* = 8.1 Hz, 2H), 6.89 (bs, 1H), 4.89 (d, *J* = 4.5 Hz, 1H), 4.77 (dd, *J* = 4.5, 2.5 Hz, 1H), 4.28 (t, *J* = 6.6 Hz, 2H), 3.13 (s, 3H), 1.75 (quintet, *J* = 7.1 Hz, 2H), 1.26-1.42 (m, 14H), 0.89 (t, *J* = 6.7 Hz, 3H).

Procedure for the *N*-Methylthiolation of Lactams 7.

To a solution of ***cis*-6a** (455 mg, 1.91 mmol) in 10 ml of dry CH_2Cl_2 was added *N*-(methylthio)phthalimide (410 mg, 2.10 mmol) and 0.25 ml of triethylamine. The resultant mixture was refluxed overnight. The solvent was removed under reduced pressure to yield a brown solid. The brown solid was redissolved in CH_2Cl_2 and washed with 1% aqueous NaOH. The organic layer was dried over anhydrous $MgSO_4$. The solvent was removed under reduced pressure to yield a brown oil, which after purification by column chromatography on silica gel (1:4 EtOAc:hexanes) yielded 0.356 g (66%) of ***cis*-7a** as a white solid. mp 118-120 °C. ^{1}H NMR (250 MHz) δ 8.03 (d, *J* =

8.1 Hz, 2H). 7.45 (d, *J* = 8.1 Hz, 2H), 7.21 (d, *J* = 8.9 Hz, 2H), 6.77 (d, *J* = 8.9 Hz 2H), 3.18 (s, 3H), 5.22 (d, *J* = 4.7 Hz, 1H), 4.84 (d, *J* = 4.7 Hz, 1H), 3.90 (s, 3H), 3.72 (s, 3H). ^{13}C NMR (63 MHz) δ 170.2, 167.0, 138.7, 130.7, 129.6, 128.8, 86.7, 65.8, 58.5, 52.2, 22.1.

An analogous procedure was used to prepare lactams **7b-e**.

***cis*-4-(4-Ethoxycarbonylphenyl)-3-methoxy-*N*-methylthio-2-azetidinone (*cis*-7b)**. White solid, mp 113-114 °C, 70%. ^{1}H NMR (250 MHz) δ 8.03 (d, *J* = 8.1 Hz, 2H), 7.45 (d, *J* = 8.1 Hz, 2H), 7.22 (d, *J* = 8.9 Hz, 2H), 6.77 (d, *J* = 8.9 Hz, 2H), 5.22 (d, *J* = 4.8 Hz, 1H), 4.84 (d, *J* = 4.8 Hz, 1H), 4.37 (q, *J* = 7.1 Hz, 2H), 3.73 (s, 3H), 3.19 (s, 3H), 1.38 (t, *J* = 7.1 Hz, 3H). ^{13}C NMR (63 MHz) δ 170.1, 166.2, 138.6, 131.0, 129.5, 128.8, 86.7, 65.8, 61.1, 58.4, 22.1, 14.3.

***cis*-3-Methoxy-*N*-methylthio-4-(4-pentoxycarbonylphenyl)-2-azetidinone (*cis*-7c)**. White solid, mp 84-85 °C, 79%. ^{1}H NMR (250 MHz) δ 8.07 (d, *J* = 8.0 Hz, 2H), 7.44 (d, *J* = 8.0 Hz, 2H), 4.88 (d, *J* = 4.8 Hz, 1H), 4.82 (d, *J* = 4.8 Hz, 1H), 4.32 (t, *J* = 6.5 Hz, 2H), 3.17 (s, 3H), 2.39 (s, 3H), 1.77 (m, 2H), 1.41 (m, 4H), 0.93 (t, J = 6.5 Hz, 3H). ^{13}C NMR (63 MHz) δ 170.2, 166.3, 138.6, 131.1, 129.5, 128.8, 86.8, 66.0, 65.4, 58.4, 28.3, 28.2, 22.1, 22.0, 13.9.

cis*-4-(4-Heptyloxycarbonylphenyl)-3-methoxy-*N*-methylthio-2-azetidinone** (cis*-7d**). White solid, mp 51-52 °C, 70%. ^{1}H NMR (250 MHz) δ 8.08 (d, *J* = 8.3 Hz, 2H), 7.45 (d, *J* = 8.3 Hz, 2H), 4.88 (d, *J* = 4.9 Hz, 1H), 4.82 (d, *J* = 4.9 Hz, 1H), 4.33 (t, *J* = 6.6 Hz, 2H), 3.18 (s, 3H), 2.39 (s, 3H), 1.75 (m, 2H), 1.25-1.42 (m, 8H), 0.90 (m, 3H). ^{13}C NMR (63 MHz) δ 170.1, 166.1, 138.5, 131.3, 129.5, 128.8, 87.0, 65.4, 65.0, 58.4, 31.7, 29.1, 28.9, 26.0, 23.0, 22.6, 14.1.

***trans*-4-(4-Heptyloxycarbonylphenyl)-3-methoxy-*N*-methylthio-2-azetidinone (*trans*-7d).**

White solid, 53-55 °C, 68%. ^{1}H NMR (250 MHz) δ 8.09 (d, *J* = 7.9 Hz, 2H). 7.38 (d, *J* = 7.9 Hz, 2H), 4.67 (app s, 1H), 4.44 (app s, 1H), 4.33 (t, *J* = 6.5 Hz, 2H), 3.53 (s, 3H), 2.43 (s, 3H), 1.77 (m, 2H), 1.25-1.41 (m, 8H), 0.89 (m, 3H). ^{13}C NMR (63 MHz) δ 170.1, 166.0, 140.9, 131.2, 130.3, 126.8, 91.7, 66.2, 65.4, 58.4, 31.7, 29.7, 28.9, 26.0, 22.6, 21.8, 14.0.

***cis*-4-(4-Decyloxycarbonylphenyl)-3-methoxy-*N*-methylthio-2-azetidinone (*cis*-7e).**

White solid, 45-46 °C, 81%. ^{1}H NMR (250 MHz) δ 8.06 (d, *J* = 8.0 Hz, 2H), 7.43 (d, *J* = 8.0 Hz, 2H), 4.88 (d, *J* = 5.0 Hz, 1H), 4.82 (d, *J* = 5.0 Hz, 1H), 4.31 (t, *J* = 6.7 Hz, 2H), 3.15 (s, 3H), 2.38 (s, 3H), 1.76 (m, 2H), 1.26-1.42 (m, 14H), 0.87 (m, 3H), ^{13}C NMR (63 MHz) δ 170.1, 166.2, 138.6, 131.0, 129.5, 128.8, 86.7, 65.8, 65.3, 58.5, 31.8, 29.5, 29.3, 28.7, 26.0, 22.7, 22.1, 14.0.

Procedure for the Synthesis of 2-Ethoxycarbonylbenzaldehyde (9)

To a stirred solution of 2-carboxybenzaldehyde **8** (5.00 g, 33.3 mmol) in dry acetone (20 ml) was added K_2CO_3 (4.60g, 40.0 mmol) and the solution was stirred for 1h. To this was added dropwise a solution of ethyl iodide (3.2 ml, 40 mmol) in dry acetone (1 ml), and the mixture was refluxed for overnight. The solvent was removed under reduced pressure to yield a brown semi-solid. The brown solid was redissolved in EtOAc, and washed with water. The organic layer was dried over anhydrous $MgSO_4$. The crude material was purified by column chromatography on silica gel (1:9 EtOAc:hexanes) to yield 1.07 g (18%) of aldehyde **9** as a colorless semi-solid. ^{1}H NMR (250 MHz) δ 10.58

(s, 1H), 7.88-7.96 (m, 2H), 7.53-7.63 (m, 2H), 4.41 (q, *J* = 7.1 Hz, 2H), 1.39 (t, *J* = 7.1 Hz, 3H). ^{13}C NMR (63 MHz) δ 192.2, 136.9, 132.9, 132.4, 132.2, 130.7, 130.3, 128.3, 62.0, 14.2.

Procedure for the Synthesis of *N*-(4-Methoxyphenyl)-4-ethoxycarbonyl phenylimine (10).

To a solution of *p*-anisidine (0.55 g, 4.5 mmol) in 10 ml of CH_2Cl_2 was added aldehyde **9** (0.80 g, 4.5 mmol) and a catalytic amount of camphorsulfonic acid. The resultant mixture was stirred at rt until TLC indicated the disappearance of both starting materials. The solvent was removed under reduced pressure, and the crude material was purified by recrystallization from methanol to yield 0.76 g (60%) of imine **9** as a yellow solid. mp 52-53 °C. ^{1}H NMR (250 MHz) δ 9.23 (s, 1H), 8.22 (d, *J* = 7.5 Hz, 1H), 7.95 (d, *J* = 7.5 Hz, 1H), 7.58 (t, *J* = 7.1 Hz, 1H), 7.46 (t, *J* = 7.4 Hz, 1H), 7.28 (d, *J* = 8.6 Hz, 2H), 6.91 (d, *J* = 8.6 Hz, 2H), 4.38 (q, *J* = 7.1 Hz, 2H), 3.79 (s, 3H),1.38 (t, *J* = 7.1 Hz, 3H). ^{13}C NMR (63 MHz) δ 166.9, 158.3, 157.6, 144.8, 137.3, 132.1, 130.7, 130.3, 129.9, 128.1, 122.5, 114.2, 61.3, 55.4, 14.2.

Synthesis of 4-(2-Ethoxycarbonylphenyl)-3-methoxy-*N*-(4-methoxyphenyl)-2-azetidinone (*cis* and *trans* adduct).

To a stirred solution of imine **4** (0.34 g, 1.21 mmol) and triethylamine (0.51 ml, 3.63 mmol) was added dropwise over 10 minutes a solution of methoxyacetyl chloride (0.22 ml, 2.42 mmol) in CH_2Cl_2. The resultant mixture was refluxed for overnight. The solvent was removed under reduced pressure to yield a brown oil. The crude material was

purified by flash column chromatography on silica gel (1:4 EtOAc:hexanes) to afford 0.18 g (36%) of lactam **11,** Brown semisolid (cis:trans = 1:1 mixture), ^{1}H NMR (250 MHz) δ 1.40 (t, J=7.1 Hz, 3H), 3.19 (s, 3H), 3.73 (s, 3H), 4.37 (q, J=7.1 Hz, 2H), 4.84 (d, J=4.8 Hz, 1H,), 5.22 (d, J=4.8 Hz, 1H,), 6.77 (d, J=8.9 Hz 2H), 7.22 (d, J=8.9 Hz, 2H), 7.45 (d, J=8.1 Hz, 2H), 8.03 (d, J=8.1 Hz, 2H). ^{13}C NMR (63 MHz) δ 14.3, 22.1, 58.4, 61.1, 65.8, 86.7, 128.8, 129.5, 131.0, 138.6, 166.2, 170.1.

Procedure for synthesis of 3-Methoxy-4-(2-ethyloxycarbonyl)phenyl-2-azetidinone (12)

To a solution of **10** (0.18 g, 0.52 mmol) in 1 ml of CH_3CN in an ice-water bath was added a solution of ceric ammonium nitrate (0.86 g, 1.57 mmol) in 1 ml of water. The resultant mixture was stirred for 5 min, and 2 mL of water was added. The solution was extracted (3 x 5 ml) with EtOAc. The combined organic layers were washed with 5% $NaHSO_3$, 5% $NaHCO_3$, and dried over anhydrous $MgSO_4$. The solvent was removed under reduced pressure to yield a brown oil, which was purified by flash column chromatography on silica gel (1:2 EtOAc:hexanes) to afford 47 mg (36%) of lactam **11** as a brown semi-solid (1:1 *cis:trans* mixture). ^{1}H NMR (250 MHz) δ 8.08 (d, *J* = 7.5 Hz, 1H). 8.02 (dd, *J* = 7.5, 1.5 Hz, 2H), 7.41 (m, 8H), 7.28 (m, 8H), 6.78 (two d, *J* = 9.0 Hz, 6H), 6.01 (d, *J* = 5.1 Hz, 1H), 5.98 (s, 2H), 4.95 (d, *J* = 5.1 Hz, 1H), 4.43 (q, *J* = 7.1 Hz, 4H), 3.71 (s, 6H), 3.59 (s, 6H), 1.42 (two t, *J* = 7.1 Hz, 6H), ^{13}C NMR (63 MHz) δ 166.9, 166.6, 164.6, 163.9, 156.3, 137.8, 136.0, 132.8, 132.4, 131.2, 131.0, 130.7, 130.3, 129.4, 129.2, 128.1, 127.8, 126.1, 118.9, 118.6, 114.3, 91.5, 85.6, 61.5, 61.2, 60.3, 59.1, 58.9, 57.9, 55.3, 30.9, 14.3.

Procedure for the Synthesis of N-Methylthiolation of β-Lactams 13.

To a solution of **12** (47 mg, 0.19 mmol) in 2 ml of dry CH_2Cl_2 was added N-(methylthio)phthalimide (55 mg, 0.28 mmol) and 3-5 drops of triethylamine. The resultant mixture was refluxed overnight. The solvent was removed under reduced pressure to yield a brown solid. The brown solid was redissolved in methylene chloride, and washed with 1% sodium hydroxide. The organic layer was dried over magnesium sulphate. The solvent was removed under reduced pressure to yield a brown semi-solid. The crude material was purified by column chromatography on silica gel using a gradient elution (1:19, 1:9 and 1:4 EtOAc:hexanes) to yield 23 mg (35%) of *cis*-lactam **13a** and 24 mg (37%) of *trans*-lactam **13b** as white solids (total 72% yield).

***cis*-4-(2-Ethoxycarbonylphenyl)-3-methoxy-*N*-methylthio-2-azetidinone (13a)**.

White solid, mp 95-97 °C, 35%. ^{1}H NMR (250 MHz) δ 8.06(m, 1H). 7.61(m, 1H), 7.43 (m, 2H), 5.72 (d, *J* = 5.1 Hz, 1H), 4.95 (d, *J* = 5.1 Hz, 1H), 4.39 (q, *J* = 7.1 Hz, 2H), 3.23 (s, 3H), 2.48 (s, 3H), 1.43 (t, *J* = 7.1 Hz 3H). ^{13}C NMR (63 MHz) δ 171.3, 166.7, 136.1, 132.4, 130.9, 129.8, 127.9, 87.6, 63.8, 61.2, 58.9, 29.7, 21.5, 14.3.

***trans*-4-(2-Ethoxycarbonylphenyl)-3-methoxy-*N*-methylthio-2-azetidinone (13b)**.

White solid, mp 75-76 °C, 37%. ^{1}H NMR (250 MHz) δ 8.01 (m, 1H), 7.58 (m, 1H), 7.43(m, 1H), 7.29 (m, 1H), 5.71 (d, *J* = 1.9 Hz, 1H), 4.41 (q, *J* = 7.1 Hz, 2H), 4.40 (d, *J* = 1.9 Hz, 1H), 3.56 (s, 3H), 2.46 (s, 3H), 1.41 (t, *J* = 7.1 Hz, 3H). ^{13}C NMR (63 MHz) δ 171.1, 166.8, 137.6, 132.6, 131.1, 130.3, 128.2, 126.3, 92.3, 62.0, 61.5, 58.2, 21.6, 14.2.

Procedure for the Synthesis of 3-Acetoxy-*N*-(4-Methoxyphenyl)-substituted β–Lactams 14.

To a stirred solution of imine **4a** (0.50 g, 1.9 mmol) and triethylamine (0.56 g, 5.6 mmol) was added dropwise over 10 min a solution of acetoxyacetyl chloride (0.24 ml, 2.2 mmol) in dry CH_2Cl_2 (10 ml). The resultant mixture was stirred at rt for overnight. The solvent was removed under reduced pressure, and the crude material was purified by column chromatography on silica gel by gradient elution (1:9 then 1:4 EtOAc: hexanes) to yield 175 mg (25%) of lactam **14a** (1:1 *cis*:*trans* mixture) as a brown semi-solid. ^{1}H NMR (250 MHz) δ 8.00 (two d, *J* = 8.9 Hz, 4H), 7.38 (two d, *J* = 8.9 Hz, 4H), 7.20 (two d, *J* = 8.9 Hz, 4H), 6.77 (two d, *J* = 8.9 Hz, 4H), 5.94 (d, *J* = 4.8 Hz, 1H), 5.37 (d, *J* = 4.8 Hz, 1H), 5.32 (s, 1H, *trans* isomer), 4.94 (s, 1H, *trans* isomer), 3.89 (s, 6H), 3.72 (s, 3H), 3.71 (s, 3H), 2.17(s, 3H), 1.67 (s, 3H).

An analogous procedure was used to prepare β-lactams **14b-e**.

3-Acetoxy-4-(4-ethoxycarbonylphenyl)-*N*-(4-methoxyphenyl)-2-azetidinone (14b). Brown semi-solid, 20:1 *cis:trans* mixture, 43%. Data for *cis* isomer:^{1}H NMR (250 MHz) δ 8.02 (d, *J* = 7.9 Hz, 2H). 7.37 (d, *J* = 7.9 Hz, 2H), 7.23 (d, *J* = 8.5 Hz, 2H), 6.79 (d, *J* = 8.5 Hz, 2H), 5.96 (d, *J* = 4.5 Hz, 1H), 5.38 (d, *J* = 4.5 Hz, 1H), 4.36 (q, *J* = 7.0 Hz, 2H), 3.73 (s, 3H), 1.69 (s, 3H), 1.37 (t, *J* = 7.0 Hz, 3H). ^{13}C NMR (63 MHz) δ 169.1, 166.0, 161.0, 156.7, 137.4, 130.9, 130.0, 129.7, 127.9, 118.7, 114.4, 76.3, 61.2, 61.1, 55.4, 19.9, 14.3.

3-Acetoxy-*N*-(4-methoxyphenyl)-4-(4-pentoxycarbonylphenyl)-2-azetidinone (14c). Brown semi-solid, 1:5 *cis:trans* mixture, 12%. Data for the *trans* isomer: ^{1}H NMR (250 MHz) δ 8.03 (d, *J* = 8.2 Hz, 2H), 7.40 (d, *J* = 8.2 Hz, 2H), 7.18 (d, *J* = 8.9 Hz, 2H), 6.76 (d, *J* = 8.9 Hz, 2H), 5.31 (s, 1H), 4.95 (s, 1H), 4.27 (t, *J* = 6.5 Hz, 2H), 3.70 (s, 3H), 2.17 (s, 3H), 1.72 (m, 2H), 1.37 (m, 4H), 0.89 (m, 3H). ^{13}C NMR (63 MHz) δ 169.7, 165.9,

160.7, 156.6, 140.0, 131.1, 130.3, 129.9, 126.4, 118.8, 114.4, 82.3, 65.2, 63.3, 55.3, 28.3, 28.1, 20.4, 13.9.

3-Acetoxy-*N*-(4-methoxyphenyl)-4-(4-heptyloxycarbonylphenyl)-2-azetidinone (14d). Brown semi-solid, 1:2 *cis:trans* mixture, 40%. ^{1}H NMR (250 MHz) δ 8.04 (two d, *J* = 8.6 Hz, 3H), 7.42 (two d, *J* = 8.6 Hz, 3H), 7.20 (two d, *J* = 8.7 Hz, 3H), 6.79 (two d, *J* = 8.7 Hz, 3H), 5.97 (d, *J* = 4.6 Hz, 0.5H, *cis* isomer), 5.39 (d, *J* = 4.6 Hz, 0.5H, *cis* isomer), 5.33 (s, 1H, *trans* isomer), 4.95 (s, 1H, *trans* isomer), 4.30 (t, *J* = 6.5 Hz, 3H), 3.73 (s, 4.5H), 2.19 (s, 3H), 1.74 (m, 3H), 1.69 (s, 1.5 H), 1.25-1.37 (m, 12H), 0.88 (m, 4.5H).

3-Acetoxy-4-(4-decyloxycarbonylphenyl)-*N*-(4-methoxyphenyl)-2-azetidinone (14e). Brown semi-solid, 1:1 *cis:trans* mixture, 57%. ^{1}H NMR (250 MHz) δ 8.04 (two d, *J* = 8.5 Hz, 4H). 7.40 (two d, *J* = 8.5 Hz, 4H), 7.22 (two d, *J* = 8.9 Hz, 4H), 6.79 (two d, *J* = 8.9 Hz, 4H), 5.96 (d, *J* = 4.8 Hz, 1H, *cis* isomer), 5.39 (d, *J* = 4.8 Hz, 1H, *cis* isomer), 5.33 (s, 1H, *trans* isomer), 4.96 (s, 1H, *trans* isomer), 4.38 (m, 4H), 3.74 (s, 3H), 3.73 (s, 3H), 2.19 (s, 6H), 1.73 (m, 4H), 1.69 (s, 6 H), 1.26-1.69 (m, 28H), 0.87 (m, 6H).

Procedure for the Synthesis of *N*-Methylthio-substituted β–Lactams 15.

To a solution of **14a** (100 mg, 0.27 mmol) in 2.5 ml of CH_3CN in an ice-water bath was added ceric ammonium nitrate (0.450 g, 0.81 mmol) in 2.5 ml of water. The resultant mixture was stirred for 5 min, and 5 ml of water was added. The solution was extracted (3x5 ml) with EtOAc. The combined organic layers were washed with 5% $NaHSO_3$, 5% $NaHCO_3$, and dried over anhydrous $MgSO_4$. The solvent was removed under reduced pressure to yield a crude brown oil, which was dissolved in 10 ml of dry CH_2Cl_2 and *N*-(methylthio)phthalimide (52 mg, 0.268 mmol) and 3-5 drops of triethylamine were added.

The resultant mixture was refluxed for overnight. The solvent was removed under reduced pressure to yield a brown solid. The brown solid was redissolved in CH_2Cl_2, and washed with 1% NaOH. The organic layer was dried over anhydrous $MgSO_4$. The solvent was removed under reduced pressure to yield a brown semi-solid, which was purified by column chromatography on silica gel with gradient elution (1:9 then 1:4 EtOAc:hexanes) to yield 23.6 mg (18%) of a brown semi-solid containing lactams as a mixture of *cis:trans* isomers. The *cis* and *trans* isomers were separated by recrystallization in methanol to give ***cis*-15a** (8 mg) and ***trans*-15a** (11 mg) in combined 18% yield.

cis*-3-Acetoxy-4-(4-methoxycarbonylphenyl)-*N*-methylthio-2-azetidinone** (cis*-15a**). White solid, mp 81-83 °C, 8%. ^{1}H NMR (250 MHz) δ 8.05 (d, *J* = 8.2 Hz, 2H), 7.35 (d, *J* = 8.2 Hz, 2H), 5.92 (d, *J* = 5.0 Hz, 1H), 5.08 (d, *J* = 5.0 Hz, 1H), 3.93 (s, 3H), 2.45 (s, 3H), 1.69 (s, 3H). ^{13}C NMR (63 MHz) δ 168.7, 168.1, 166.5, 137.6, 130.8, 129.5, 128.6, 78.1, 65.4, 52.2, 22.1, 19.8.

trans*-3-Acetoxy-4-(4-methoxycarbonylphenyl)-*N*-methylthio-2-azetidinone** (trans*-15a**).

White solid, mp 66-68 °C, 10%. ^{1}H NMR (250 MHz) δ 8.09(d, *J* = 8.2 Hz, 2H), 7.40 (d, *J* = 8.2 Hz, 2H), 5.38 (d, *J* = 1.5 Hz, 1H), 4.72 (d, *J* = 1.5 Hz, 1H), 3.92 (s, 3H), 2.43 (s, 3H), 2.16 (s, 3H). ^{13}C NMR (63 MHz) δ 169.4, 168.0, 166.4, 140.0, 131.0, 130.2, 127.1, 82.7, 66.0, 52.3, 21.8, 20.4.

An analogous procedure was used to prepare lactams **15b-e**.

cis*-3-Acetoxy-4-(4-ethoxycarbonylphenyl)-*N*-methylthio-2-azetidinone** (cis*-15b**). White solid, mp 95-97 °C, 12%. ^{1}H NMR (250 MHz) δ 8.06 (d, *J* = 8.3 Hz, 2H), 7.35 (d,

J = 8.3 Hz, 2H), 5.93 (d, *J* = 5.0 Hz, 1H), 5.07 (d, *J* = 5.0 Hz, 1H), 4.39 (q, *J* = 7.1 Hz, 2H), 2.45 (s, 3H), 1.71 (s, 3H), 1.41 (t, *J* = 7.1 Hz, 3H). ^{13}C NMR (63 MHz) δ 14.3, 20.0, 22.1, 61.2, 65.4, 78.1, 128.6, 129.5, 131.1, 138.0, 166.9, 168.6, 169.2.

3-Acetoxy-*N*-methylthio-4-(4-pentyloxycarbonylphenyl)-2-azetidinone (***trans*-15c**). Brown oil, 1:7 *cis:trans* mixture, 5%. Data for *trans* isomer: ^{1}H NMR (250 MHz) δ 8.11(d, *J* = 8.3 Hz, 2H), 7.41 (d, *J* = 8.3 Hz, 2H), 5.39 (d, *J* = 1.9 Hz, 1H), 4.72 (d, *J* = 1.9 Hz, 1H), 4.33 (t, *J* = 6.6 Hz, 2H), 2.45 (s, 3H), 2.18 (s, 3H), 1.78 (m, 2H), 1.42 (m, 4H), 0.91 (m, 3H). ^{13}C NMR (63 MHz) δ 7.8, 20.6, 23.7, 24.3, 28.1, 28.4, 65.4, 66.1, 82.7, 127.1, 130.2, 131.2, 139.9, 166.4, 167.9, 169.3.

trans*-3-Acetoxy-4-(4-heptyloxycarbonylphenyl)-*N*-methylthio-2-azetidinone** (trans*-15d**).

Brown oil, 2%. ^{1}H NMR (250 MHz) δ 8.05 (d, *J* = 8.1 Hz, 2H), 7.37 (d, *J* = 8.1 Hz, 2H), 5.35 (app s, 1H), 4.70 (app s, 1H), 4.28 (t, *J* = 6.6 Hz, 2H), 2.40 (s, 3H), 2.12 (s, 3H), 1.72 (m, 2H), 1.21-1.36 (m, 8H), 0.84 (m, 3H). ^{13}C NMR (63 MHz) δ 169.4, 168.0, 165.9, 139.8, 131.3, 130.1, 127.1, 82.7, 65.9, 65.3, 31.6, 28.9, 28.6, 25.9, 22.1, 21.7, 20.3, 14.0.

***cis*-3-Acetoxy-4-(4-decyloxycarbonylphenyl)-*N*-methylthio-2-azetidinone (*cis*-15e)**. Brown oil, 9%. ^{1}H NMR (250 MHz) δ 8.06 (d, *J* = 8.3 Hz, 2H), 7.36 (d, *J* = 8.3 Hz, 2H), 5.93 (d, *J* = 5.0 Hz, 1H), 5.08 (d, *J* = 5.0 Hz 1H), 4.33 (t, *J* = 6.7 Hz, 2H), 2.46 (s, 3H), 1.77 (m, 2H), 1.71 (s, 3H), 1.28-1.43 (m, 14H), 0.88 (t, *J* = 6.2 Hz, 3H). ^{13}C NMR (63 MHz) δ 168.9, 168.3, 166.6, 137.7, 131.1, 129.5, 128.6, 78.1, 65.4, 31.9, 29.5, 29.3, 28.6, 26.0, 22.1, 19.9, 14.1.

trans*-3-Acetoxy-4-(4-decyloxycarbonylphenyl)-*N*-methylthio-2-azetidinone** (trans*-15e**).

Brown oil, 12%. ^{1}H NMR (250 MHz) δ 8.07 (d, *J* = 8.3 Hz, 2H), 7.39 (d, *J* = 8.3 Hz, 2H), 5.37 (d, *J* = 2.0 Hz, 1H), 4.71 (d, *J* = 2.0 Hz, 1H), 4.30 (t, *J* = 6.6 Hz, 2H), 2.42 (s, 3H), 2.14 (s, 3H), 1.74 (m, 2H), 1.24-1.40 (m, 14H), 0.85 (m, 3H). ^{13}C NMR (63 MHz) δ 169.4, 168.0, 165.9, 139.8, 131.3, 130.2, 127.1, 82.7, 66.0, 65.3, 31.8, 29.5, 29.2, 28.6, 26.0, 22.6, 21.8, 20.3, 14.1.

Procedure for the Synthesis of 3-Acetoxy-*N*-(4-methoxyphenyl)-4-phenyl-2-azetidinone (16).

To a stirred solution of *N*-(4-methoxyphenyl)imine (5.31 g, 25.2 mmol) and triethylamine (7.64 g, 75.5 mmol) was added a solution of acetoxyacetyl chloride (5.15 g, 37.7 mmol) in methylene chloride dropwise over 10 minutes. The resultant mixture was stirred at rt until TLC indicated the disappearance of starting material. The solvent was removed under reduced pressure, and the crude material was purified by washing with ice-cold methanol to give 6.89 g (89%) of **16** as white solid, mp 153-155 ^{o}C. ^{1}H NMR (250 MHz) δ 7.34-7.30 (t, 5H), 7.28 (d, *J* = 8.9 Hz, 2H) 6.79 (d, *J* = 8.9 Hz, 2H), 5.92 (d, *J* = 4.8 Hz, 1H), 5.33 (d, *J* = 4.8 Hz, 1H), 3.74 (s, 3H), 1.66 (s, 3H). ^{13}C NMR (63 MHz) δ 169.1, 161.2, 156.5, 132.2, 130.2, 128.7, 128.4, 127.8, 118.7, 61.3, 55.3, 19.7.

Procedure for the Synthesis of 3-Hydroxy-*N*-(4-methoxyphenyl)-4-phenyl-2-azetidinone (17).

To a solution of β-lactam **15** (21.2 g, 68.3 mmol) in 500 ml of acetone was added KOH (3.83 g, 68.3 mmol) in 50 ml of methanol. The resultant mixture was stirred for 5 minutes, and 300 ml of water was added. The product was precipitated and isolated by filtration to yield 18.0 g (98%) of **17** as a white solid, mp 199-202 ^{o}C. ^{1}H NMR (250

MHz) δ 7.44-7.28 (m, 7H), 6.83-6.79 (q, 2H), 5.29 (d, *J* = 5.2 Hz, 1H), 5.90 (d, *J* = 5.2 Hz, 1H), 3.76 (s, 3H), 2.10 (bs, 1H). ^{13}C NMR (63 MHz, DMSO-d_6), δ 166.7, 155.9, 135.2, 131.1, 128.5, 128.4, 128.1, 114.8, 77.2, 62.2, 55.5.

Procedure for the Synthesis of 3-(methoxycarbonyl)oxy-*N*-(4-methoxyphenyl)-4-phenyl-2-azetidinone (**18a**).

To a solution of β-lactam **17** (500 mg, 1.86 mmol) in 5 ml of freshly distilled CH_2Cl_2 was added NaH (60% suspension in mineral oil, 74.4 mg, 1.86 mmol), and the mixture was stirred for 15 min. Methyl chloroformate (0.17 ml, 2.23 mmol) was then added, and the resultant mixture was stirred for 5 h or until TLC indicated the disappearance of starting material. The reaction was quenched with a 5% solution of NH_4Cl and extracted (3x20 ml) with CH_2Cl_2. The combined organic layers were dried over anhydrous $MgSO_4$ and purified with column chromatography on silica gel (1:4, EtOAc:hexanes) to give 0.35 g (55%) of **17a** as a white solid, mp 123-124 °C. ^{1}H NMR (250 MHz) δ 7.35 (s, 5H), 7.28 (d, *J* = 8.9 Hz, 2H) 6.81 (d, *J* = 8.9 Hz, 2H), 5.86 (d, *J* = 4.8 Hz, 1H), 5.36 (d, *J* = 4.8 Hz, 1H), 3.75 (s, 3H), 3.55 (s, 3H). ^{13}C NMR (63 MHz) δ 160.2, 156.6, 154.0, 131.8, 130.2, 129.0, 128.6, 127.9, 118.8, 114.4, 78.5, 61.3, 55.4, 55.3.

An analogous procedure was used to prepare β–lactams **18b-e**.

3-(Ethoxycarbonyl)oxy-*N*-(4-methoxyphenyl)-4-phenyl-2-azetidinone (**18b**).

White solid, mp 105-106 °C, 39%. ^{1}H NMR (250 MHz) δ 7.35 (s, 5H), 7.28 (d, *J* = 9.0 Hz, 2H) 6.81 (d, *J* = 9.0 Hz, 2H), 5.83 (d, *J* = 4.8 Hz, 1H), 5.36 (d, *J* = 4.8 Hz, 1H), 3.96 (q, *J* = 7.1 Hz, 2H), 3.75 (s, 3H), 1.03 (t, *J* = 7.1 Hz, 3H). ^{13}C NMR (63 MHz) δ 160.2,

156.6, 154.0, 131.8, 130.2, 128.9, 128.6, 128.0, 118.8, 114.4, 78.4, 64.7, 61.4, 55.4, 13.9.

3-(1,1-Dimethylethoxy)carbonyloxy-*N*-(4-methoxyphenyl)-4-phenyl-2-azetidinone (**18c**).

White solid, mp 169-170 °C , 98 %. ^{1}H NMR (250 MHz) δ 7.35 (s, 5H), 7.28 (d, *J* = 8.9 Hz, 2H) 6.80 (d, *J* = 8.9 Hz, 2H), 5.74 (d, *J* = 4.7 Hz, 1H), 5.33 (d, *J* = 4.7 Hz, 1H), 3.75 (s, 3H), 1.20 (s, 9H). ^{13}C NMR (63 MHz) δ 160.2, 156.6, 154.0, 131.8, 130.2, 129.0, 128.6, 127.9, 118.8, 114.4, 78.5, 61.3, 55.4, 55.3.

3-Phenoxycarbonyloxy-*N*-(4-methoxyphenyl)-4-phenyl-2-azetidinone (**18d**).

White solid, mp 154-155 °C, 21%. ^{1}H NMR (250 MHz) δ 7.42 (s, 5H), 7.34-7.19 (m, 5H), 6.83 (d, *J* = 8.9 Hz, 2H) 6.73 (d, *J* = 8.9 Hz, 2H), 5.89 (d, *J* = 4.8 Hz, 1H), 5.40 (d, *J* = 4.8 Hz, 1H), 3.75 (s, 3H). ^{13}C NMR (63 MHz) δ 159.8, 156.7, 152.0, 150.5, 131.7, 130.1, 129.5, 129.1, 128.7, 128.2, 126.3, 120.9, 120.7, 118.9, 114.4, 78.9, 61.3, 55.4.

3-(methoxydithiocarbonyl)oxy-*N*-(4-methoxyphenyl)-4-phenyl-2-azetidinone (**18e**).

White solid, mp 125-126 °C , 15%. ^{1}H NMR (250 MHz) δ 7.32 (s, 5H), 7.29 (d, *J* = 9.0 Hz, 2H) 6.81 (d, *J* = 9.0 Hz, 2H), 6.67 (d, *J* = 4.8 Hz, 1H), 5.41 (d, *J* = 4.8 Hz, 1H), 3.75 (s, 3H), 2.28 (s, 3H). ^{13}C NMR (63 MHz) δ 160.6, 156.6, 131.9, 130.1, 128.9, 128.4, 128.2, 118.9, 114.7, 81.7, 61.7, 55.5, 18.9.

Procedure for the 3-(Ethoxycarbonyl)oxy-4-phenyl-2-azetidinone (19a).

To a solution of **18a** (330 mg, 1.01 mmol) in 5 ml of CH_3CN was added ceric ammonium nitrate (1.66 g, 3.03 mmol, 3 eq.) in 5 ml of water. The resultant mixture was stirred for 5 min, and 10 ml of water was added. The solution was extracted (3x10 ml) with EtOAc. The combined organic layers were washed with 5% $NaHSO_3$, 5% $NaHCO_3$, and dried

over anhydrous $MgSO_4$. The solvent was removed under reduced pressure to yield a brown oil. The crude material was purified by flash column chromatography on silica gel (1:2 EtOAc:hexanes) to give 150 mg (63%) of **19a** as a brown semi-solid. ^{1}H NMR (250 MHz) δ 7.37-7.28 (m, 5H), 6.90 (bs, 1H), 5.75 (dd, *J* = 4.7, 2.7 Hz, 1H), 5.03 (d, *J* = 4.7 Hz, 1H), 3.52 (s, 3H).

An analogous procedure was used to prepare β–lactams **19b-e**.

3-(Ethoxycarbonyl)oxy-4-phenyl-2-azetidinone (19b).

Brown semi-solid, 2%. ^{1}H NMR (250 MHz) δ 7.35-7.31 (m, 5H), 7.02 (bs, 1H), 5.73 (dd, *J* = 4.7, 2.7 Hz, 1H), 5.01 (d, *J* = 4.7 Hz, 1H), 4.08 (q, *J* = 7.1 Hz, 2H), 1.22 (t, 3H).

3-(1,1-Dimethylethoxy)carbonyloxy-4-phenyl-2-azetidinone (19c).

Brown semi-solid, 72%. ^{1}H NMR (250 MHz) δ 7.35 (s, 5H), 6.67 (bs, 1H), 5.65 (dd, *J* = 4.5, 2.8 Hz, 1H), 5.02 (d, *J* = 4.5 Hz, 1H), 1.19 (s, 9H).

3-Phenoxycarbonyloxy-4-phenyl-2-azetidinone (19d).

Brown semi-solid, 78%. ^{1}H NMR (250 MHz) δ 7.43 (s, 5H), 7.30-7.20 (m, 3H), 7.17 (bs, 1H), 6.72 (m, 2H), 5.78 (dd, *J* = 4.5, 2.8 Hz, 1H), 5.05 (d, *J* = 4.5 Hz, 1H).

3-(methoxycarbonyl)oxy-4-phenyl-2-azetidinone (19e).

Brown semi-solid, 1%. ^{1}H NMR (250 MHz) δ 7.33 (s, 5H), 6.61 (dd, *J* = 4.7, 2.5 Hz, 1H), 6.53 (bs, 1H), 5.03 (d, *J* = 4.7 Hz, 1H), 2.31 (s, 3H).

Procedure for Synthesis of *N*-Methylthio-3-methoxycarboxy-4-phenyl-2-azetidinone (20a).

To a solution of **19a** (200 mg, 0.90 mmol) in 5 ml of dry CH_2Cl_2 was added *N*-(methylthio)phthalimide (260 mg, 1.35 mmol) and 3-5 drops of triethylamine. The resultant mixture was refluxed overnight. The solvent was removed under reduced

pressure to yield a brown solid. The brown solid was redissolved in methylene chloride, and washed with 1% sodium hydroxide. The organic layer was dried over magnesium sulphate. The solvent was removed under reduced pressure to yield a brown oil. The crude material was purified by column chromatography (1:4 ethyl acetate: hexanes) to yield 11.8 mg (5%) of **20a** as a white solid. mp 83-84 °C. ^{1}H NMR (250 MHz) δ 7.29-7.41 (m, 5H), 5.83 (d, *J* = 5.0 Hz, 1H), 5.03 (d, *J* = 5.0 Hz, 1H), 3.54 (s, 3H), 2.43 (s, 3H). ^{13}C NMR (63 MHz) δ 167.3, 153.6, 131.9, 129.2, 128.7, 128.5, 80.1, 65.7, 55.4, 22.1.

3-(Ethoxycarbonyl)oxy-*N*-methylthio-4-phenyl-2-azetidinone (20b).

White solid, mp 71-72 °C, 35%. ^{1}H NMR (250 MHz) δ 7.30-7.40 (m, 5H), 5.80 (d, *J* = 4.9 Hz, 1H), 5.02 (d, *J* = 4.9 Hz, 1H), 3.93 (q, *J* = 7.1 Hz, 2H), 2.43 (s, 3H), 1.01 (t, *J* = 7.1 Hz, 3H). ^{13}C NMR (63 MHz) δ 167.4, 153.7, 132.0, 129.1, 128.8, 128.4, 80.1, 65.8, 64.8, 22.1, 13.8.

3-(1,1-Dimethylethoxy)carbonyloxy-*N*-methylthio-4-phenyl-2-azetidinone (20c).

White solid, mp 81-83 °C, 1%. ^{1}H NMR (250 MHz) δ 7.30-7.39 (m, 5H), 5.69 (d, *J* = 4.8 Hz, 1H), 5.01 (d, *J* = 4.8 Hz, 1H), 2.44 (s, 3H), 1.16 (s, 9H). ^{13}C NMR (63 MHz) δ 167.5, 151.1, 132.1, 128.9, 128.3, 128.4, 83.3, 79.8, 66.0, 27.2, 22.2.

***N*-Methylthio-3-phenoxycarbonyloxy-4-phenyl-2-azetidinone (20d).**

White solid, mp 117-118 °C, 53%. ^{1}H NMR (250 MHz) δ 7.18-7.49 (m, 8H), 6.69 (m, 2H), 5.87 (d, *J* = 4.9 Hz, 1H), 5.09 (d, *J* = 4.9 Hz, 1H), 2.48 (s, 3H). ^{13}C NMR (63 MHz) δ 166.8, 151.7, 150.4, 131.8, 129.4, 128.9, 128.6, 126.4, 120.6, 80.5, 66.7, 22.2.

***N*-Methylthio-3-methoxydithiocarboxy-4-phenyl-2-azetidinone (20e).**

White solid, mp 77-78 °C, 1%. ^{1}H NMR (250 MHz) δ 7.28-7.37 (m, 5H), 6.61 (d, *J* = 4.9 Hz, 1H), 5.09 (d, *J* = 4.9 Hz, 1H), 2.45 (s, 3H), 2.31 (s, 3H).

References

1. T. E. Long and E. Turos, *Curr. Med. Chem. –Anti-Infective Agents* **2002**, *1*, 251.
2. (a) X. F. Ren, M. I. Konaklieva, H. Shi, S. Dickey, D. V. Lim, J. Gonzalez, E. Turos, *J. Org. Chem*. **1998**, *63*, 8898. (b) E. Turos, M. I. Konaklieva, X. F. Ren, H. Shi, J. Gonzalez, S. Dickey, D. V. Lim, *Tetrahedron* **2000**, *56*, 5571.
3. E. Turos, T. E. Long, M. I. Konaklieva, C. Coates, J.-Y. Shim, S. Dickey, D. V. Lim, A. Cannons, *Bioorg. Med. Chem. Lett.* **2002**, *12*, 2229.
4. T. E. Long, E. Turos, M. I. Konaklieva, A. L. Blum, A. Amry, E. A. Baker, L. S. Suwandi, M. D. McCain, M. F. Rahman, S. Dickey, D. V. Lim, *Bioorg. Med. Chem.* **2002**, *11*, 1859.
5. Gomez-Gallego, M.; Mancheno, M. J.; Sierre, M. A. *Tetrahedron* **2000**, *56*, 5743.
6. Delpiccolo, C. M. L.; Mata, E. G. *Tetrahedron: Asymmetry* **2002**, *13*, 905.
7. Banik, I.; Becker, F. F.; Banik, B. K. *J. Med. Chem.* **2003**, *46*, 12.
8. Banik, I.; Hackfeld, L.; Banik, B. K. *Heterocycles* **2003**, *59*, 505.

Chapter Three

Polymeric Nanoparticles Containing an N-Methylthio β-Lactam

3.1 Introduction

In recent years, there has been a rapid growth in the area of drug discovery. This has been facilitated by novel technologies such as combinatorial chemistry and high-throughput screening.[1,2,3] These novel approaches have led to numerous drug candidates within very short periods of time compared with the conventional drug discovery method. Many of these analogs show promising biological activity in vitro and in vivo. However, most of them do not progress to commercialization because of the problems of unwanted cytotoxicity (no targeting and no controlled release), very poor water solubility and, consequently, low bioavailability. These problems are closely related to optimal drug delivery systems in the human body which is why research on drug delivery systems has been and remains a hot topic in drug discovery.[4,5]

Fig. 3-1 shows a hypothetical comparison of the concentration of drug found in the plasma as a function of time following conventional drug release versus controlled drug release by oral drug administration**.** As can be seen in Fig. 3-1, the conventional oral drug administration does not provide ideal pharmacokinetic profiles, especially for drugs which display high toxicity and/or narrow therapeutic periods of

time. For such drugs, if they can be conjugated to an optimal drug delivery system, the ideal pharmacokinetic profile can be achieved wherein the drug concentration reachs therapeutic levels without exceeding the maximum tolerable dose, and maintains these concentrations for extended periods of time until the desired therapeutic effect is reached. Therefore, optimizing drug delivery is a good answer for treatments that involve highly cytotoxic drugs such as certain anticancer agents, so that toxic side effects and damage to healthy tissues are minimized.

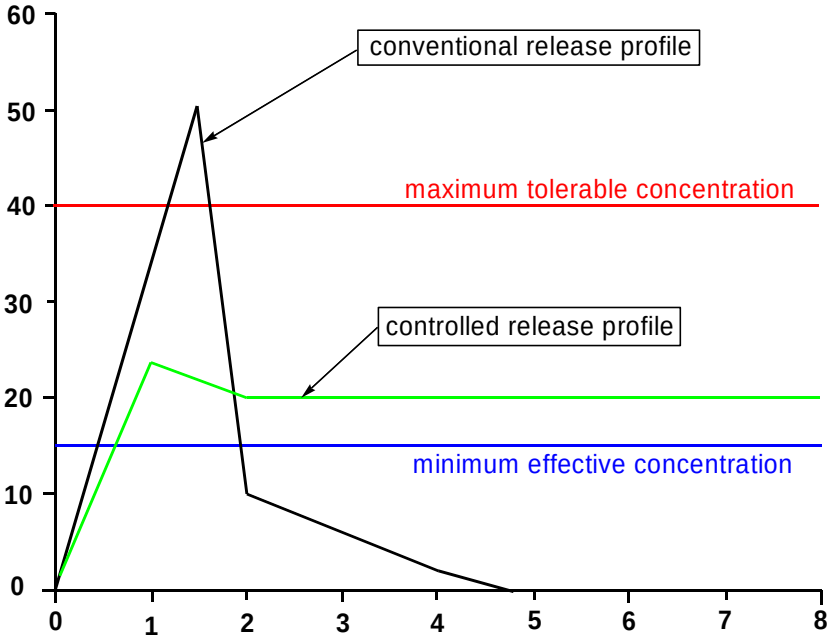

Fig. 3-1[6] Comparison of conventional and controlled release profile

In recent years, significant effort has been devoted to developing micro or nano-size microsphere technology for drug delivery.[7,8,9] These microspheres offer a suitable means of delivering small molecular weight drugs, as well as biomacromolecules such as proteins, peptides or genes by either sustained or targeted

delivery to the tissue of interest. This technology focuses on formulating therapeutic agents in biocompatible or biodegradable polymeric nanocomposites such as nanoparticles or nanocapsules. Since these systems are often polymeric and submicron in size, they have multiple advantages in drug delivery. These systems in general can be used to provide cellular or tissue delivery of drugs, to improve oral bioavailability, to sustain drug/gene effect in target tissue, to enhance the water solubility of drugs for intravascular delivery, and to improve the stability of therapeutic agents against enzymatic degradation (nucleases and proteases).[7] However, the majority of current technologies are focusing on controlled or sustained release systems via drug encapsulation methods using biodegradable polymeric nanoparticles, even though the nanometer-size ranges of these delivery systems offer certain distinct advantages for drug delivery. Therefore, if nanoparticles can penetrate deep into tissues and through endocytosis are taken up efficiently by the cells[10], this allows efficient delivery of therapeutic agents to target sites in the body. Also, by modulating polymer characteristics, one can control the release of the drug from nanoparticles to achieve a desired therapeutic level in target tissue for optimal therapeutic effects. Further, nanoparticles can be delivered to target sites either by localized delivery using an enhanced permeation and retention (EPR) effect[11, 12] or by targeted delivery through conjugation to a biospecific ligand which could direct them to the target tissue or organ.[7]

In this research, microemulsion polymerization was done in aqueous solution to form hydrophilic polymeric nanoparticles containing a highly water-insoluble solid antibiotic, an *N*-methylthio β-lactam. *N*-Methylthio β-lactams are a new family of

potent antibacterial compounds that selectively inhibit the growth of methicillin-resistant *Staphylococcus aureus* (MRSA). These drugs tend to be insoluble in water, and it was hoped that this method could enhance water solubility and bioavailability of these drugs. In addition, the antibacterial activity of these resulting polymeric nanoparticles was investigated against MRSA strains.

The synthesis of *N*-thiolated β-lactam acrylic monomers for radical polymerization, and the conjugation of these acrylic monomers into a polymeric nanoparticle using a novel microemulsion polymerization method, are described herein. We also describe the characterization of the polymer, its antibacterial properties, and the relationship that may exist between antibacterial activity, % drug content, and particle size.

Finally, the preparation and the characterization of a fluorescence-active nanoparticle is reported in chapter four for diagnostic purposes such as elucidating the biological mode of action, acting as a biological sensor and biological imaging.

3.2 Conventional Microemulsion Polymerization

Microemulsion polymerization was first reported in the early 1980's.[13, 14] This process can produce transparent or translucent polymeric microlatexes with particle diameters of 50nm or higher. Over 45% of all industrial polymers have been prepared by using emulsion polymerization. The main advantages of this process are: a) water is used as the sole solvent, b) the viscosity of emulsion is relatively low and independent of the polymer molecular weight, and c) high molecular weight polymers with a narrow weight distribution can be produced in a controlled environment.

Therefore, this emulsion polymerization is bringing about the renaissance in the industrial polymer area.

A conventional emulsion polymerization consists of dispersing a water insoluble acrylic monomer phase, which is the low viscosity liquid phase, in an aqueous phase with the aid of surfactants. Polymerization is then brought about by free radical initiation in the water phase. The polymer formed is stabilized within the emulsion by absorption onto surfactants to form a protective colloid form as the polymerization proceeds. The resultant products are homogeneous and relatively stable emulsified polymeric microspheres. The surfactant is a hydrocarbon chain with one end being hydrophobic and the other hydrophilic. If the concentration of surfactant is high enough, the hydrophobic ends of several surfactants form aggregates known as micelles. The surfactant serves as a stabilizer for the polymer particles and the monomer droplets. Therefore, the hydrophobic ends will attach to the particles while the hydrophilic ends will remain in the water phase. The charges on these surfactants form what is known as an electrical double layer which prevents the particles from coagulating. In other words, the emulsifier serves to keep the particles suspended in the water. The micelles can also be the location of particle nucleation. The monomer is present in the reaction mixture in the form of large droplets. These droplets act as reservoirs of the monomer. The monomer in the droplets can diffuse through the water phase and into the micelles. When the initiator is added to the reaction mixture it dissociates into two radicals in the presence of heat. The initiator radicals are very reactive towards any monomer in the water phase. The monomer in the water phase continues to add to the radical until the chain grows long enough such that it is no

longer soluble in water. The oligomeric radical chain (multiple monomeric units) is now hydrophobic enough to enter a polymer particle or to enter a micelle to nucleate a new particle. Thus, the conventional emulsion polymerization will occur in three stages. The first stage involves the nucleation (birth) of polymer particles. This can occur by either micellar or homogeneous nucleation. The second stage involves the growth of the particles until the monomer droplets disappear. The third and final stage begins with the disappearance of the monomer droplets and continues until the end of the reaction (Fig. 3-2).[15, 16]

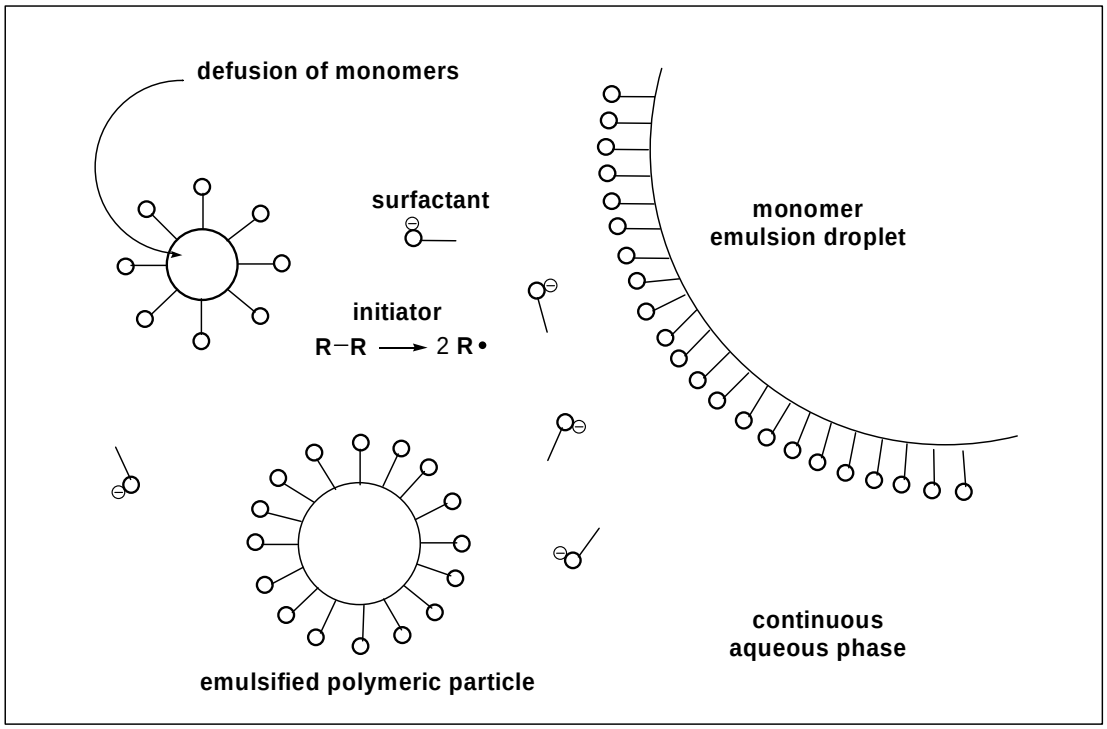

Fig. 3-2 Schematic representation of an emulsion polymerization system[15]

Conventional emulsion polymerization methods are difficult to use for the preparation of polymeric microspheres for drug delivery systems, since most drugs are either partially or completely insoluble in water, and as such cannot form the

liquid droplet in the emulsion polymerization process. The acrylic part on the original chemical structure of the drug has to be introduced synthetically for free radical polymerization without losing activity. Therefore, the challenge is to prepare polymeric microspheres for drug delivery systems using a new emulsion polymerization method which can overcome these problems.

3.3 Synthesis of C_3-Acryloyl *N*-Methylthio β-Lactam as a Key Monomer

The acrylation of *N*-methylthio β-lactams is required for microemulsion polymerization using free radicals. Acrylation can be accomplished at either the C_3 or the C_4 position of the β-lactam. In this study, the C_3-acrylation of the β-lactam was studied. The synthesis of C_3-acryloyl *N*-methylthio β-lactam is summarized in Scheme III-1. The key step is to introduce the acryloyl group at the C_3-position, which can then participate in the radical copolymerization with the other acrylic co-monomer.

2-Chlorobenzaldehyde (**21**) was coupled with *p*-anisidine, to give imines **22**. Staudinger coupling of acetoxyacetyl chloride with imine **22** gave C_3-acetoxy *N*-aryl protected β-lactam **23**. Hydrolysis of acetoxy group under basic conditions gave the C_3-free hydroxyl β-lactam **24.** Acrylation of free hydroxyl β-lactam **24** with acryloyl chloride gave C_3-acryloyl *N*-aryl protected β-lactam **25**. Dearylation of β-lactam **25** with ceric ammonium nitrate gave N-dearylated β-lactam **26**, followed by methylthiolation with N-methylthio- phthalimide affords C_3-acryloyl *N*-methylthio β-

lactam **27** which is a white solid, mp 92-93 ^{o}C . The ^{1}H NMR spectra of C_3-acryloyl *N*-methylthio β-lactam **27** is displayed in Fig. 3-3.

Scheme III-1

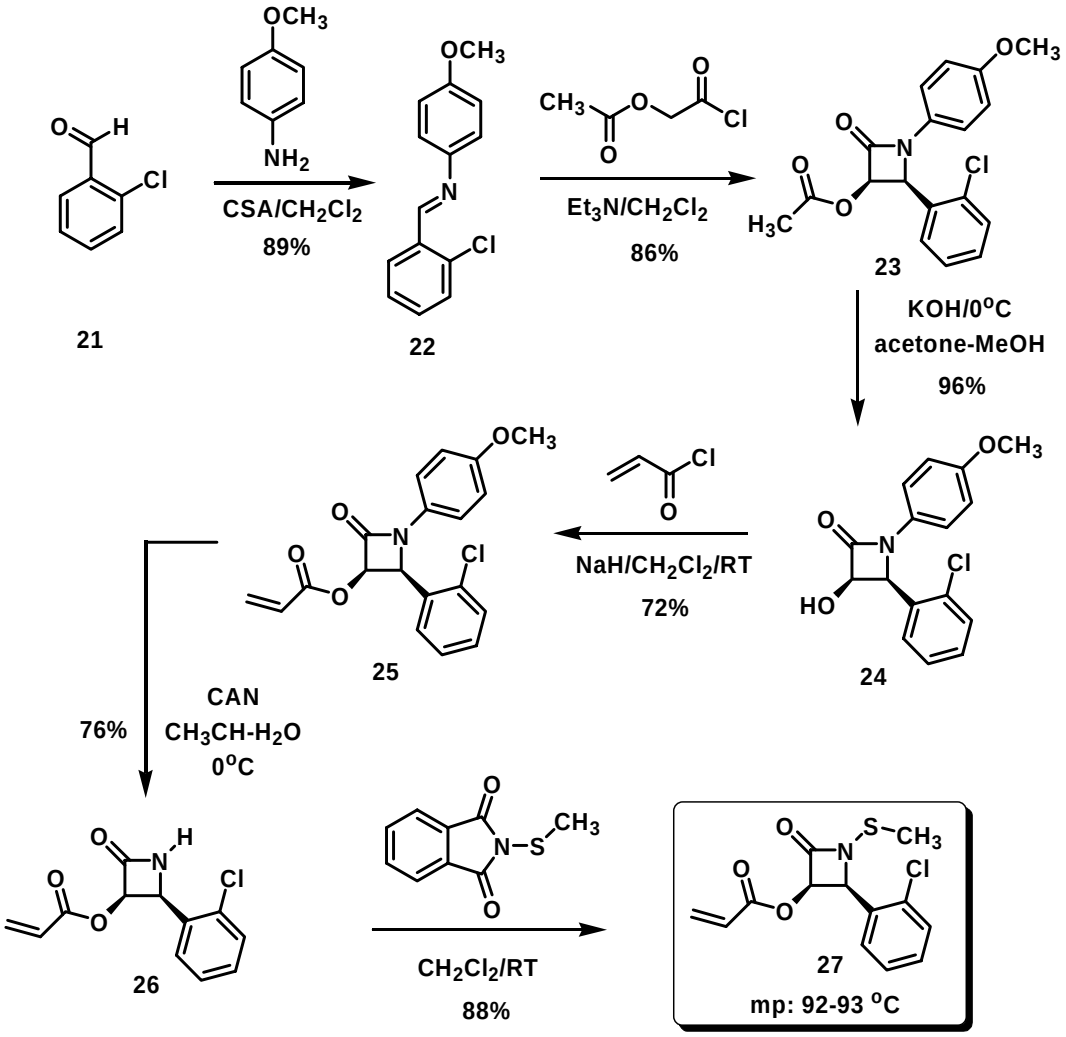

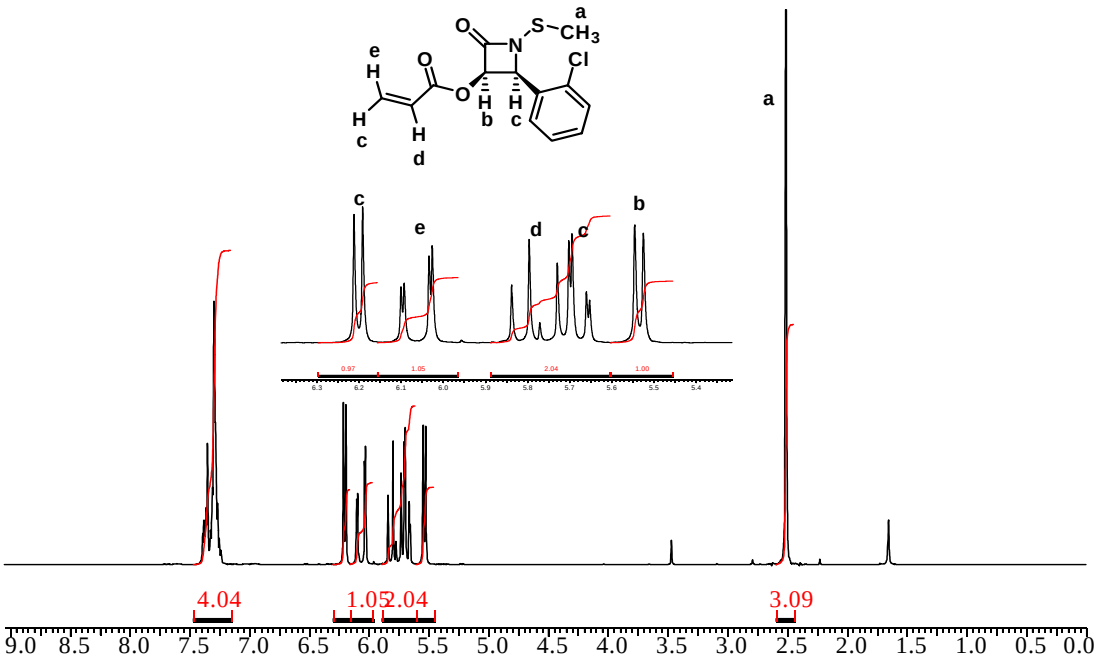

Fig. 3-3 ^{1}H NMR Spectra of C_3-acryloyl N-methylthio β-lactam

3.4 Main Components for Microemulsion Polymerization

The microemulsion polymerization used to prepare the polymeric nanoparticles consists of four major components: 1) acrylic drug monomer, 2) acrylic co-monomer, 3) surfactant, and 4) deionized water. The selection and requirement of each of these components are described below.

3.4.1 Choice of Drug Monomer

The drug monomer needs to contain three essential parts; the first one is the drug itself, the second one is the acrylic moiety for radical polymerization and the third one is the linker that connects the drug with the acrylic moiety such that it can break down biologically or enzymatically. The general features are shown in Fig. 3-4.

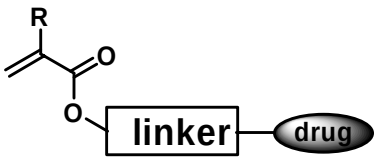

Fig. 3-4 Structure of drug monomer

A wide variety of drugs (antibacterial, antiviral, antifungal and anticancer agents, etc.) can potentially be used in this method, including those which have little or no water solubility as well as those that have good water solubility.

A variety of acrylic monomers can conceivably be synthetically coupled with a drug containing a functional group such as a carboxylic acid, an amine or an alcohol. Examples of such monomers include acryloyl chloride, methacryloyl chloride, acrylic acid, maleic acid, itaconic acid, crotonic acid, N-methylol acrylamide, acrylonitrile, 2-hydroxyethyl acrylate, 2-hydroxypropyl acrylate, 2-hydroxyethyl methacrylate

Modified acrylamide, modified methacrylamide, (PEG) modified acrylate, amino acid oligomeric acrylate etc. also can be possibly used for specific controlled release system since the amino acid oligomer which is active for a specific enzyme can be selectively cleaved under certain biological conditions.

3.4.2 Choice of Co-monomer

Commercial acrylic or vinyl monomers can be used as the co-monomers. The choice of co-monomers is entirely dependent on the chemical and physical properties of the drug monomer. It is a critical that the commercial or synthetically modified acrylic monomers are able to play two roles in the polymerization process: (1) as the co-monomer for the radical emulsion polymerization and (2) as the solvent for

dissolving the synthetically modified drug monomers in order to make homogeneous liquid phase. Therefore, it is very important to find a specific acrylic co-monomer that matches a specific drug monomer, and this is accomplished by trial and error. Fortunately, there are many acrylic monomers available commercially and/or synthetically: acrylonitrile, acrylic acid, maleic acid, methyl acrylate, ethyl acrylate, butyl acrylate, 2-ethylhexyl acrylate, methoxyethyl acrylate, dimethylamino acrylate, methacrylic acid, methyl methacrylate, ethyl methacrylate, butyl methacrylate, isobutyl methacrylate, 2-ethyl hexyl methacrylate, lauryl methacrylate, stearic methacrylate, dimethyl amino methacrylate, allyl methacrylate, 2-hydroxyethyl acrylate, 2-hydroxypropyl acrylate, 2-hydroxyethyl methacrylate, modified acrylamide, modified methacrylamide, glycidyl acrylate, styrene, vinyl acetate, vinyl toluene, and all synthetically modified acrylics can be used.

3.4.3 Choice of Surfactant

The surfactant that is used in emulsion polymerizations has two ends of different solubility. One end, termed the tail, is a long hydrocarbon that is soluble in nonpolar, organic compounds. The other end, the head, is often a hydrophilic functional sodium or potassium salt, which is water soluble. The water soluble salt can be the salt of a carboxylic acid or sulfonic acid. The technical term for the chemical display of "dual personalities" is *amphipathic*.

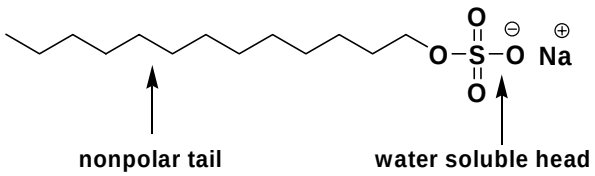

Sodium Lauryl Sulfate

The selection of emulsifiers (or the surfactants) is very important for a successful formulation as it can control many of the properties of emulsion polymers. There is a critical concentration below which an emulsifier will not form micelles. The minimum level required for micelle formation is known as the critical micelle concentration (CMC). Emulsifiers are classified according to the ionic type of the hydrophilic group, ionic or non-ionic. Ionic emulsifiers generally have a lower CMC than non-ionic emulsifiers and they provide low particle size emulsions. However, there is a problem with long term storage of these compounds. In the case of non-ionic emulsifiers, they need higher CMC level because of their low water solubility so that it leads to the formation of small aggregates or grainy emulsions. However, once the particles are formed they are very stable in aqueous systems. As a result of these advantages and disadvantages, ionic/non-ionic emulsifier mixtures can be employed in emulsion polymerization. Therefore, the factors for selecting the emulsifiers are totally dependent on the chemical or physical properties of the applied drug monomer and co-monomer, radical initiator and aqueous system.

As the choice of surfactants, anionic, cationic and nonionic surfactants such as lauryl alcohol (+6EO), nonyl phenol (+10EO, +15EO, +30EO), sodium lauryl sulphate, sodium lauryl sulphate (+2EO, +4EO), sodium dodecylbenzenesulphonate,

sodium dioctyl sulphosuccinate, polyvinyl alcohol, polyol, unsaturated and saturated fatty acid sodium and potassium salts, and synthetically modified PEG surfactants can, in principle, be used.

3.4.4 Choice of Radical Initiator

The initiator must be water soluble and the free radicals have to be generated thermally or by use of an oxidation-reduction (or redox) couple. The major initiators used in emulsion polymerization are persulphates.

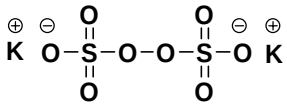

Potassium Persulfate

Even though the initiating efficiency and the half life of persulphates vary, ammonium persulphate is preferred in practice because of its better solubility. Hydroperoxides are often used particularly as a post reaction initiator to kill the unreacted monomers after emulsion polymerization. The rate of free radical generation increases with temperature, and it is normal to employ reaction temperatures of 60-90^{o}C when using thermal generation techniques. However, when redox couples (thiosulphates, metabissulphites and hydrosulphides) are employed, the rate of free radical generation is increased to that provided by thermal generation at the same temperature. Therefore, when using redox couples, reaction temperatures can be as low as 30^{o}C. Possible free-radical initiators for use in the initiating step of

polymerizations include: peroxides; persulphates; alkyl hydroperoxides; persulphates with sodium, ammonium and potassium; thiosulphates; metabisulphites; and hydrosulphides.

3.4.5 Choice of Aqueous Media

The aqueous media is the major part of the emulsion polymerization. The ions or metals in the aqueous media can act as a radical scavenger. Therefore the aqueous media used has to be either de-ionized water or nano-pure water for biological purposes. It is sometimes necessary to use a buffer solution depending on the surfactant and the particle stabilization.

3.5 The Preparation of Polymeric Nanoparticles Using Microemulsion Polymerization

Polymeric nanoparticles of N-methylthio β-lactam were prepared by a novel microemulsion polymerization technique described in Scheme III-2. The key point of this method was the complete dissolution of the solid drug monomer in a commercial acrylic monomer at elevated temperature, followed by its dispersion into an aqueous media containing a surfactant for the stabilization of the suspension. Therefore, it is very critical to get a homogeneous liquid mixture. In the first example studied, C_3-acryloyl N-methylthio β-lactam **21** and ethyl acrylate were combined at 70^{o}C. The mixture was then dispersed into an aqueous media containing a surfactant, sodium lauryl sulphate, to allow the formation of droplets with vigorous stirring until a milky suspension was formed. The emulsion radical polymerization then was launched by

adding the initiator, potassium persulfate, at 70°C to afford the polymeric nanoparticles as a milky colloidal suspension (Fig. 3-5).

Scheme III-2

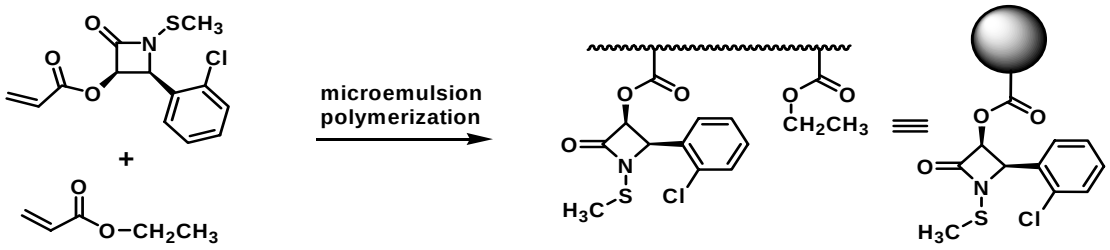

Fig. 3-5 β-lactam polymeric emulsion

Other anaologs were prepared by emulsion polymerization by varying the ratios of monomers and reaction conditions. The formulations of polymerization are summarized in Table 3-1.

Table III-1 Formulation of Microemulsion Polymerization

entry	mole ratio	monomers(mg)		surfactant (mg)	initiator(mg)	water (ml)	rxn. temp.(^{o}C)
	EA[1] : β-lactam[1]	β-lactam[1]	EA[1]	lauryl sulphate[1]	persulphate[1]		
1	EA homo	0	1000	20	5.0	5.0	60
2[2]	20 : 1	100	700	16	4.0	4.0	70
3[2]	13 : 1	100	456	12	3.0	2.8	70
4[2]	10 : 1	100	350	9	2.5	2.3	70
5[2]	7 : 1	100	245	7	1.8	1.8	70
6[2]	5 : 1	100	175	6	1.5	1.4	70
7[2]	2.5 : 1	100	88	3	0.8	0.7	70

[1] EA:ethyl acrylate, β-lactam: C_3-acryloyl *N*-methylthio β-lactam, lauryl sulphate: sodium salt, persulphate: potassium salt

[2] The scale was varied several times based on volume.

3.6 Characterization of Emulsion

3.6.1 Scanning Electron Microscopy (SEM)

The morphology and the particle size of the emulsified particles were examined by Scanning Electron Microscopy (SEM). The sample of nanoparticles was prepared on the silicon wafer by air blowing and then was coated with gold sputter under high vacuum. The gold-coated nanoparticles were then observed by SEM (Hitach S800). The SEM images of the copolymeric nanoparticles for the β-lactam and ethyl acrylate are shown in Fig. 3-6 through Fig. 3-12.

The SEM image of the polymeric nanoparticles for homo poly (ethyl acrylate): Fig. 3-6 shows the polymeric nanoparticles deformed by the electron beam of SEM because of the low Tg, -23 ^{o}C of homo poly(ethyl acrylate). The SEM images

of the copolymeric nanoparticles, (20:1 through 2.5:1 for ethyl acrylate: β-lactam) show that the particles have microspherical morphology with the particle size distribution of 40 nm to 150 nm in diameter. It is very interesting that the 7:1 copolymeric nanoparticles have the smallest particle size distribution (40-80 nm), while the 2.5:1 copolymeric nanoparticles had a uniform particle size of 70 nm. The particle size distribution of the copolymeric nanoparticles for the β-lactam and ethyl acrylate, determined by SEM analyses, are summarized in Fig. 3-13.

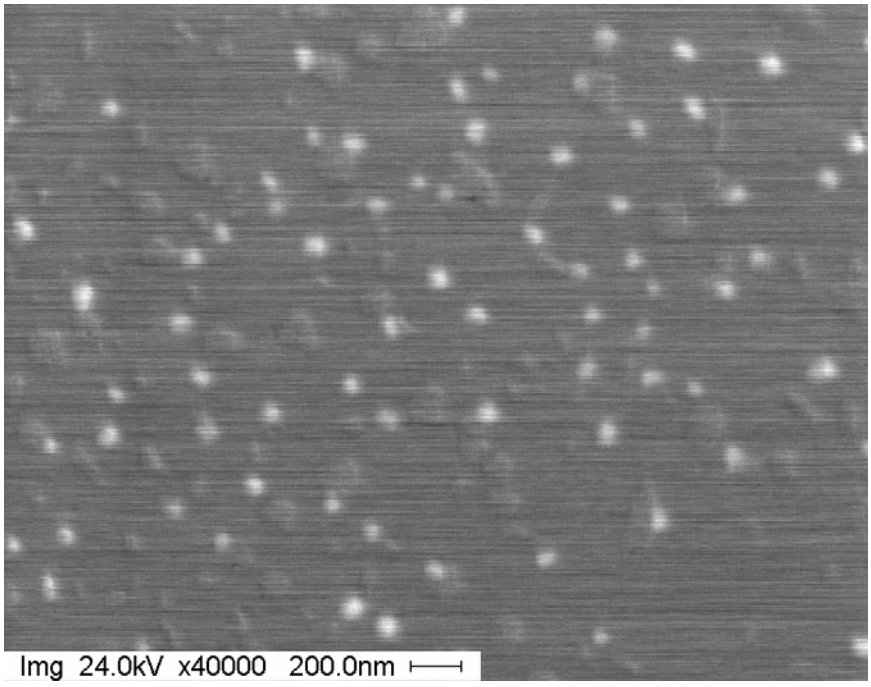

Fig. 3-6 SEM picture for homo ethyl acrylate polymeric nanoparticles

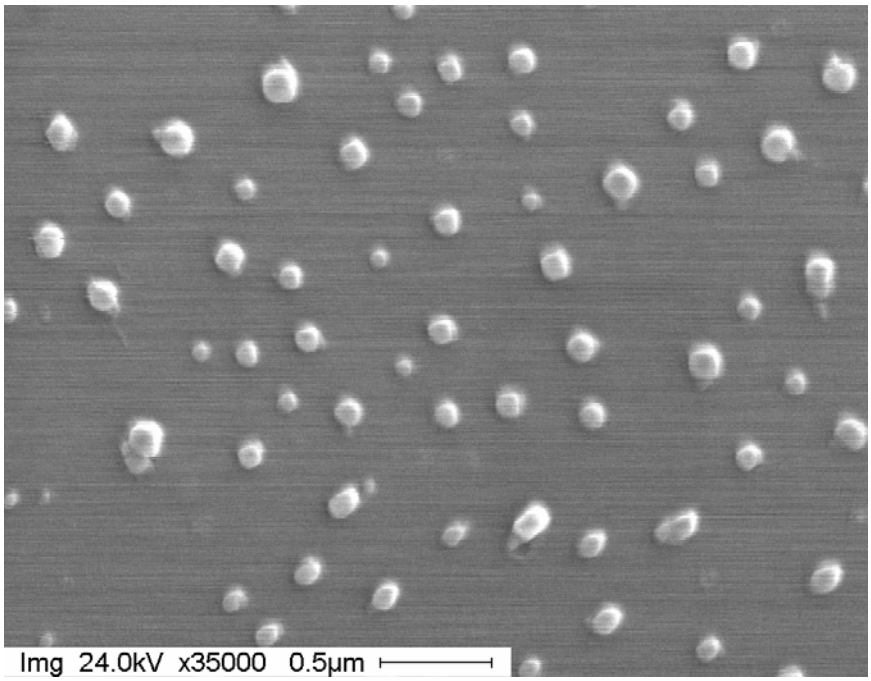

(a)

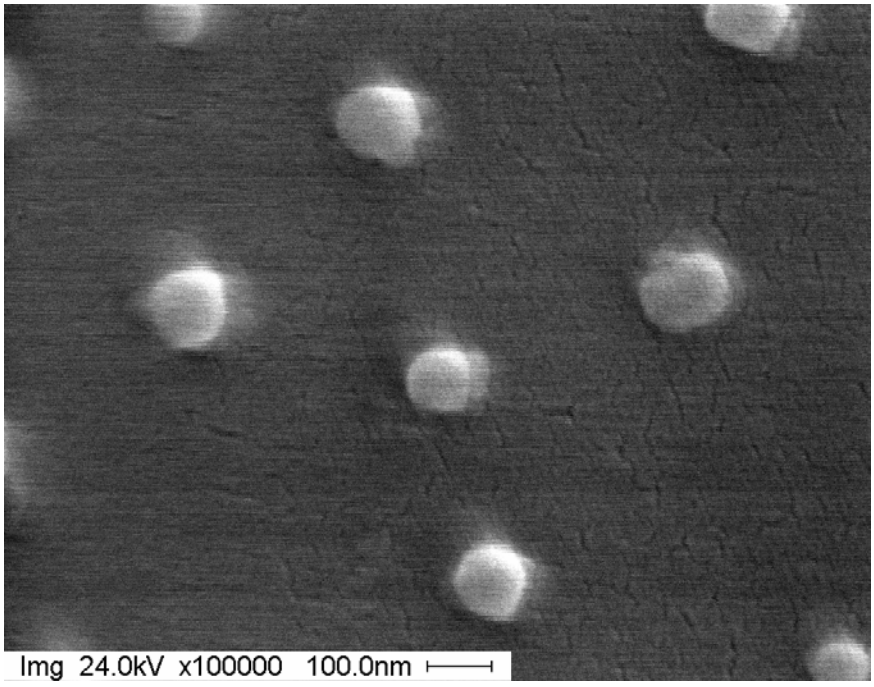

(b)

Fig. 3-7 SEM pictures for 20:1 copolymeric nanoparticles which has particle size, 60-150 nm; (a) and (b)

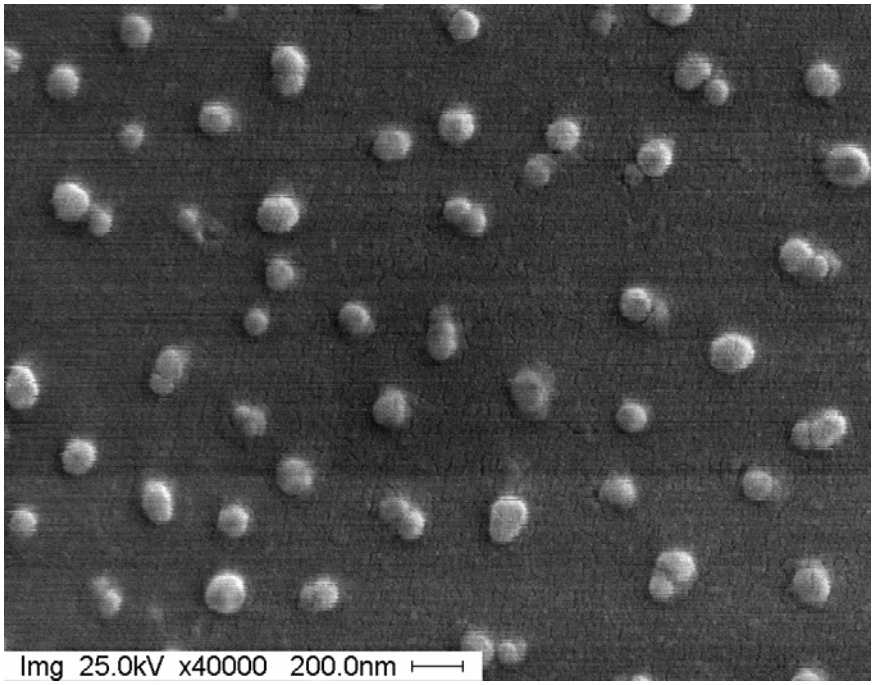

(a)

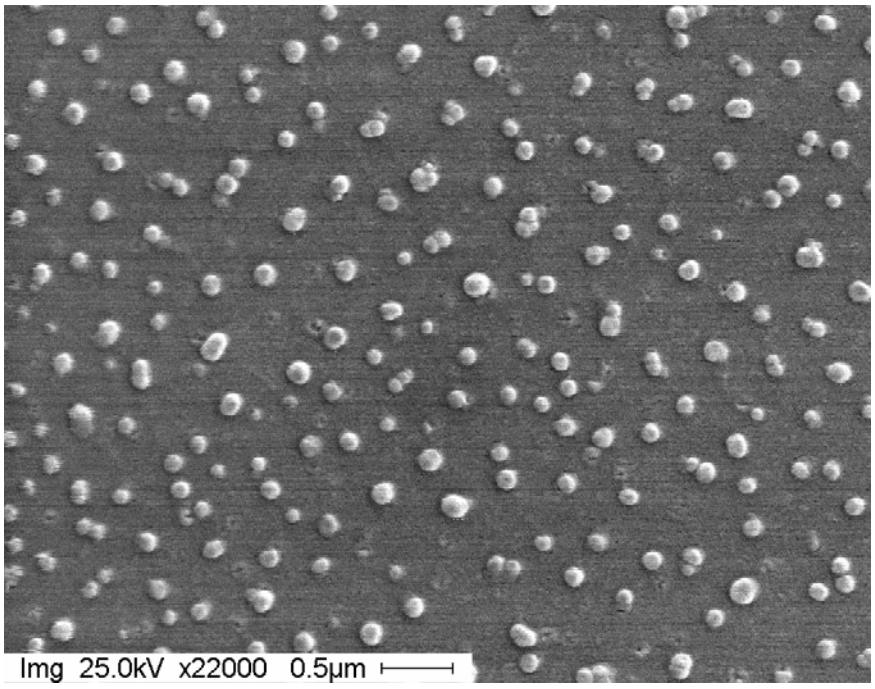

(b)

Fig. 3-8 SEM pictures for 13:1 copolymeric nanoparticles which has particle size, 60-150 nm; (a) and (b)

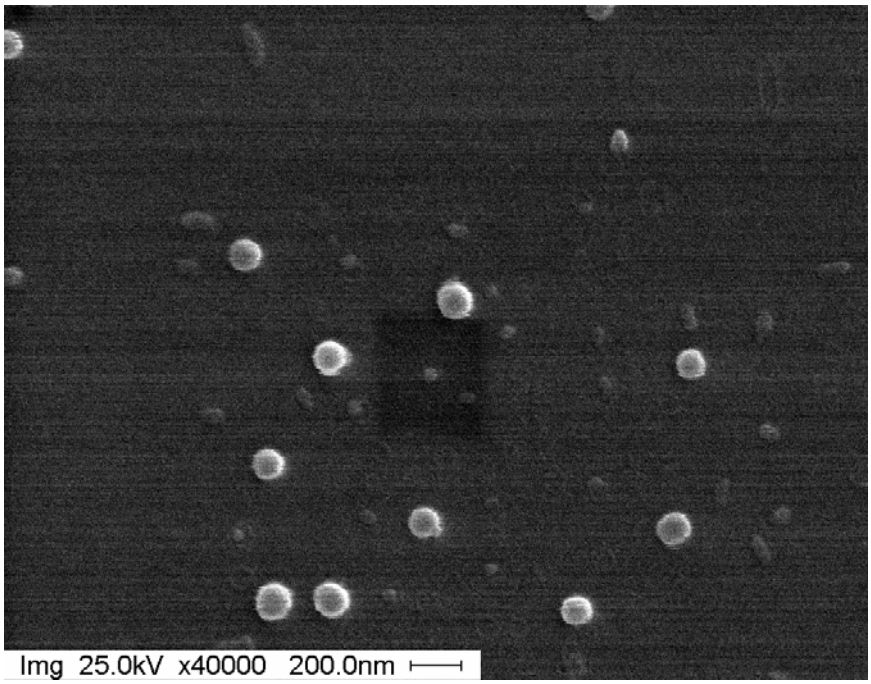

(a)

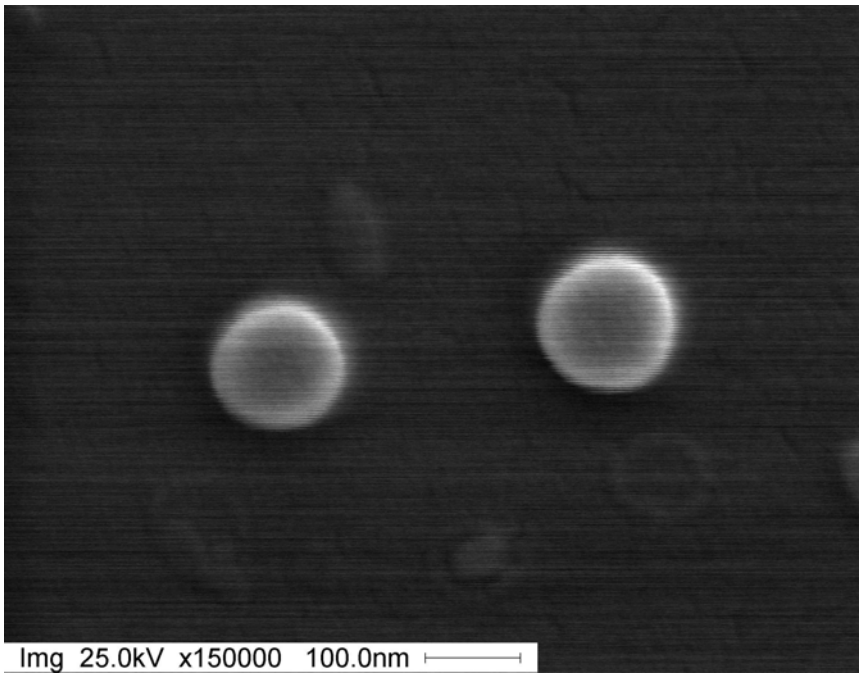

(b)

Fig. 3-9 SEM pictures for 10:1 copolymeric nanoparticles which has particle size, 100-130 nm; (a) and (b)

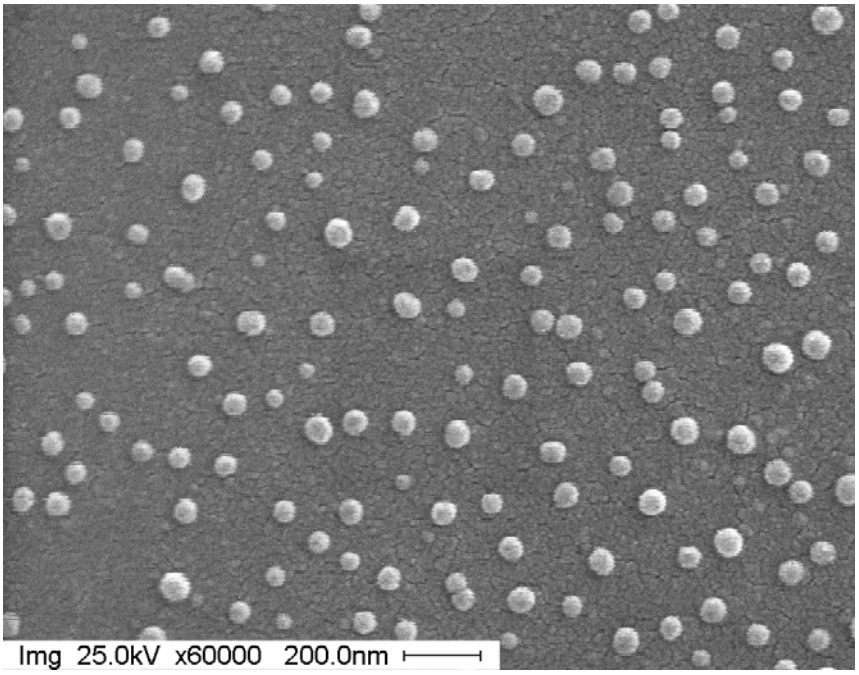

(a)

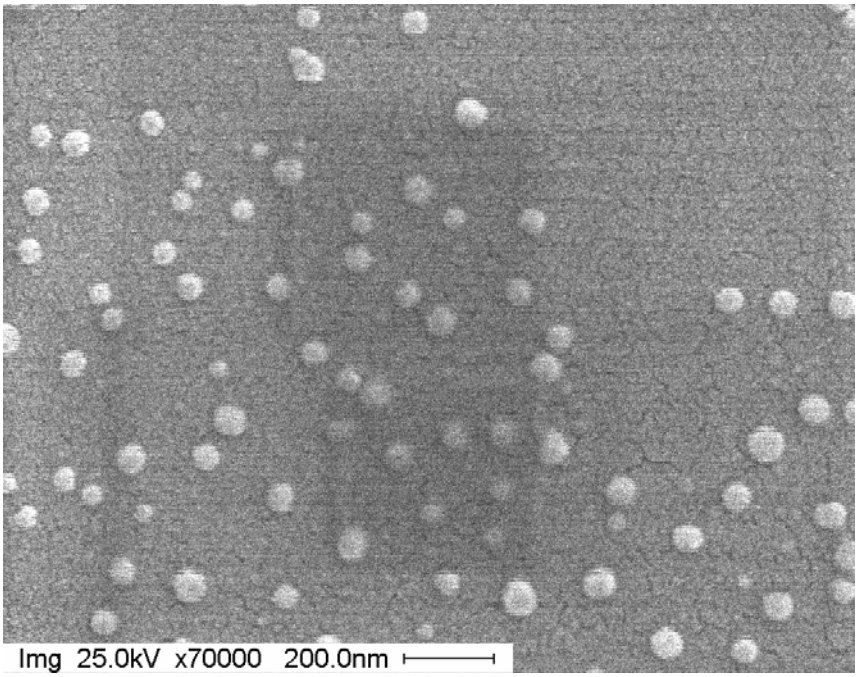

(b)

Fig. 3-10 SEM pictures for 7:1 copolymeric nanoparticles which has particle size, 40-80 nm; (a) and (b)

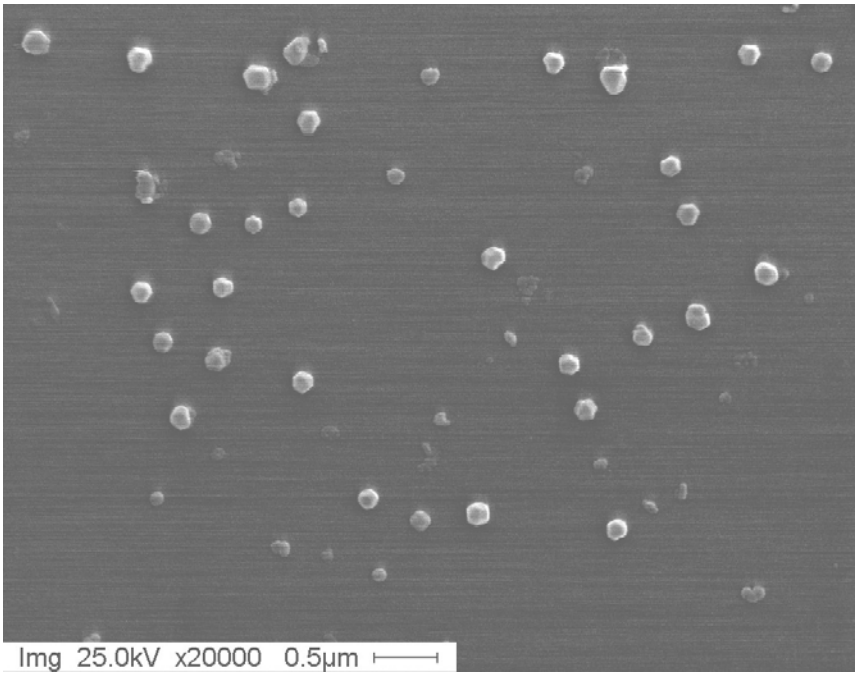

(a)

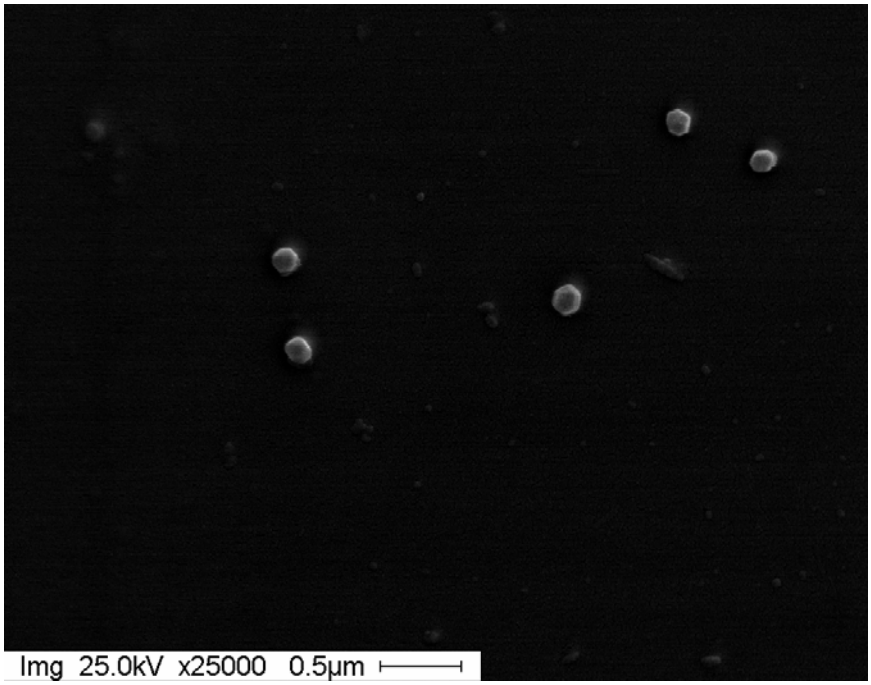

(b)

Fig. 3-11 SEM pictures for 5:1 copolymeric nanoparticles which has particle size, 130-150 nm; (a) and (b)

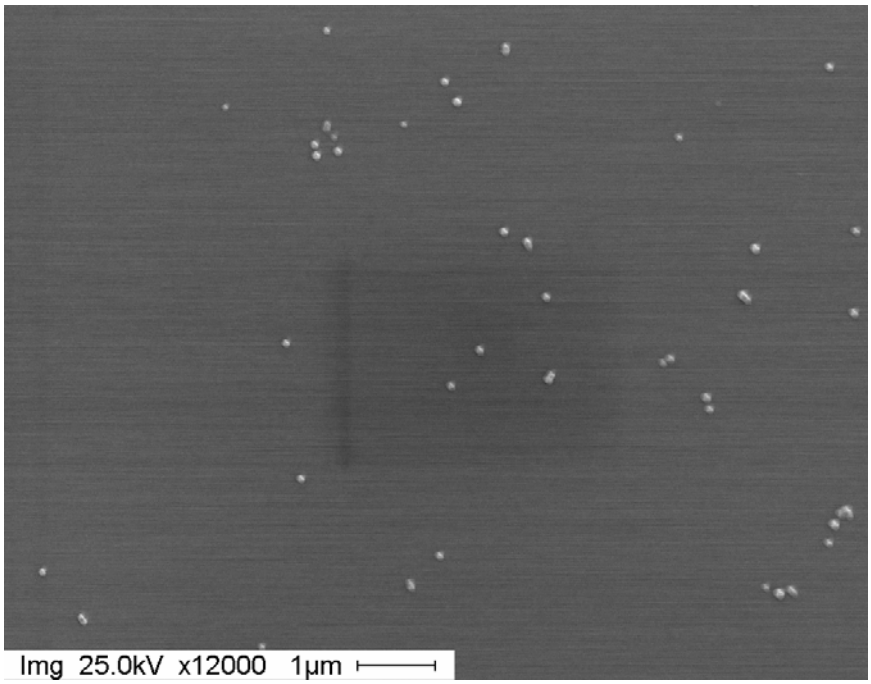

(a)

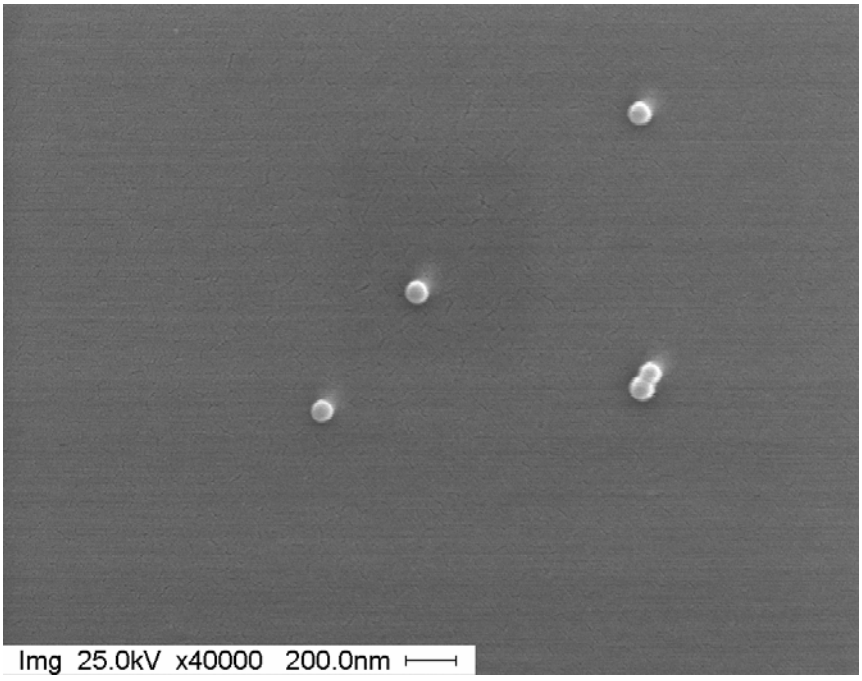

(b)

Fig 3-12. SEM pictures for 2.5:1 copolymeric nanoparticles which has particle size, 70nm; (a) and (b)

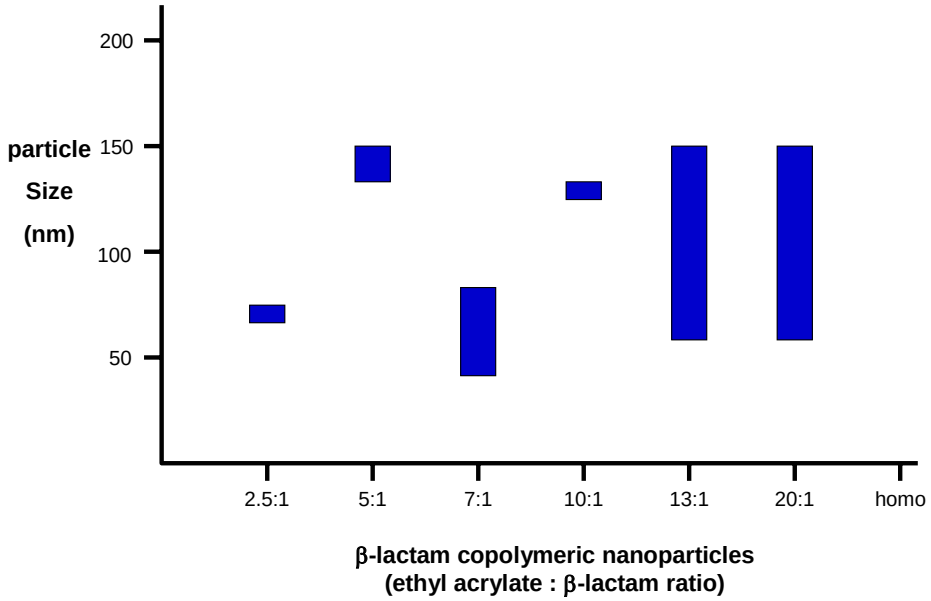

Fig. 3-13 Particle size distribution of β-lactam copolymeric nanoparticles

3.6.2 Coalescing Process [15,16]

For further characterization of β-lactam copolymeric nanoparticles, thin films were prepared by a coalescing process. The polymeric particles experience an irreversible structural change during film formation. The particles, upon evaporation of water, come into contact, fuse and form a uniform film through a process called coalescense. In general it is assumed that the film formation can be separated into the following three stages:

Stage 1: Water evaporates slowly and thus polymer particles become concentrated.

Stage 2: The particles deform to form a dense closed packing.

Stage 3: The fully coalesced particles produce a uniform film.

The coalescing process is summarized in Fig. 3-14.

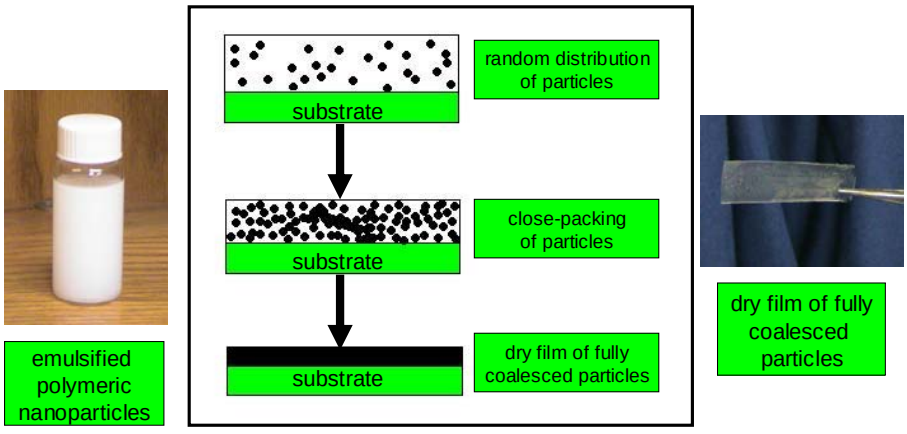

Fig. 3-14 Representation of the coalescing process [15]

3.6.3 Determination of Solid Content (%)

The measurement of the non-volatile solid (β-lactam) content in polymer is critical for determining the amount of the drug in the polymeric emulsion. The solid content is defined as the weight percent of the non-volatile solid among total weight of the emulsion. The weight percent of polymer in the emulsion can be calculated quantitatively after film formation via the coalescence process. The calculation method is described in Fig. 3-15. All solid content measurements were done in triplicate and the average value is reported.

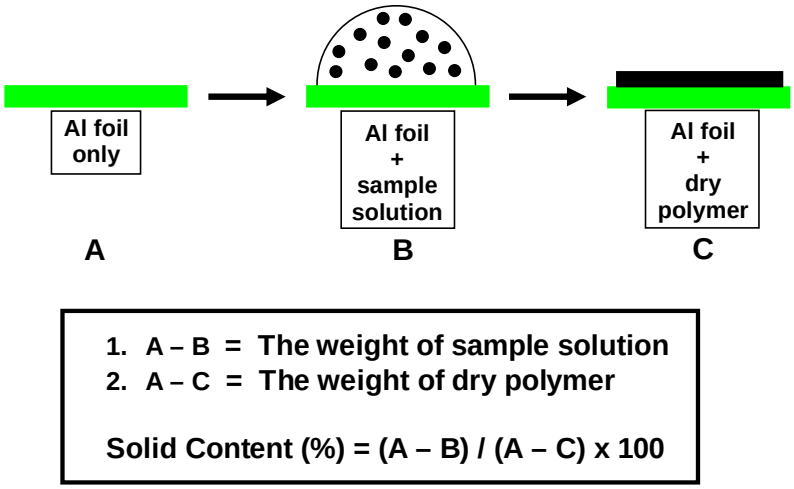

Fig. 3-15 Determination of solid content (%)

3.6.4 ^{1}H NMR Spectra Analysis

^{1}H NMR spectroscopy is a very powerful tool to analyze chemical structure of organic molecules. It can also be used to determine the mole ratio of each of the monomeric units, (β-lactam and ethyl acrylate) in copolymers. Fig. 3-16 shows the cumulated ^{1}H NMR spectra for the dry films obtained by coalescing the nanoparticle emulsions of homopoly(ethyl acrylate) and six different copolymers of the β-lactam and ethyl acrylate. Signals at (d) 2.6, (b) 5.6 and (c) 6.1 ppm are assigned to S-CH_3, C_3-H and C_4-H on β-lactam respectively. The signal at (a) 4.0 ppm is assigned to the methylene proton of ethyl acrylate. The olefin protons of acrylate in the range of 5.6-6.1 ppm do not show in the spectrum. That indicates that all of the monomeric β-lactam acrylate and ethyl acrylate was converted to polymeric particles. In addition, the composition of the polymeric nanoparticles can be determined by ^{1}H NMR spectroscopy as mentioned. The mole ratio of β-lactam and ethyl acrylate in the copolymer was determined from the peak integration of the methylene proton (**a**) of ethyl acrylate and a proton of C_3 (**b**) or C_4 (**c**) on the β-lactam respectively. Fig. 3-16 also shows the solid content of each of the polymers. The β-lactam loading amount on the each polymers can be calculated quantitatively based on these parameters, based on the mole ratio of each monomers, the loading volume and the solid content.

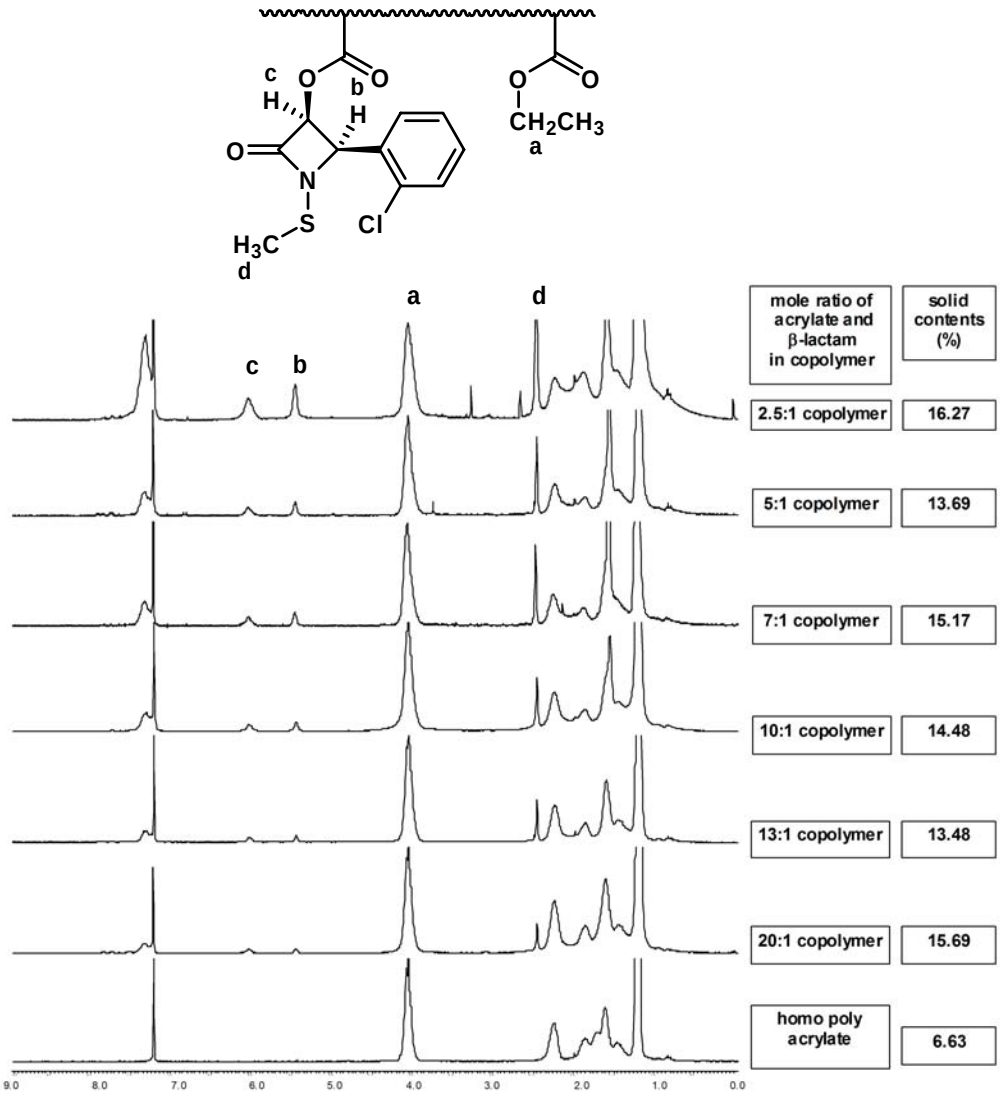

Fig. 3-16 ^{1}H NMR Spectra, the mole ratio and the solid content of β-lactam and ethyl acrylate copolymers

3.7 Biological Activity Against MRSA

3.7.1 Initial Testing

The N-methylthio β-lactam-conjugated polymeric nanoparticles and their coalesced plastic films were tested for antibacterial activity using the Kirby-Bauer method of disc diffusion on agar plates. The 7:1 (ethyl acrylate : lactam) copolymeric nanoparticles and their plastic film as well as the homo poly(ethyl acrylate) nanoparticles and their plastic film, were also tested against a strains of methicillin-resistant *Staphylococcus aureus* (MRSA). Fig. 3-17 shows the results of this testing. It is obvious that the plastic films of the 7:1 copolymer and the homo polymer, as well as the homo poly(ethyl acrylate) nanoparticles have no activity against MRSA. However, the 7:1 copolymeric nanoparticles surprisingly have strong activity against MRSA. That means the film polymers, whether they contain the drug or not, have no activity, and the nanoparticles that do not bear a drug, also have no activity. This initial result indicates that further research should be focused on nanoparticles having the attached β-lactam drug.

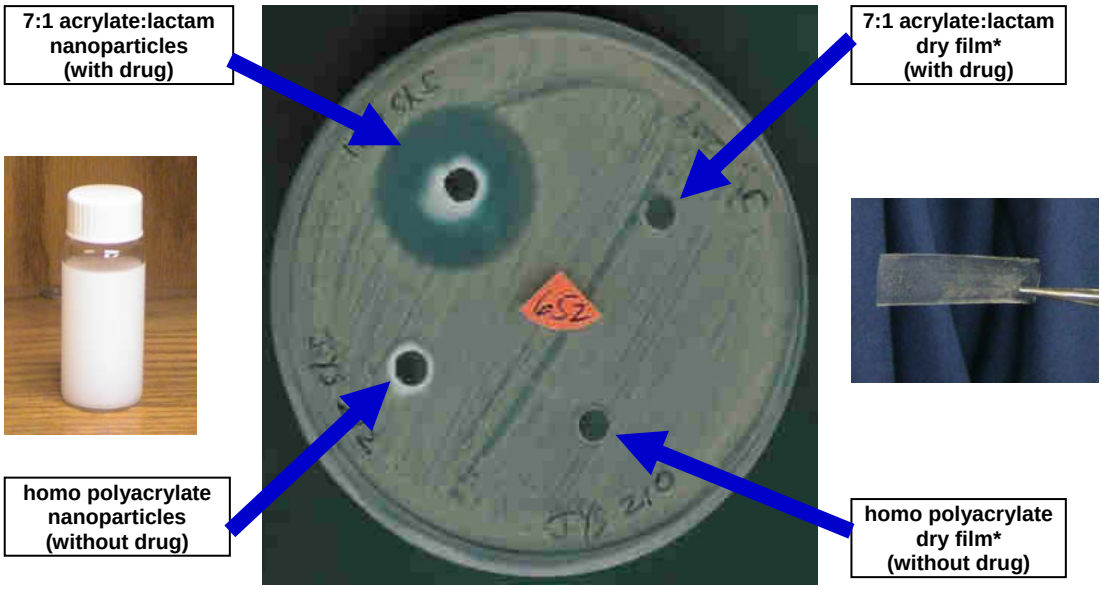

*Dry film was dissolved in DMSO for testing.

Fig. 3-17 Initial antibacterial testing of nanoparticles and polymer films against MRSA 652

3.7.2 Antibacterial Testing of Homo Poly(ethyl acrylate) Nanoparticles (Without N-Methylthio β-Lactam)

The antibacterial testing of homo poly(ethyl acrylate) nanoparticles was performed as a control experiment. A sample of the nanoparticle suspension was tested against MRSA on an agar plate, with increasing disk loading amounts from 20 μl to 100 μl. No activity was observed even at 100 μl of disk loading (Fig. 3-18). This result is consistent with that of the initial testing showing that the polymeric nanoparticle which has no drug, has no activity. Therefore, the focus next was to the test the antibacterial activity of the nanoparticles that do contain the N-methylthio β-lactam drug.

Fig. 3-18 Antibacterial testing of homo poly(ethyl acrylate) nanoparticle against MRSA

3.7.3 Antibacterial Testing of Lactam-containing Nanoparticles Against MRSA

Nanoparticles containing the N-methylthio β-lactam were evaluated for antibacterial activity against ten MRSA strains by Kirby-Bauer of disc diffusion on agar plates. Six different samples of the nanoparticle emulsions were tested, varying in the relative amounts of drug to ethyl acrylate used to prepare the particles (20:1 to 2.5:1). Table 3-2 displays the observed zones of inhibition for the nanoparticles. It is very interesting that all samples containing the N-methylthio β-lactam are active against the MRSA strains as well as the non-resistant strain of *S. aureus*. In addition, the strongest bioactivity was observed for the 7:1 (acrylate:lactam) nanoparticles, which have the smallest particle size distribution, 40-80 nm. Therefore, these facts

indicate that research should be focused on the biological mode of action of these conjugated nanoparticles, and the relationship of particle size to biological activity. The images of the agar plates used to test against MRSA and *S. aureus* are displayed in Fig. 3-19 through Fig. 3-29.

Table III-2. Zones of inhibition obtained from agar well diffusion experiments using 20 μl of the emulsified suspension of the test nanoparticles. The values correspond to the diameters in mm for the zone of growth inhibition appearing around the well after 24 hours. *Staphylococcus aureus* and β-lactamase-producing strains of methicillin-resistant *Staphylococcus aureus* (labeled MRSA USF652-659) were obtained from a clinical testing laboratory at Lakeland Regional Medical Center, Lakeland, FL or from ATCC sources.

	nanoparticles having monomer ratio of EA* : β-lactam						
strains	homo EA	20 : 1	15 : 1	10 : 1	7 : 1	5 : 1	2.5 : 1
MRSA 652	0	14	11	18	23	16	17
653	0	15	13	24	28	24	24
654	0	14	12	15	23	17	16
655	0	0	11	18	22	17	15
656	0	12	15	18	23	17	18
657	0	12	12	18	24	17	16
658	0	0	12	17	24	18	16
659	0	0	14	16	22	17	17
919	0	0	11	17	22	17	17
920	0	0	12	16	23	18	16
S. aureus 849	0	13	16	18	24	20	19

* ethyl acrylate (EA)

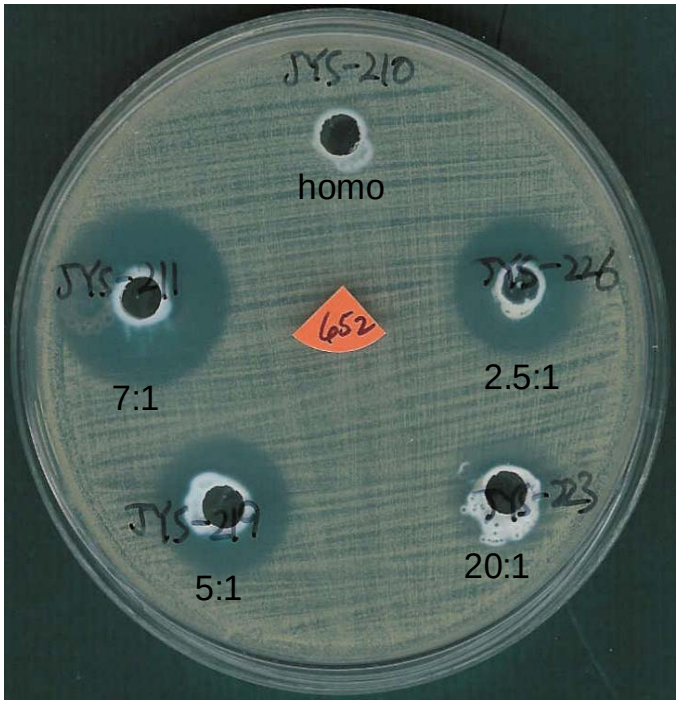

Fig. 3-19 Antibacterial testing of drug-embedded nanoparticles against MRSA 652 (ratios of ethyl acrylate : lactam indicated)

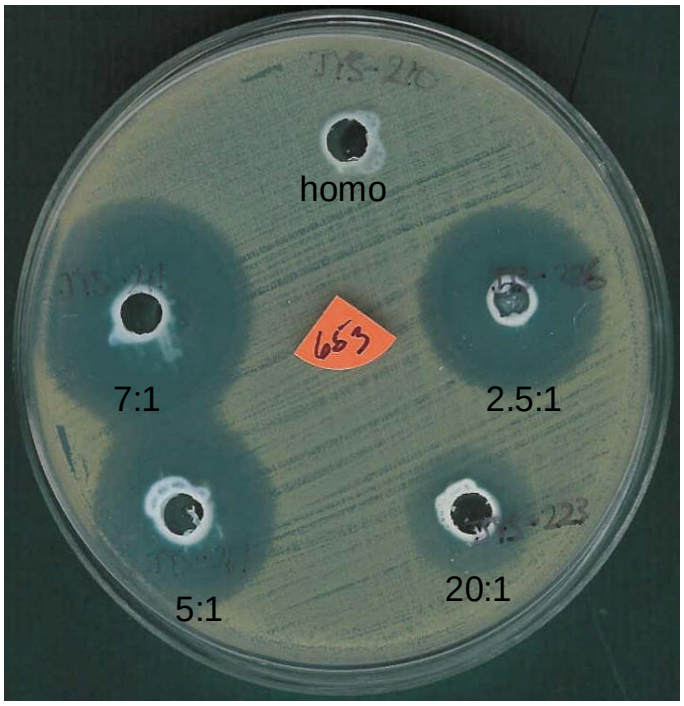

Fig. 3-20 Antibacterial testing of drug-embedded nanoparticles against MRSA 653 (ratios of ethyl acrylate : lactam indicated)

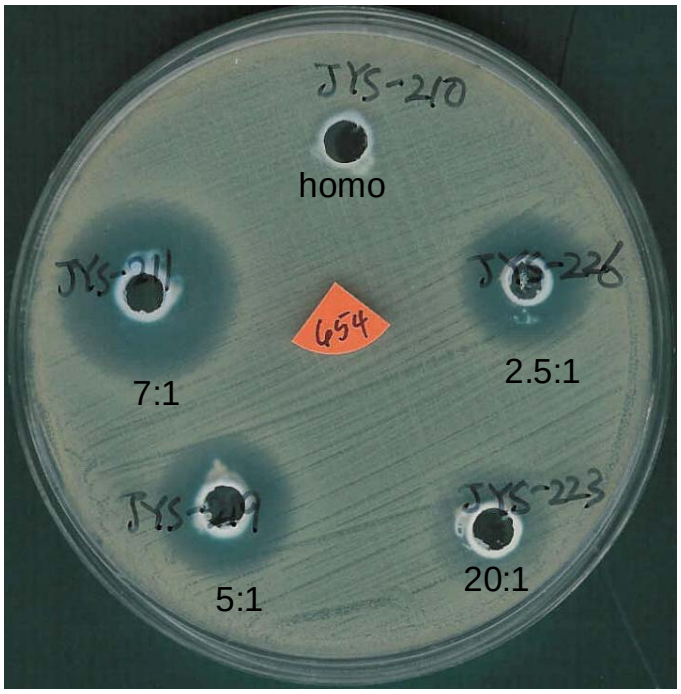

Fig. 3-21 Antibacterial testing of drug-embedded nanoparticles against MRSA 654 (ratios of ethyl acrylate : lactam indicated)

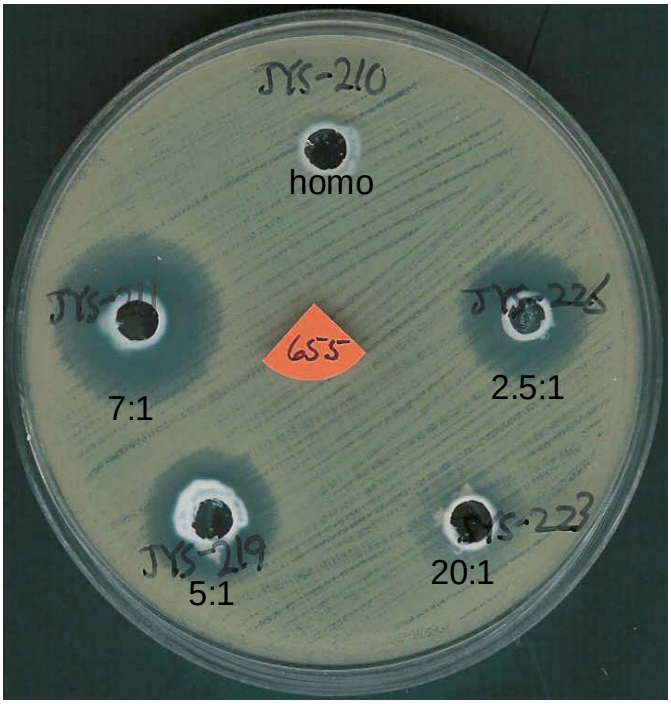

Fig. 3-22 Antibacterial testing of drug-embedded nanoparticles against MRSA 655 (ratios of ethyl acrylate : lactam indicated)

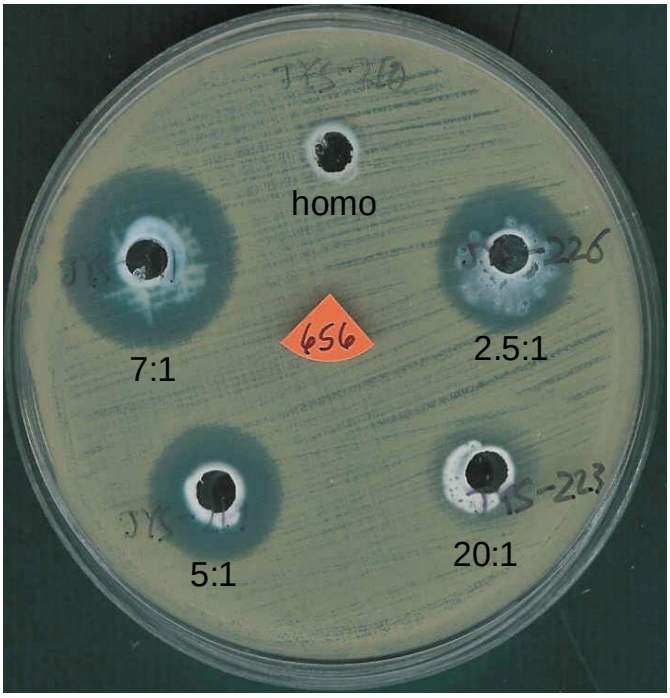

Fig. 3-23 Antibacterial testing of drug-embedded nanoparticles against MRSA 656 (ratios of ethyl acrylate : lactam indicated)

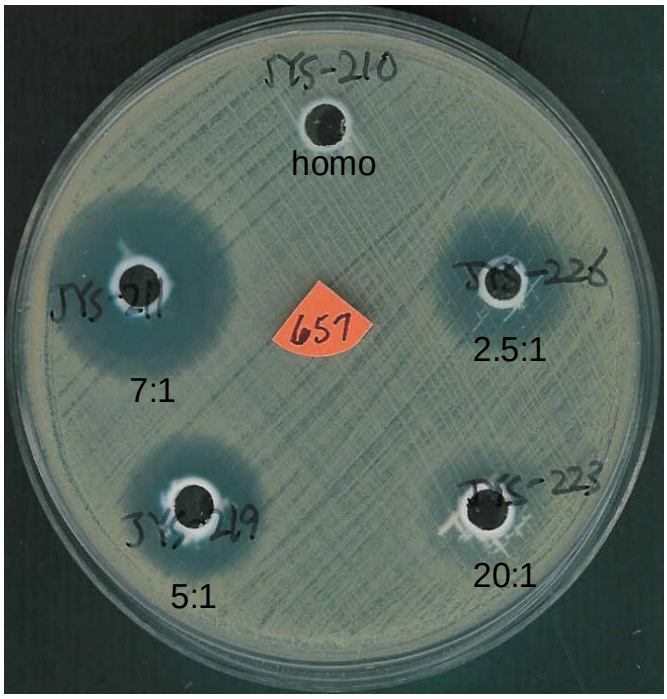

Fig. 3-24 Antibacterial testing of drug-embedded nanoparticles against MRSA 657 (ratios of ethyl acrylate : lactam indicated)

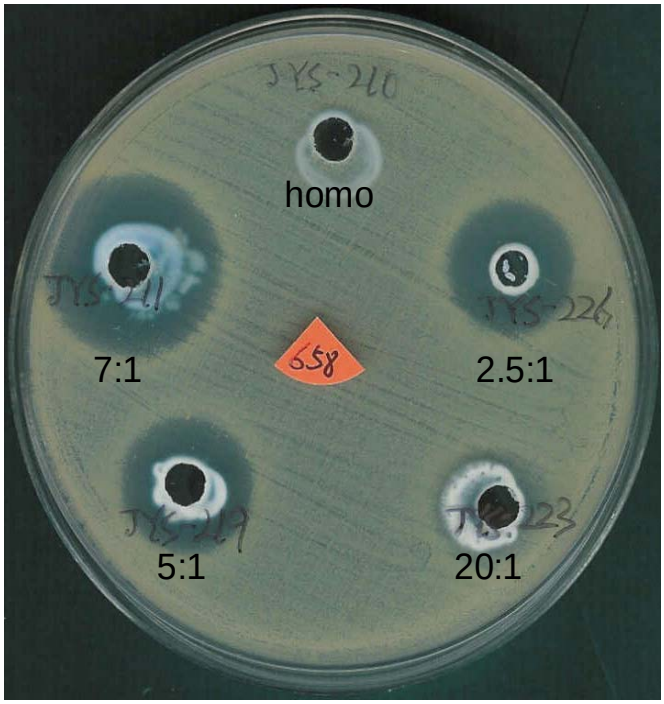

Fig. 3-25 Antibacterial testing of drug-embedded nanoparticles against MRSA 658 (ratios of ethyl acrylate : lactam indicated)

Fig. 3-26 Antibacterial testing of drug-embedded nanoparticles against MRSA 659 (ratios of ethyl acrylate : lactam indicated)

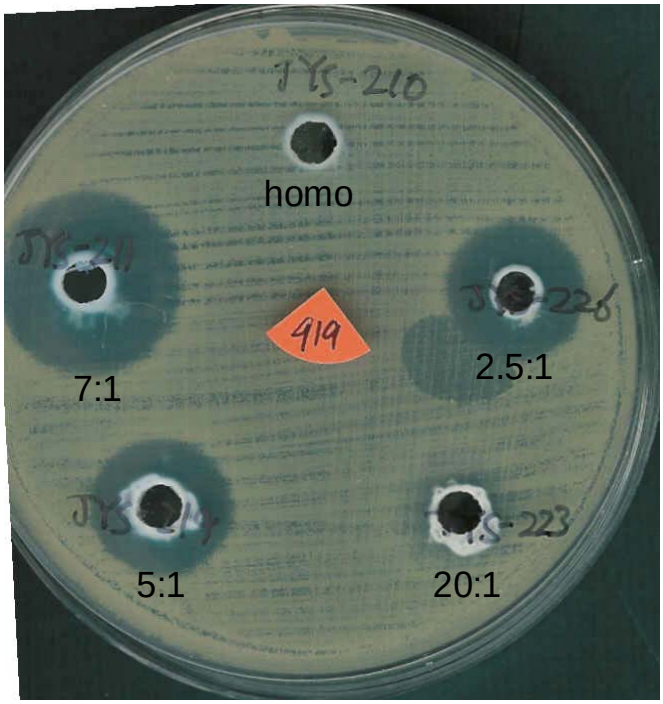

Fig. 3-27 Antibacterial testing of drug-embedded nanoparticles against MRSA 919 (ratios of ethyl acrylate : lactam indicated)

Fig. 3-28 Antibacterial testing of drug-embedded nanoparticles against MRSA 920 (ratios of ethyl acrylate : lactam indicated)

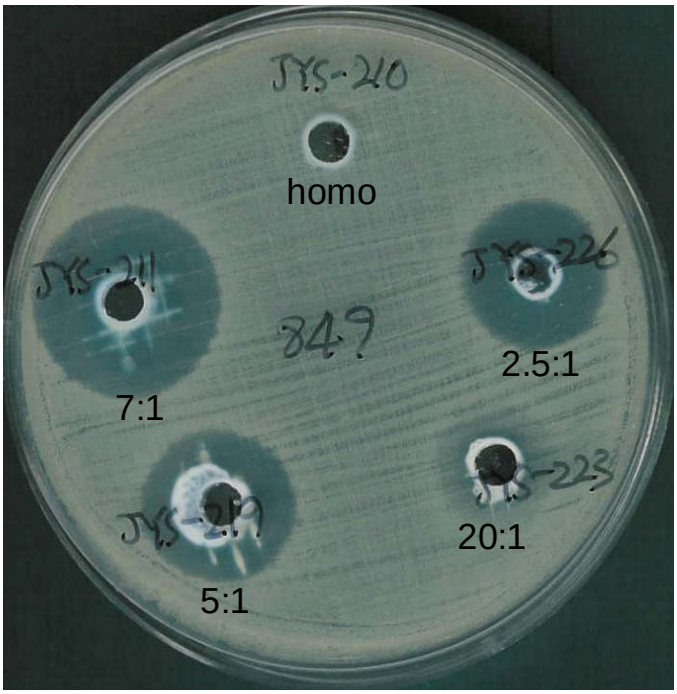

Fig. 3-29 Antibacterial testing of drug-embedded nanoparticles against *S. aureus* 849 (ratios of ethyl acrylate : lactam indicated)

3.8 Antifungal Testing of Nanoparticle Emulsions

In the previous section the 7:1 (acrylate:drug) nanoparticles showed the most promising antibacterial activity against MRSA strains. Thus, it is very meaningful to extend the testing of these emulsions to fungus, because N-methylthio β-lactams have previously been found (Marci Culbreath, unpublished results) to have activity against fungal strains. The antifungal testing of these nanoparticles was performed by Kirby-Bauer disc diffusion on agar plates against eight genera of fungi. Table 3-4 displays the zones of inhibition observed nanoparticles. It is very interesting that nanoparticles are very active against all of the fungal strains, with antifungal activity of the N-thiolated lactam (1 μg) in the nanoparticles being similar to that of the standard,

clotrimazole (50 μg). That means the 7:1 (acrylate:lactam) nanoparticles are fifty times more potent than clotrimazole. This indicates that drug containing nanoparticles are promising leads to new antifungal agents as well as an antibacterial antibiotics.

Table III-4. Zones of inhibition obtained from agar well diffusion experiments using 20 ml of 7:1 (ethyl acrylate:lactam) nanoparticle emulsion. This corresponds to 1 mg of active drug in the particle. The values correspond to the diameters in mm for the zone of growth inhibition appearing around the well after 48 hours.

fungal strains*	nanoparticles				standard clotrimazole (50 μg)
	1st	2nd	3rd	average	
C. albicans	26			26	20
C. tropicalis	20	24		22	20
C. glabrata	19	20	16	18	14
C. kefyr	21	23	20	21	37
C. krusei	24	27	29	27	27
C. lusitaniae	31	32	32	32	25
C. parapsilosis	19	20	22	20	32
C. utilis	22	23	23	23	24

* Fungi were chosen on the basis of their potential pathogenicity. *C. albicans* and *C. tropicalis* were donated by Dr. Ray Widen from the University of South Florida, School of Medicine. *C. glabrata* (ATCC 15126), *C. krusei* (ATCC 14243), *C. keyfr* (ATCC 20409), *C. parapsilosis* (ATCC 22019), *C. lusitaniae* (ATCC 34449) and *C. utilis* (ATCC 29950) were obtained commercially.

3.9 Discussion

Nanoparticles comprised of poly(ethyl acrylate) were made by a novel microemulsion polymerization procedure. This method has the advantage over conventional emulsion polymerization methods because a solid co-monomer (β-lactam drug) is utilized. This method may open a new area in drug delivery and help to solve the main problems in drug discovery: unwanted cytotoxicity, water insolubility and low bioavailability of drug. The core feature of this method, as mentioned in section 3.5, is to make a homogeneous solution of monomeric substances at elevated temperature (60 ^{o}C or 70 ^{o}C) and to disperse this mixture in aqueous media containing a suitable surfactant (to stabilize the nanoparticles). Radical polymerization within these pre-formed particles then ensues to make the nanospherical polymers.

A water-insoluble solid antibiotic, N-methylthio β-lactam, was synthetically converted to a C_3-acryloyl β-lactam derivative and its homogenized into a liquid state with ethyl acrylate as a co-monomer was generated at 70 ^{o}C. The N-methylthio β-lactam-containing nanoparticles were then prepared by free radical microemulsion polymerization after dispersing in an aqueous phase. Thus, it was demonstrated that the N-methylthio β-lactam could be incorpoated as a monomer to generate a new N-methylthio β-lactam-containing nanoparticle. It is likely that this new method can be applied to many other water-insoluble solid drugs (or those having high viscosity).

The N-methylthio β-lactam-containing nanoparticles were subjected to antibacterial testing against various MRSA strains. Fig. 3-30 displays a comparison of

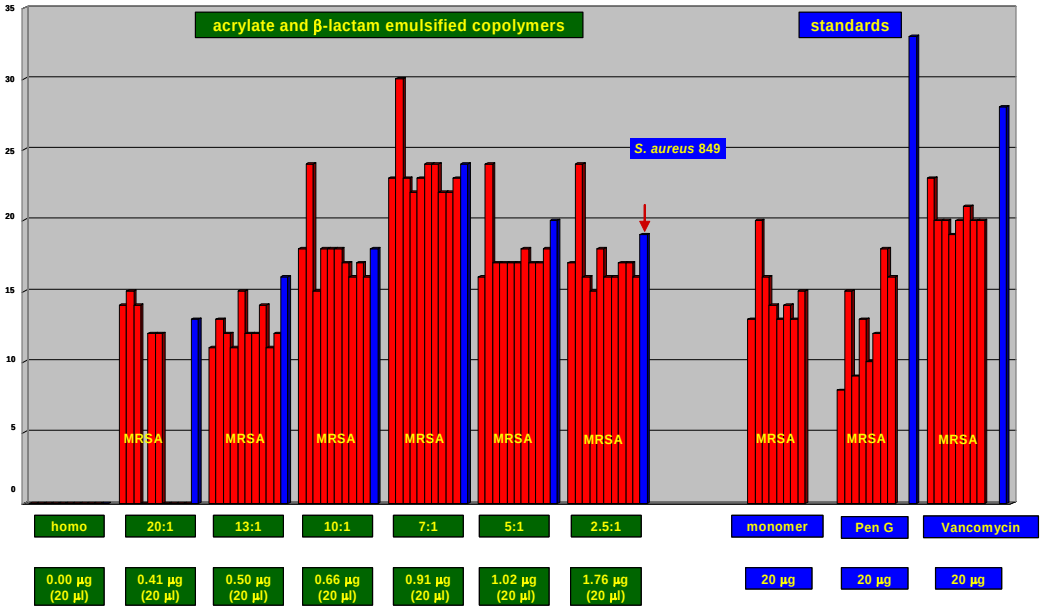

Fig. 3-30 Comparison of antibacterial activities of N-thiolated β-lactam-containing emulsified nanoparticles.

antibacterial activities for each of the different emulsified nanoparticles to penicillin G (Pen. G), vancomycin, and C_3-acryloyl β-lactam **27** as standards. It also shows the actual amounts of drug contained within 20 μl of the nanoparticle emulsion tested.

It is apparent that all N-methylthio β-lactam containing nanoparticles are active against MRSA strains as well as the non-resistant strain, *S. aureus* 849. Their activity trend appears to increase gradually as the portion of drug (β-lactam) increase from 20:1 (ethyl acrylate:antibiotic)to the 7:1 and reachs the maximum at the 7:1. However, the bioactivity decreased for particles having an ethyl acrylate:lactam ratio of 5:1, and the activities of the 5:1 and 2.5:1 nanoparticles are similar even though the portion of drug (β-lactam) is increased. Therefore, the result indicates that the antibacterial performance of N-methylthio β-lactam containing nanoparticles is enhanced dramatically over that of the free antibiotic, and the 7:1 (ethyl acrylate:lactam) nanoparticles show the best activity.

The comparison of antibacterial activity of the N-methylthio β-lactam containing emulsified nanoparticles and the standards: penicillin G (Pen. G), vancomycin, and C_3-acryloyl β-lactam **27** against MRSA, shows that the emulsified nanoparticles have similar and/or better activities at very low drug amount compared with those of standards. However, the activity of 7:1 (ethyl acrylate:lactam) nanoparticles are better even at low drug amount (0.91 μg) compared with that of vancomycin (20 μg). It is likely that the activity of the 7:1 nanoparticles is over 20 times more than that of vancomycin.

Fig. 3-31 and Fig. 3-32 display a comparison of the antibacterial activities of the 2.5:1, 5:1, 7:1 and 10:1 (ethyl acrylate:lactam) nanoparticles against MRSA and non-resistant *S. aureus* with decreasing sample loading volume (20 μl to 12 μl). The amount of sample was proportional to the bioactivity. However, the N-methylthio β-lactam containing nanoparticles still possess good activities even at 12 μl of loading volume. Most notably the 7:1 copolymeric nanoparticles still show the strongest activity.

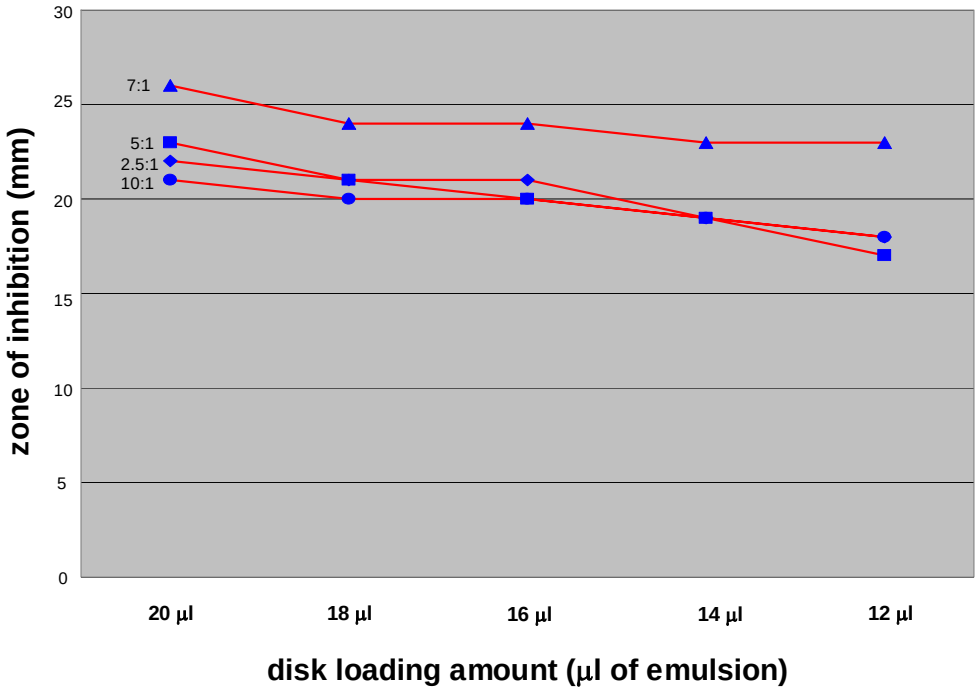

Fig. 3-31 Bioactivity of polymeric nanoparticles as a function of disk loading amounts (MRSA 653)

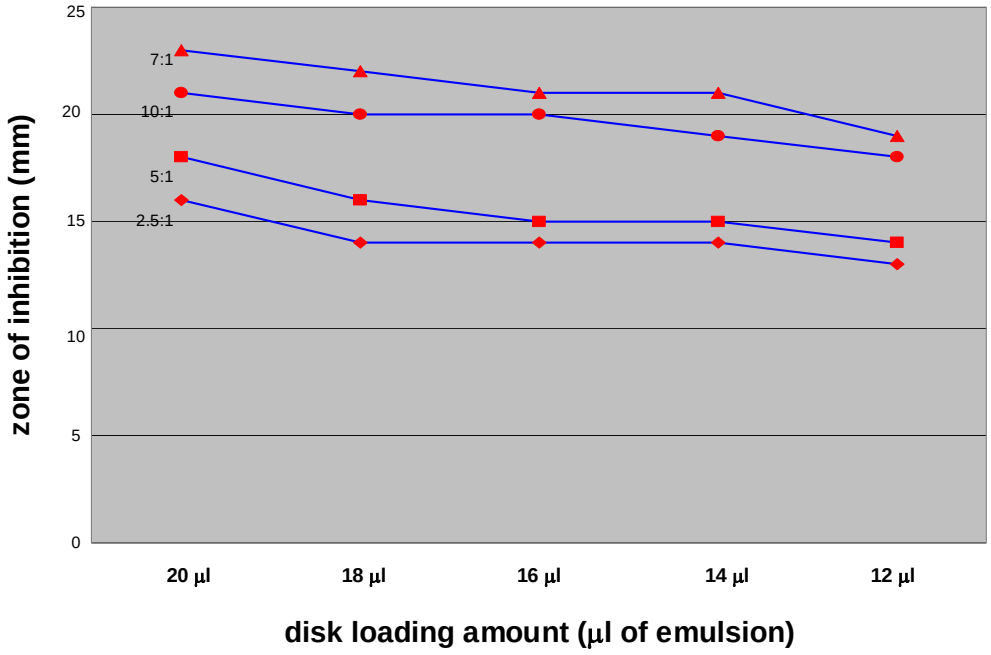

Fig. 3-32 Bioactivity of polymeric nanoparticles as a function of disk loading amounts for *S. aureus* 849

Fig. 3-33 displays antibacterial activity of the 7:1 nanoparticles as the sample loading volume is decreased from 20 µl to 2 µl against MRSA and *S. aureus*. Surprisingly, the activity of the 7:1 nanoparticles for MRSA maintained a strong level of potency (over 20 mm zone of inhibition) until the volume was reduced to 6 µl (0.27 µg) and even at 2 µl (0.09 µg, 14 mm in the zone of inhibition). In addition, against *S. aureus* the particles also show a good level of antibiotic activity until the loading amount is reduced to 6 µl (0.27 µg, 16 mm zone of inhibition).

The relative antibacterial activities for 7:1 (ethyl acrylate:lactam) nanoparticles, Pen G, vancomycin, and C_3-acryloyl N-methylthio β-lactam **27** were also evaluated at

1 μg since 20 μl of volume for the 7:1 nanoparticles contains approximately 1 μg of β-lactam.

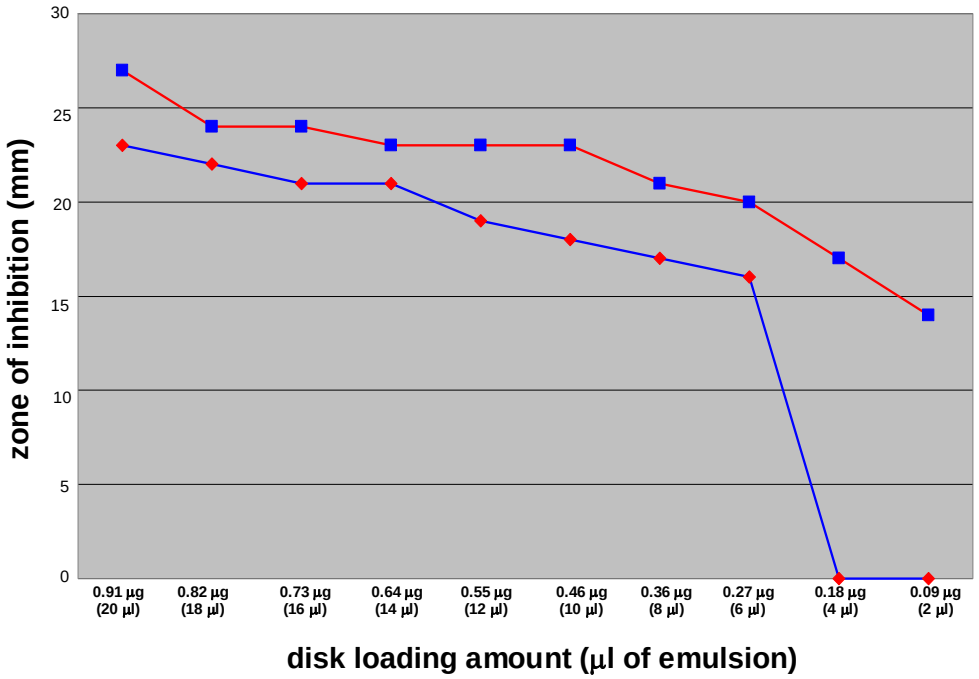

Fig. 3-33 Bioactivity of 7:1 copolymeric nanoparticles as a function of decreasing disk loading amounts

Fig. 3-33 shows a comparison of relative antibacterial activities against MRSA. It is obvious that Pen G and C_3-acryloyl N-methylthio β-lactam have no activity and vancomycin is very weak at 1 μg of drug amount level. However, the 7:1 (ethyl acrylate:lactam) nanoparticles show very strong activity.

Therefore, it is a natural question to ask why the N-methylthio β-lactam-containing nanoparticles have such enhanced antibacterial activities even at very low concentrations.

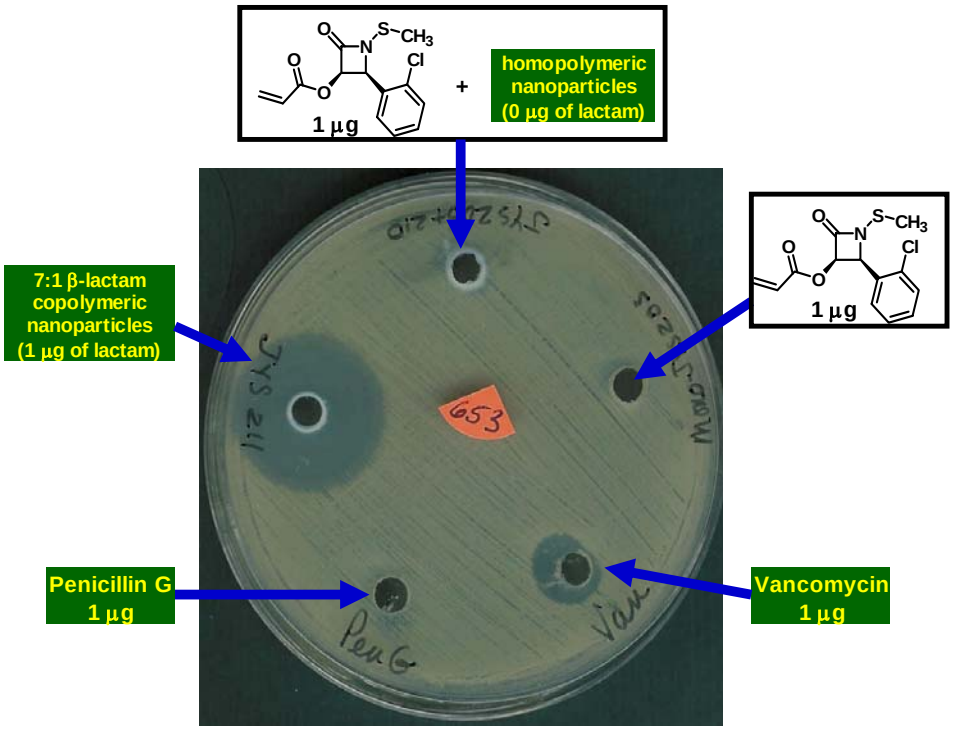

Fig. 3-34 Comparison of antibacterial activities against MRSA 653

Though the mode of antibacterial action of these nanoparticles is unknown, one possible answer is that N-methylthio β-lactam-containing nanoparticles have nano-size diameters (40–150 nm) and can easily penetrate into the bacteria cell through a process called endocytosis, and thus, the bioavailability of the antibiotic can be dramatically increased. Fig. 3-33 shows an example of the endocytosis process for a polymer drug. To study this proposed mechanism, the relationship between particle size and bioactivity, as well as the preparation of fluorescence probe containing nanoparticles, are the subject of our current investigations.

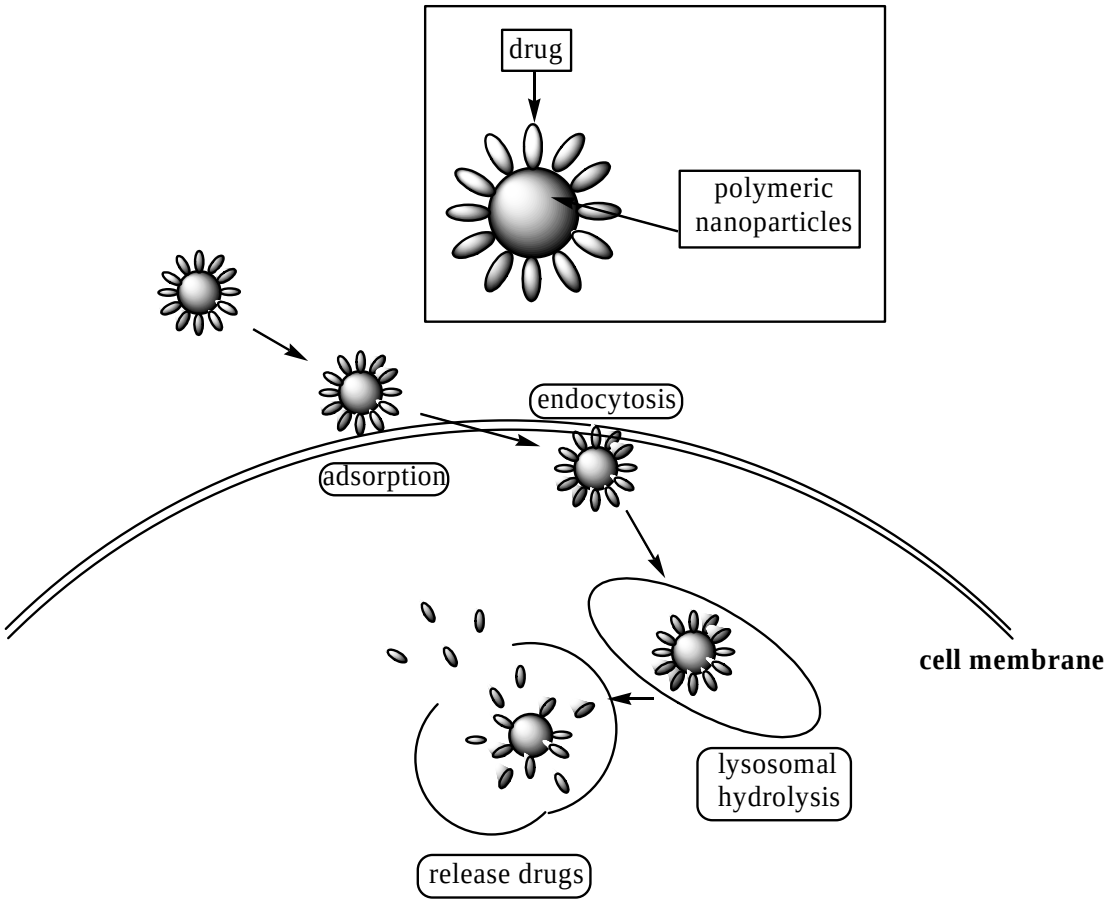

Fig. 3-35 Proposed mechanism of drug delivery by endocytosis[13]

3-10 Conclusions

N-Methylthio β-lactam containing nanoparticles were prepared by a novel nanoemulsion polymerization technique with ethyl acrylate as a co-monomer. This method has advantages over the conventional emulsion polymerization methods because a solid co-monomer (β-lactam drug) can be utilized.

SEM studies show that the polymeric nanoparticles have a microspherical morphology with particle sizes of 40-150 nm, and the 7:1 copolymeric nanoparticles have the smallest particle sizes (40-80 nm). The *N*-thiolated β-lactam containing

nanoparticles display potent anti-MRSA activity at low drug amount compared with penicillin G and vancomycin. The strongest bioactivity was observed in the 7:1 (ethyl acrylate:lactam) nanoparticles, which correlates with it having the smallest particle size (40-80 nm). Although at this time, the relationship between particle size and activity is not clear and the mode of action is unknown, the *N*-thiolated β-lactam containing nanoparticles dramatically enhance bioactivity, possibly due to increased bioavailability of the antibiotic via endocytosis. Further examination of this proposed mechanism is the subject of our current investigations.

3.11 Experimental

All reagents were purchased from Sigma-Aldrich Chemical Company and used without further purification. Solvents were obtained from Fisher Scientific Company. Thin layer chromatography (TLC) was carried out using EM Reagent plates with a fluorescence indicator (SiO_2-60, F-254). Products were purified by flash chromatography using J.T. Baker flash chromatography silica gel (40 μm). NMR spectra were recorded in $CDCl_3$ unless otherwise noted. ^{13}C NMR spectra were proton broad-band decoupled.

Procedure for the Synthesis of *N*-(4-Methoxyphenyl)-(2-chlorophenyl)imine (22). To a solution of *p*-anisidine (9.64 g, 78 mmol) in 25 ml of CH_2Cl_2 was added 2-chlorobenzaldehyde **21** (10.50 g, 64 mmol) and a catalytic amount of camphor-sulfonic acid. The resultant mixture was stirred until TLC indicated the disappearance

of starting materials. The solvent was removed under reduced pressure, and the crude material was purified by recrystallization from methanol to yield 15.56 g (89%) of **22** as a yellow solid. mp 56-57 °C. ^{1}H NMR (250 MHz) δ 8.95 (s, 1H), 8.25 (m, 1H), 7.43-7.35 (m, 3H), 7.29 (d, *J* = 8.6 Hz, 2H), 6.96 (d, *J* = 8.6 Hz, 2H), 3.85 (s, 3H). ^{13}C NMR (63 MHz) δ 158.6, 154.6, 144.5, 135.7, 133.4, 131.7, 129.8, 128.3, 127.0, 122.5, 114.3, 55.4.

Procedure for the Synthesis of 3-Acetoxy-*N*-(4-methoxyphenyl)-4-(2-chlorophenyl)-2-azetidinone (23).

To a stirred solution of *N*-(4-methoxyphenyl)-(2-chlorophenyl)imine **22** (17.00 g, 69.15 mmol) and triethylamine (26.8 g, 36 ml, 207.6 mmol) was added a solution of acetoxyacetyl chloride (9.76 g, 7.69 ml, 90.0 mmol) in methylene chloride (30 ml) dropwise over 10 minutes. The resultant mixture was stirred at rt until TLC indicated the disappearance of starting material. The solvent was removed under reduced pressure, and the crude material was purified by washing with ice-cold methanol to give 19.48 g (86%) of **23** as white solid, mp 130-132 ^{o}C. ^{1}H NMR (250 MHz) δ 7.43 (d, *J* = 7.8 Hz), 7.29-7.24 (m, 5H), 6.83 (d, *J* = 8.3 Hz, 2H), 6.16 (d, *J* = 4.6 Hz, 1H), 5.78 (d, *J* = 4.6 Hz, 1H), 3.76 (s, 3H), 1.76 (s, 3H). ^{13}C NMR (63 MHz) δ 168.7, 161.4, 156.7, 133.8, 130.2, 130.0, 129.8, 128.7, 126.8, 118.6, 114.5, 75.4, 58.2, 55.4, 19.9.

Procedure for the Synthesis of 3-Hydroxy-*N*-(4-methoxyphenyl)-4-(2-chloro phenyl)-2-azetidinone (24).

To a solution of β-lactam **23** (8.00 g, 23.1 mmol) in 50 ml of acetone was added KOH (1.30 g, 23.1 mmol) in 20 ml of methanol at 0^{o}C. The resultant mixture was stirred for 5

minutes, and 50 ml of water was added. The product was precipitated and isolated by filtration to yield 6.8 g (96%) of **24** as a white solid, mp 178-180 ^{o}C. ^{1}H NMR (250 MHz) δ 7.48 (d, J = 7.3 Hz, 1H), 7.34-7.24 (m, 5H), 6.85 (d, *J* = 9.0 Hz, 2H), 5.63 (d, *J* = 5.1 Hz, 1H), 5.34 (d, *J* = 5.1 Hz, 1H), 3.78 (s, 3H), 1.74 (bs, 1H). ^{13}C NMR (63 MHz, DMSO-d_6), δ 166.6, 156.1, 133.1, 132.9, 131.0, 129.8, 129.6, 128.9, 127.4, 118.6, 115.0, 77.2, 60.0, 55.7.

Procedure for the Synthesis of 3-acryloyl-*N*-(4-methoxyphenyl)-4-(2-chlorophenyl)-2-azetidinone (**25**).

To a solution of C_3-hydroxy β-lactam **24** (5.80 g, 19.1 mmol) in 30 ml of freshly distilled CH_2Cl_2 was added NaH (60% suspension in mineral oil, 0.83 g, 21.0 mmol), and the mixture was stirred for 15 min at room temperature. Acryloyl chloride (2.59 g, 28.64 mmol) was then added dropwise and the resultant mixture was stirred until TLC indicated the disappearance of starting material. The reaction was quenched with a 5% solution of NH_4Cl and extracted (3x20 ml) with CH_2Cl_2. The combined organic layers were dried over anhydrous $MgSO_4$ and purified with column chromatography on silica gel (1:4, EtOAc:hexanes) to give 4.92 g (72 %) of **25** as a white solid, mp 99-100 °C. ^{1}H NMR (250 MHz) δ 7.33 (d, J = 7.9 Hz, 1H), 7.23-7.10 (m, 5H), 6.75 (d, *J* = 8.9 Hz, 2H), 6.17 (d, *J* = 5.0 Hz, 1H), 5.98 (dd, *J* = 16.9, 1.00 Hz, 1H), 5.74 (dd, *J* = 16.9, 10.4 Hz, 1H), 5.69 (d, *J* = 5.0 Hz, 1H), 5.59 (d, *J* = 10.4, 1.0 Hz, 1H), 3.66 (s, 3H). ^{13}C NMR (63 MHz) δ 163.6, 161.2, 156.6, 133.7, 132.3, 130.3, 130.1, 129.8, 128.5, 126.8, 126.5, 118.6, 114.4, 75.3, 61.3, 58.2, 55.3.

Procedure for the Synthesis of 3-acryloyl-*N*-methylthio-4-(2-chlorophenyl)-2-azetidinone (27).

To a solution of **25** (4.00 g, 11.2 mmol) in 40 ml of CH_3CN in an ice-water bath was added ceric ammonium nitrate (18.39 g, 33.54 mmol) in 40 ml of water. The resultant mixture was stirred for 5 min, and 20 ml of water was added. The solution was extracted (3x5 ml) with EtOAc. The combined organic layers were washed with 5% $NaHSO_3$, 5% $NaHCO_3$, and dried over anhydrous $MgSO_4$. The solvent was removed under reduced pressure to yield 2.14 g (76 %) of **26** as a crude brown oil. Without futher purification, compound **26** (2.00 g, 8.0 mmol) was dissolved in 30 ml of dry CH_2Cl_2 and *N*-(methylthio)phthalimide (2.30 g, 11.9 mmol) and 3-5 drops of triethylamine were added. The resultant mixture was refluxed for overnight. The solvent was removed under reduced pressure to yield a brown solid. The brown solid was redissolved in CH_2Cl_2, and washed with 1% NaOH. The organic layer was dried over anhydrous $MgSO_4$. The solvent was removed under reduced pressure to yield a brown semi-solid, which was purified by column chromatography on silica gel with gradient elution (1:9 then 1:4 EtOAc:hexanes) to yield 2.00 g (88%) of **27** as a white solid. ^{1}H NMR (250 MHz) δ 7.35-7.26 (m, 4H), 6.20 (d, *J* = 5.1 Hz, 1H), 6.06 (dd, *J* = 16.7, 1.9 Hz, 1H), 5.78 (dd, *J* = 16.7, 10.4 Hz, 1H), 5.68 (dd, *J* = 10.4, 1.9 Hz, 1H), 5.54 (d, *J* = 10.4 Hz, 1H), 2.51 (s, 3H). ^{13}C NMR (63 MHz) δ 168.3, 163.4, 156.6, 134.3, 132.6, 129.8, 128.6, 126.6, 126.3, 62.1, 21.9.

Procedure for the synthesis of 2.5:1 (ethyl acrylate:lactam) nanoparticles containing N-methylthio β-lactam

The mixture of 3-acryloyl *N*-methylthio β-lactam **27** (500 mg, white solid, mp 92-93 ^{o}C) and ethyl acrylate (440 mg) was warmed to 70 ^{o}C with slow stirring under a nitrogen atmosphere. Stirring was continued until the mixture was completely mixed to give a homogeneous liquid phase. Deionized water (7.94 ml) containing dodecyl sulfate, sodium salt (Acros, 15 mg) was added with vigorous stirring and the mixture was stirred for one hour to give a milky pre-emulsion state. A solution of potassium persulfate (Sigma, 4 mg) dissolved in deionized water (0.3 ml) was added under a nitrogen atmosphere and the mixture was stirred rapidly at 70 ^{o}C for 6 hr. A solution of potassium persulfate (1 mg) dissolved in deionized water (0.1 ml) was added to the emulsion and rapid stirring was continued for 1hr, to give the N-methylthio β-lactam containing nanoparticles as a milky emulsion.

Other analogs were prepared similarly based on the formulation described in Table 3-2.

Process for the preparation of samples for SEM

An aliquot (0.1 ml) of the emulsified suspension of the nanoparticles was diluted 20,000 to 30,000 times with deionized water (2000 ml- 3000 ml). One drop of the diluted emulsion was carefully applied to the surface of a silicon wafer and evaporated under a gentle stream of air. The spot of emulsion on the wafer was marked with a pen and coated with gold sputter under high vacuum. The gold coated nanoparticles were observed by SEM.

Note: it is really important to keep the silicon wafer clean from any dust. Therefore, the best way is to prepare the sample in a clean room.

Process for the preparation of thin film on the glass.

Samples of the nanoparticle emulsions were converted to thin films by coalescence as described in section 3.6.1. A rectangular cardboard frame was fixed on glass and the emulsion was poured into the frame. The emulsion was left to dry for 48 hours to give a transparent thin film.

References

1. Lebl, M. Parallel Personal Comments on "Classical" Papers in Combinatorial Chemistry. *J. Comb. Chem*. **1999**, *1*, 3.
2. a) Hudson, D. Matrix Assisted Synthetic Transformations: A Mosaic of Diverse Contributions. I. The Pattern Emerges. *J. Comb. Chem*. **1999**, *1*, 333. b) Hudson, D. Matrix Assisted Synthetic Transformations: A Mosaic of Diverse Contributions. II. The Pattern is Completed. *J. Comb. Chem*. **1999**, *1*, 403.
3. Rao, V.S.V.Vadlamudi; Thomas, P. C. High Throughput Screening: Revolution in Drug Discovery Research. *Asian Chemistry Letters* **2001**, *5*, 61.
4. Greenwald, R.B.; Choe, Y.H.; McGuire, J.; Conover, C.D. Effective drug delivery by PEGylated drug conjugates. *Advanced Drug Delivery Reviews* **2003**, *55*, 217.
5. a) Langer, R. Drug delivery and targeting. *Nature*, **1998**, *392*, 5. b) Garnett, M. C. Targeted Drug Conjugates: Principles and Progress. *Advanced Drug Delivery Reviews* **2001**, *53*, 171.
6. Internet Web Site Paper; Polymeric Drug Deliver, A Brief Review; http://www.drugdel.com/polymer.htm

7. Moghimi, S.M.; Hunter, A.C.; Murray, J.C.; Long-Circulating and Target Specific Nanoparticles: Theory to Practice. *Pharmacol. Rev.* **2001**, *53*, 283.
8. a) Langer, R. New Methods for Drug Delivery. *Science* **1990**, *249*, 1527. b) Langer, R. Perspectives: Drug Delivery-Drugs on Target. *Science*, **2001**, *293*, 58.
9. a) Lambert G.; Fattal E.; Couvreur P. Nanoparticulate Systems for the Delivery of Antisense Oligonucleotides. *Advanced Drug Delivery Reviews*. **2000**, 47, 99. b) Kawaguchi, H. Functional Polymer Microspheres. *Prog. Polym. Sci*. **2000,** *25*, 1171.
10. a) Vinagradov,S.V.; Bronich,T.K.; Kabanov, A.V. Nanosized Cationic Hydrogels for Drug Delivery: Preparation, Properties and Interactions with Cells, *Adv. Drug Del. Rev.* **2002**, *54*, 223. b) Okamoto, C.T. Endocytosis and Transcytosis. *Advanced Drug Delivery Reviews* **1998**, *29*, 215.
11. a) C. Song, V. Labhasetwar, X. Cui, T. Underwood, R.J. Levy, Arterial Uptake of Biodegradable Nanoparticles for Intravascular Local Drug Delivery: Results with an Acute Dog Model, *J. Control. Release* **1998**, *54*, 201. b) Rihova, B.; Jelinkova, M.; Strohalm, J.; Subr, V.; Plocova, D.; Hovorka, O.; Novak, M.; Plundrova, D.; Germano, Y.; Ulbrich, K. Polymeric Drugs Based on Conjugates of Synthetic and Natural Macromolecules-II. Anti-cancer Activity of Antibody or (Fab')2-Targeted Conjugates and Combined Therapy with Immunomodulators. *J. Control. Release* **2000**, *64*, 241.

12. Matsumura, Y.; Maeda, H. A New Concept for Macromolecular Therapies in Cancer Chemotherapy: Mechanism of Tumouritropic Accumulation of Proteins and Antitumour Agent SMANCS, *Cancer Res*. **1986,** *6*, 6387.
13. a) Harkins, W.D. A General Theory of the Mechanism of Emulsion Polymerization. *J. Am. Chem. Soc.* **1947**, *69*, 1428. b) Blackley, D.C. Emulsion Polymerization, Applied Science. London, **1975**. c) Stoffer, J.O.; Bone, T. *J. Polym. Sci. Polym. Chem. Ed.* **1980**, *18*, 2641. d) Stoffer, J.O.; Bone, T. *J. Dispersion Sci. Technol.* **1980**, *1*, 37.
14. a) Atik, S.S.; Thomas, J.K. Polymerized Microemulsions. *J. Am. Chem. Soc.* **1981**, *103*, 4279. b) Atik, S.S.; Thomas, J.K. Photochemistry in Polymerized Microemulsion Systems. *J. Am. Chem. Soc.* **1982**, *104*, 5868. c) Atik, S.S.; Thomas, J.K. Photoinduced Reactions in Polymerized Microemulsions. *J. Am. Chem. Soc.* **1983**, *105*, 4515.
15. Wicks, Z.W. Jr; Jones, F.N.; Pappas, S.P. Organic Coatings: Science and Technology. John Wiley & Sons, Inc., **1992**, Vol. I, p64.
16. Barbour, M.; Clarke, J.; Fone, D.; Hoggan, A.; James, R.; Jones, P.; Lam, P.; Langham, C.; O'Hara, K.; Oldring, P.; Raynor, G.; Royston, I.; Tuck, N.; Usher, R. Waterborne & Solvent Based Acrylics and Their End User Applications. SITA Technology Limited, **1996**, Vol. 1, p103.
17. Ouchi, T.; Ohya, Y. Macromolecular Prodrugs. *Prog. Polym. Sci*. **1995,** *20*, 211.

Chapter Four

Preparation of Fluorescence Active Nanoparticles

4.1 Introduction

Fluorescence has proven to be a versatile tool for numerous applications. This powerful technique enables one to study molecular interactions in life science . It is promoting the phenomenal sensitivity for the life scientist working on biological analysis. But the fluorescence technology offers much more than mere signal-gathering capabilities. New developments in instrumentation, software, probes, and applications have resulted in a burst of popularity since it was observed over 150 years ago. As the theory of fluorescence became better understood, a more powerful set of applications emerged and afforded the detailed information about complex molecules and their reaction pathways.[1,2,3]

The preparation of N-methylthio β-lactam containing fluorescence-active nanoparticles are the subject of our current investigations for studying the biological mechanism of the nanoparticles. However, there are no reports to prepare fluorescence-active polymeric nanoparticles. Therefore, it may open a new area in biological diagnostics if fluorescence-active nanoparticles are successfully prepared and applied appropriately to detection of specific biological molecules, acting as a water dispersed biological sensor or biological imaging agent.

4.2 Preparation of an Acrylated Fluorescence Monomer

The acrylation of fluorescent molecules to serve as free radical acceptors is required for microemulsion polymerization. Three compounds were selected for these studies: dansyl chloride[1] (5-dimethylamino-1-naphthalenesulfonamide, **29)**, 1-naphthoic acid[1] (**30)** and 9-anthracenecarboxylic acid[1] (**31)**. They are all fluorescence active. 2-Hydroxy ethyl acrylate was used for acrylation of each compound since the terminal hydroxyl group is easily coupled with the carboxylic acid group of each substance, and the resultant diester linker can be easily hydrolyzed in a biological environment. Dansyl chloride (**29)** was reacted with 2-hydroxyethyl acrylate using amine base, to give compound **32** with 56% yield. Both 1-naphthoic acid (**30)** and 9-anthracenecarboxylic acid (**31)** was also coupled with 2-hydroxy acrylate under EDC/DMAP conditions, to give compound **32** and **33** with 82% and 21% yield, respectively. The synthesis and ^{1}H NMR spectra are displayed in Scheme IV-1 and Fig. 4-1, respectively.

Scheme IV-1

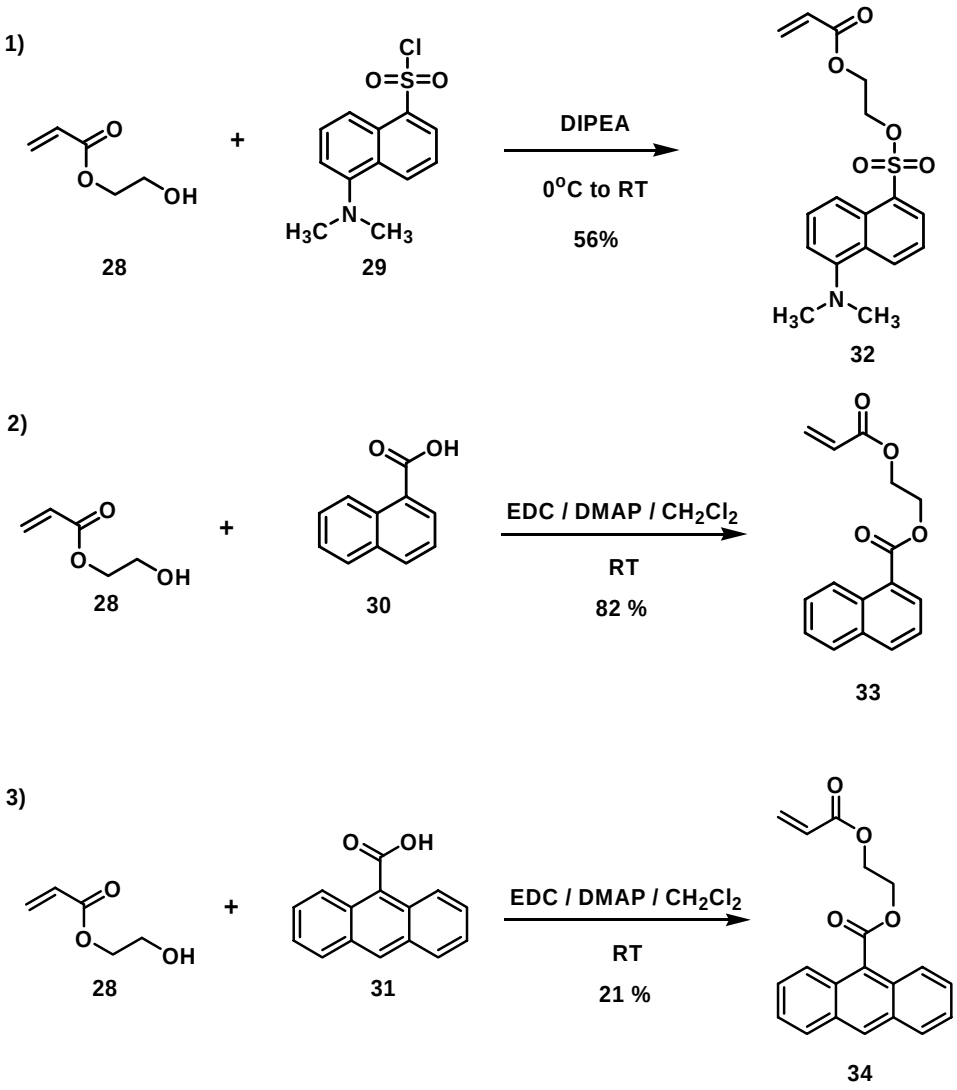

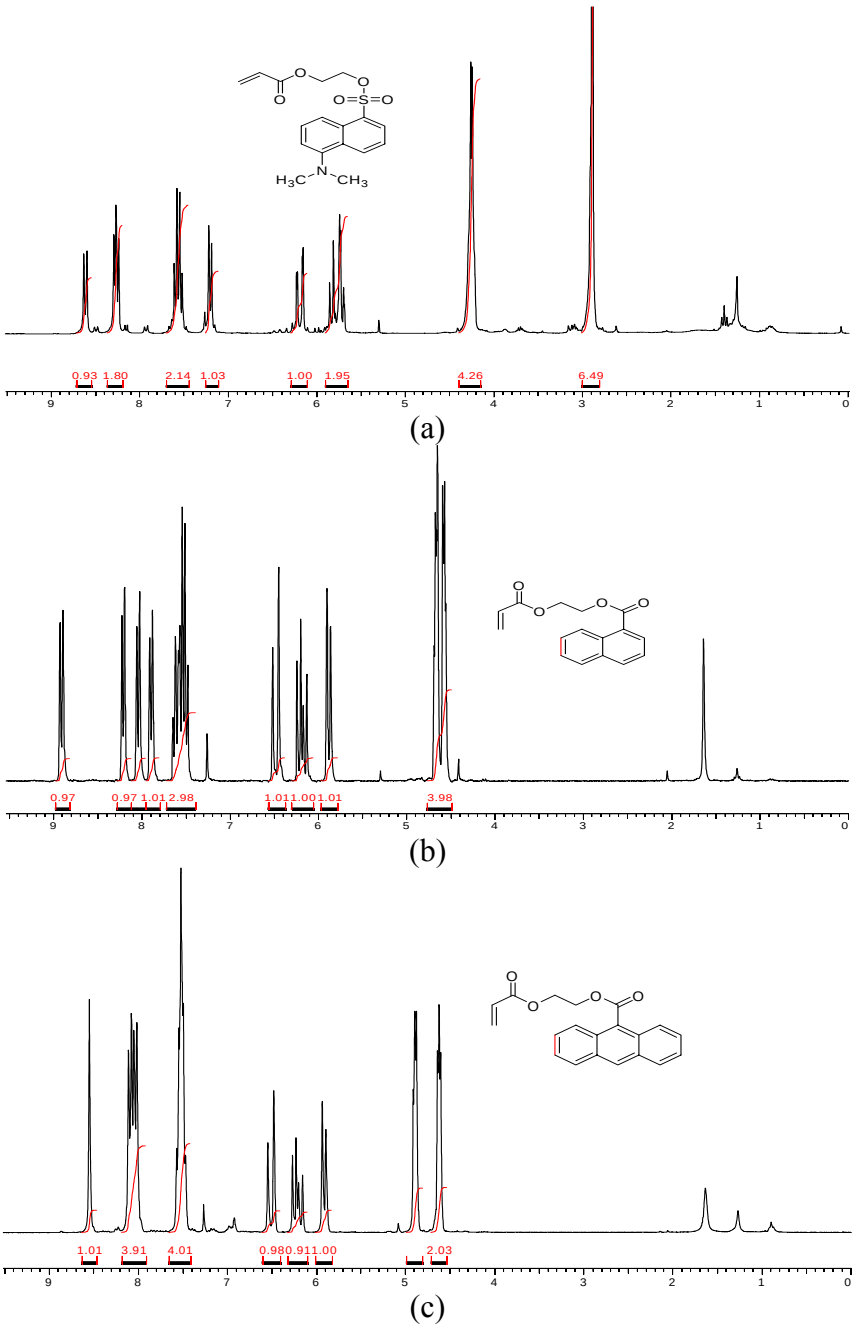

Fig. 4-1 ^{1}H NMR spectra of (a) dansyl, (b) naphthyl, and (c) anthracenyl acrylates

4.3 The Preparation of Fluorescence-Active Polymeric Nanoparticles in an Aqueous Emulsion

The microemulsion polymerization described in section was performed with the fluorescent acrylates in an attempt to prepare fluorescence-active nanoparticles.

β-Lactam containing fluorescence-active emulsified nanoparticles were successfully prepared with C_3-acryloyl N-methylthio β-lactam **27**, naphthyl acrylate **32** and ethyl acrylate at 70 ^oC. After making a homogeneous solution of these three monomeric substances at 70 ^oC, this mixture was dispersed in aqueous media containing the surfactant, sodium lauryl sulfate. Radical polymerization within this pre-formed particle mixture then was performed with an initiator (potassium persulfate) to give the nanospherical polymers. Its synthesis and formulation are described in Scheme IV-2 and Table IV-1 respectively.

Dansyl acrylate **31** could not be used in the emulsion polymerization, because it underwent the hydrolysis under the above conditions.

The naphthyl containg fluorescence-active emulsified nanoparticles (without the β-lactam drug) were prepared with naphthyl acrylate **32** and ethyl acrylate in aqueous phase. A homogeneous solution of monomeric substances could be made at room temperature and this mixture was dispersed in aqueous media with the aid of sodium lauryl sulphate at 60 ^oC. Its synthesis and formulation are displayed in Scheme IV-3 and Table IV-2 respectively.

Finally, anthracenyl fluorescence-active emulsified nanoparticles were also prepared with anthracenyl acrylate **33**, styrene and butyl acrylate in aqueous phase at 70 ^oC. A homogeneous solution of monomeric substances could be made with styrene and butyl

acrylate at 70 ^{o}C and this mixture was dispersed in aqueous media containing a surfactant, sodium lauryl sulfate, to give the anthracenyl fluorescence-active nanoparticles as a milky emulsion. However, a homogeneous solution of monomeric substances could not be obtained with either ethyl acrylate and butyl acrylate since they could not dissolve the anthracenyl acrylate **34** at 70 ^{o}C. Its synthesis and the formulation are also displayed in Scheme IV-4 and Table IV-3 respectively.

Scheme IV-2

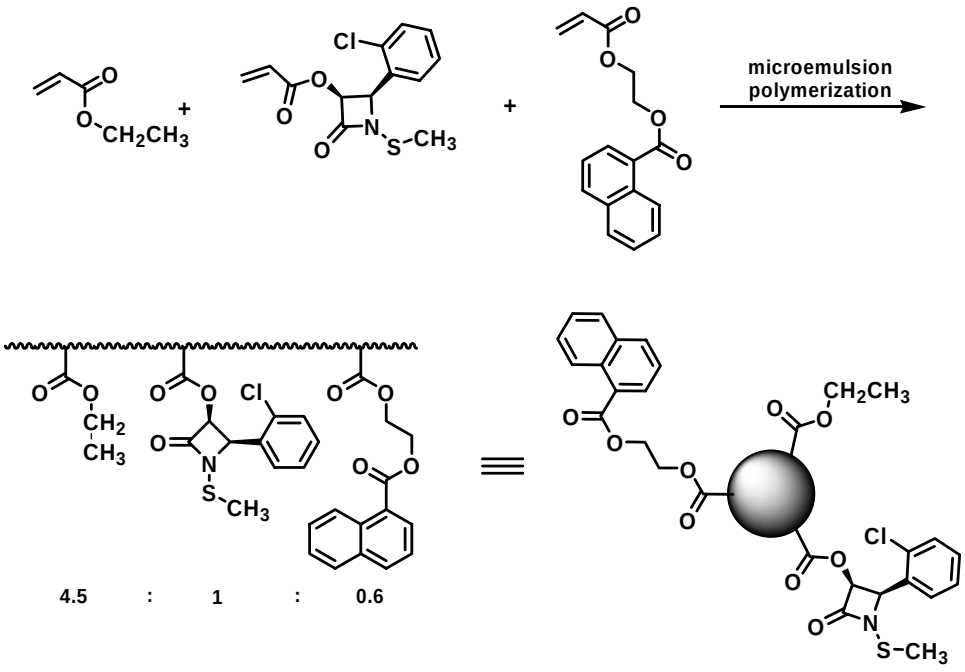

Table IV-1 Formulation of Microemulsion Polymerization for Fluorescence-Active β-Lactam Copolymeric Nanoparticles

components	amount
ethyl acrylate (mg)	170
β-lactam acrylate (27) (mg)	100
naphthyl acrylate (33) (mg)	50
surfactant[1] (mg)	7
initiator[1] (mg)	1.8
deionized water (ml)	2.0
temperature (^{o}C)	70

[1] surfactant: sodium laury sulfate; initiator: potassium persulfate

Scheme IV-3

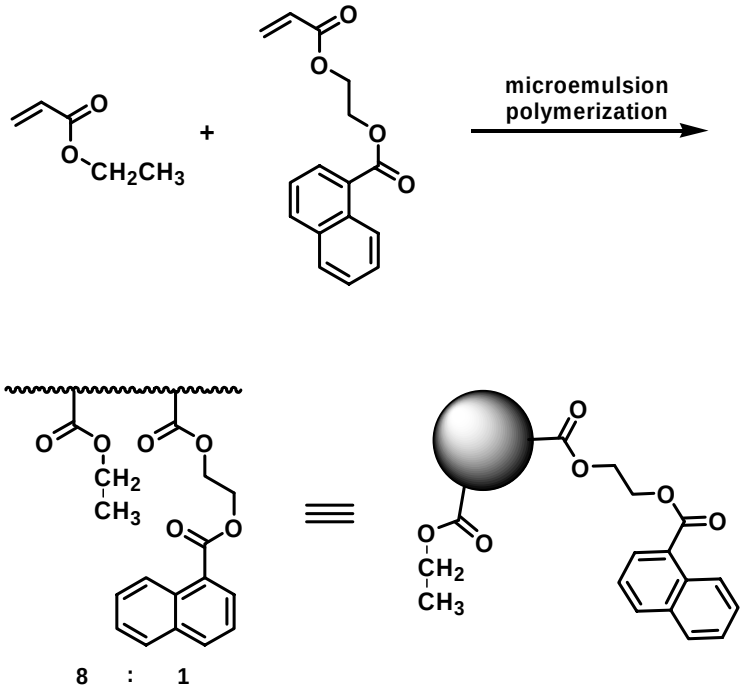

Table IV-2 Formulation of Microemulsion Polymerization for Fluorescence-Active Naphthyl Copolymeric Nanoparticles

components	amount
ethyl acrylate (mg)	300
naphthyl acrylate (33) (mg)	100
surfactant[1] (mg)	8
initiator[1] (mg)	2.0
deionized water (ml)	3.0
temperature (^{o}C)	60

[1] surfactant: sodium laury sulfate; initiator: potassium persulfate

Scheme IV-4

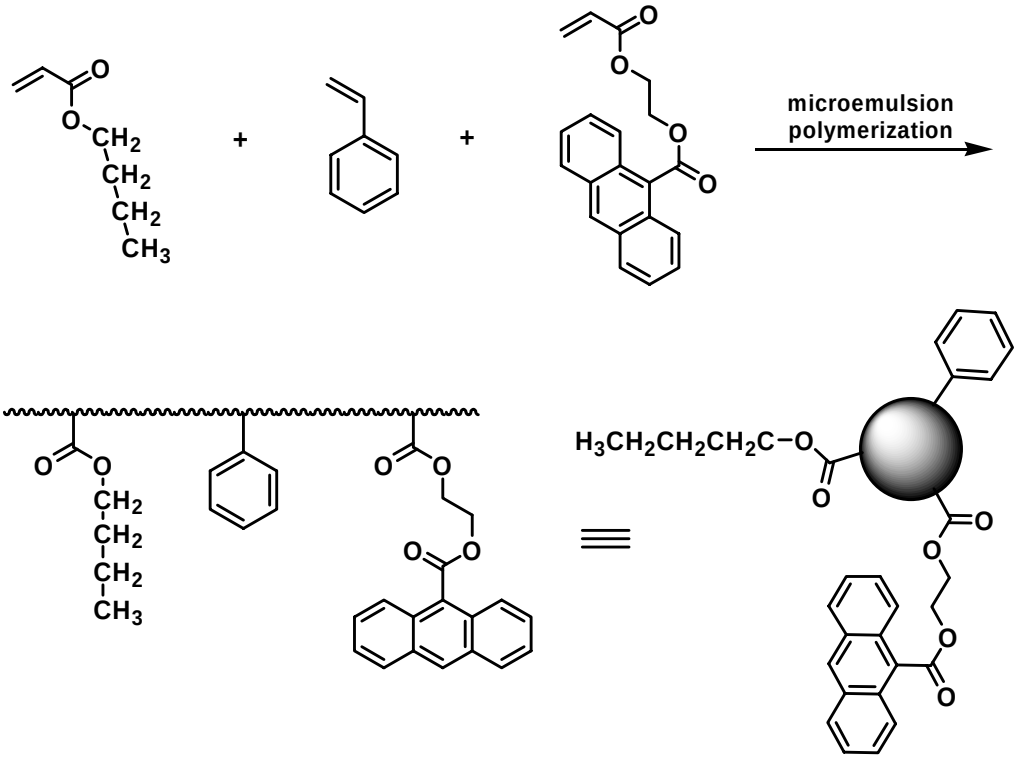

Table IV-3 Formulation of Microemulsion Polymerization for Fluorescence-Active Anthracenyl Copolymeric Nanoparticles

components	amount
butyl acrylate (mg)	700
styrene (mg)	300
anthracenyl acrylate (34) (mg)	10
surfactant[1] (mg)	20
initiator[1] (mg)	5.0
deionized water (ml)	5.0
temperature (^{0}C)	70

[1] surfactant: sodium laury sulfate; initiator: potassium persulfate

4.4 Characterization of Fluorescence Active Emulsified Nanoparticles

4.4.1 Scanning Electron Microscopy (SEM)

The morphology and the size of the emulsified particles were examined by Scanning Electron Microscopy (SEM). The sample of nanoparticles was prepared on a silicon wafer by evaporation of water under a gentle stream of air, and then coated with gold sputter under high vaccum. The gold-coated nanoparticles were then observed by SEM.

The SEM images of β-lactam, naphthyl, and anthracenyl fluorescence-active nanoparticles are displayed in Fig. 4-2, 4-3, and 4-4 respectively. The images of nanoparticles show that the particles have microspherical morphology and a particle size distribution of about 30-120 nm. Fig. 4-2 and 4-4 also show that some of particles are fused by the coalescence due to not enough dilution of the samples when they are prepared.

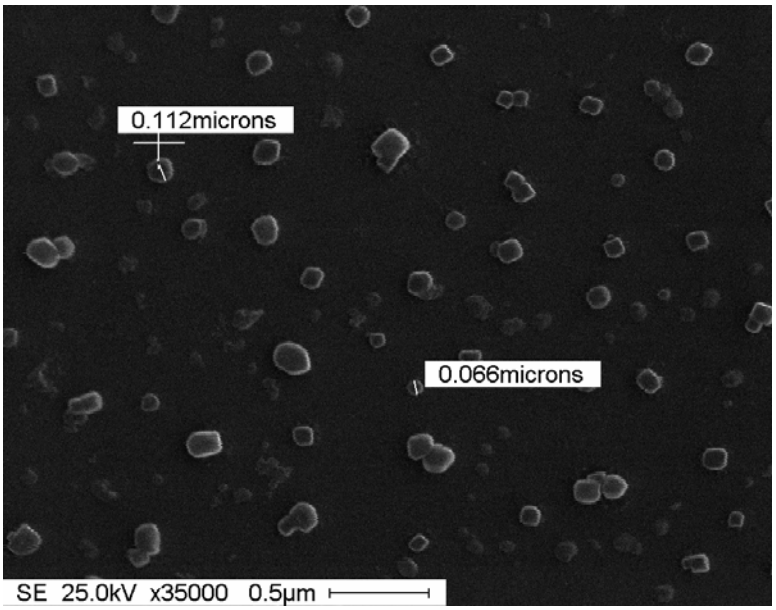

Fig. 4-2 SEM image for β-lactam fluorescence-active emulsified nanoparticles with particles size (60-120 nm)

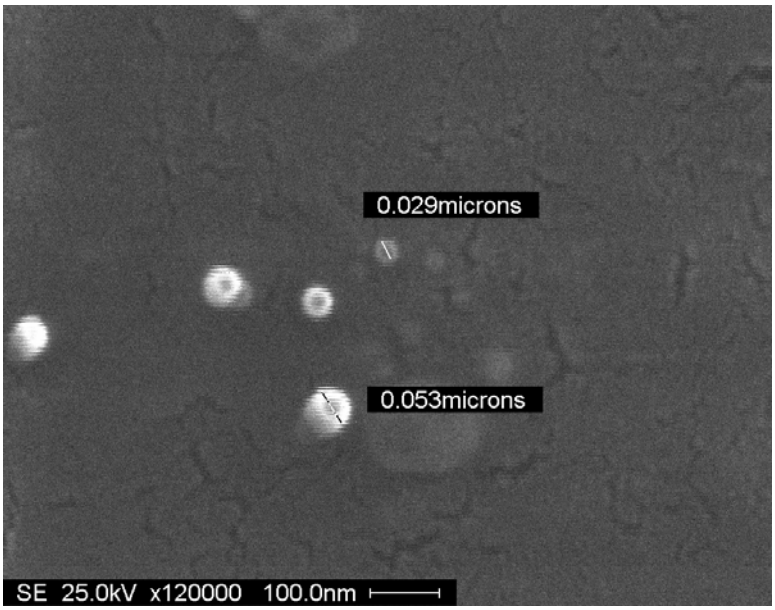

Fig. 4-3 SEM image for naphthalyl fluorescence-active emulsified nanoparticles with particle size (30-60 nm)

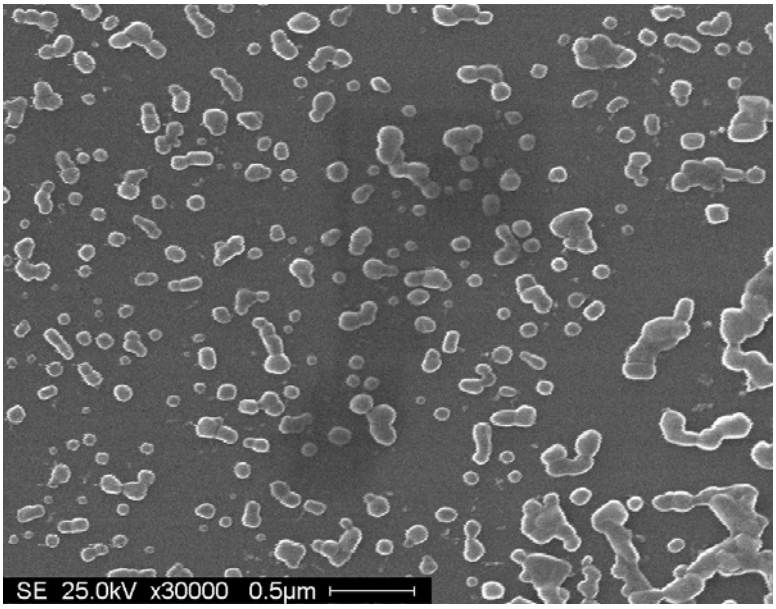

Fig. 4-4 SEM image for anthracenyl fluorescence-active emulsified nanoparticles with particle size (60-120 nm)

4.4.2 ^{1}H NMR Spectra Analysis

^{1}H NMR Spectroscopy is a very useful tool to analyze the chemical structure of organic molecules. It can also be used to determine the mole ratio of each of the monomeric units, in copolymers. Fig. 4-5 shows ^{1}H NMR spectra for the dry films obtained by coalescing the nanoparticle emulsions of naphthyl (a), β-lactam (b), and anthracenyl (c) copolymer. The olefin protons of the acrylate moiety in the range of 5.6-6.1 ppm do not appear in the spectrum, indicating that all acrylic monomers participated in polymerization. In addition, each monomer composition in the polymer was determined by the peak integration in the ^{1}H NMR spectrum. For instance, the comparison of the peak integration for C_3 or C_4 proton of β-lactam, methylene protons of ethyl acrylate, and one of aromatic protons in naphthyl group in (b) spectra gave the mole ratio of each monomer in the copolymer.

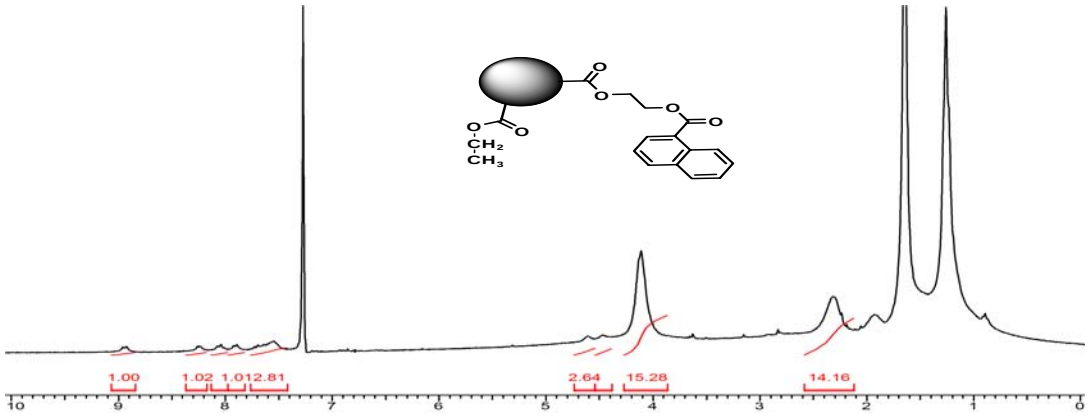

(a)

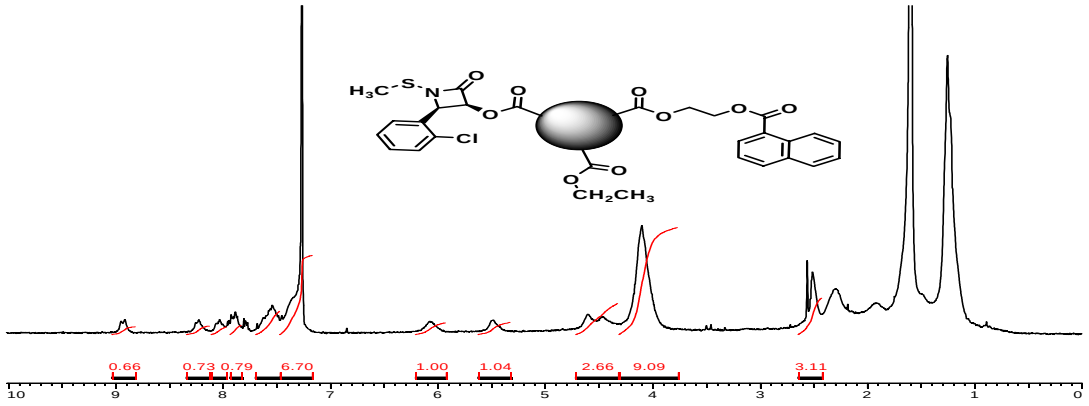

(b)

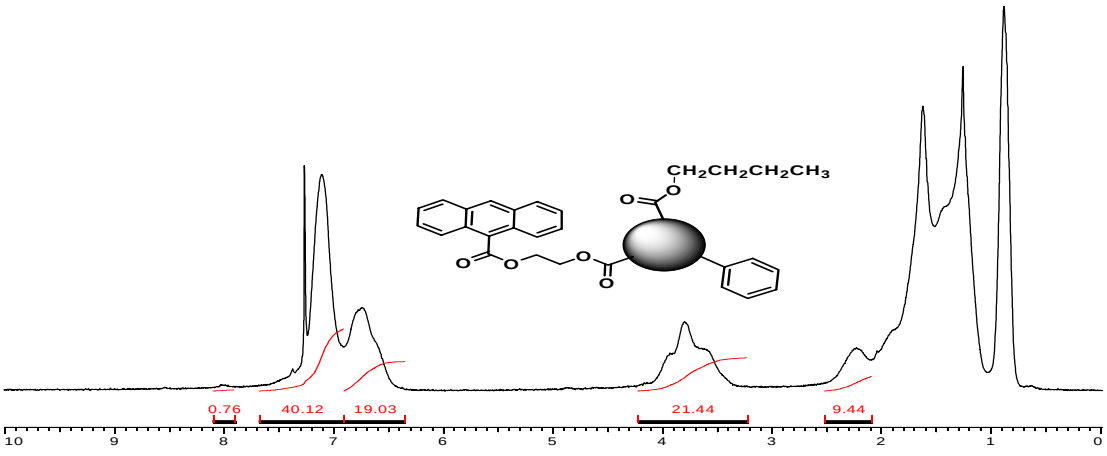

(c)

Fig. 4-5 ^{1}H NMR spectra for (a) naphthyl, (b) β-lactam and (c) anthracenyl fluorescence-active copolymer

4.5 Discussion

Fluorescence-active emulsified nanoparticles were successfully prepared by a novel microemulsion polymerization described in chapter three. The fluorescence-active nanoparticles were made for the first time and may open opportunities to construct new biological diagnostic systems to detect a certain microbe, cell, or biomolecule. This will require further development.

Acrylation with naphthyl carboxylic acid **30** and anthracenyl carboxylic acid **31** was performed with 2-hydroxy ethyl acrylate using EDC/DMAP condition to give acrylated compound **33** and **34** which are all fluorescence-active.

The β-lactam containing fluorescence active emulsified nanoparticles were prepared with the monomer combination of C_3-acryloyl N-methylthio β-lactam **27**, naphthalyl acrylate **33**, and ethyl acrylate. The homogeneous solution of monomeric substances was formed at 70 ^oC, followed by dispersion in water phase with aid of surfactants. The mole ratio of each monomer in the polymer is 1 : 4.5 : 0.6, and the particle size distribution is approximately 60-120 nm. These nanoparticles were prepared for possible use in identifying the mechanism, of how the drug enters the cell of MRSA (chapter 3).

The fluorescence-active polymeric nanoparticles without drug are also expected to be very important materials as leads to bio-diagnostics because of easy and fast detection of the fluorescence probe. First, naphthyl-contaning fluorescence-active emulsified nanoparticles were prepared with ethyl acrylate as a co-monomer using microemulsion polymerization. A water-insoluble high viscous oil, naphthyl acrylate **33,** was pre-mixed with ethyl acrylate at room temperature to give a homogeneous liquid. Following this, emulsion polymerization was performed at 60 ^oC to give naphthyl fluorescence-active

emulsified nanoparticles as a milky emulsion. The mole ratio of ethyl acrylate and naphthyl acrylate in the polymer is 8:1 and the particle size distribution is approximately 30-60 nm.

Anthracenyl fluorescence-active emulsified nanoparticles which have a different fluorescent emission were also prepared with butyl acrylate and styrene as co-monomers using microemulsion polymerization. The mole ratio of each monomer was not determined with ^{1}H NMR spectra analysis since the peak integration of anthracenyl group is too small to detect. The particle size distribution is approximately 60-120 nm. Even though the emulsion polymerization was attempted with the monomer combination of ethyl acrylate-anthracenyl acrylate and the butyl acrylate-anthracenyl acrylate respectively, the anthracenyl emulsified nanoparticles were not prepared since neither monomer combinations could form a homogeneous liquid phase at 70 ^{o}C. Thus, these experiments failed.

The fluorescent emission colors for a naphthyl and an anthracenyl emulsions and their corresponding thin films formed by coalescence were compared with non fluorescent β-lactam emulsion and its thin film upon UV irradiation. The image (a) and (a') in Fig. 4-6 displays the fluorescent emission colors for the non fluorescent β-lactam nanoparticles as well as that of naphthyl, and anthracenyl system upon UV irradiation. The non-fluorescent β-lactam emulsion shows no color change while both the naphthyl and anthracenyl nanoparticle emulsions emit a blue and a bright blue-green fluorescent color respectively. The image (b) and (b') in Fig. 4-6 also displays the fluorescent emission colors for the thin films of corresponding samples upon UV irradiation. Each sample shows the same fluorescent emission colors as in the emulsion. Therefore,

naththyl and anthracenyl emulsified nanoparticles and their corresponding thin films are all fluorescence-active and emit a blue and a bright blue-green fluorescent color respectively.

As an on-going study, the naphthyl and anthracenyl copolymeric emulsified nanoparticles are going to be prepared by using microemulsion polymerization. If the copolymeric nanoparticles emit the totally different color in fluorescent emission, that means new fluorescence-active nanoparticles can be created with simple microemulsion copolymerization of two different fluorescent probes. Therefore, this research can potentially bring significant advantages and applications in the bio-diagnostics area.

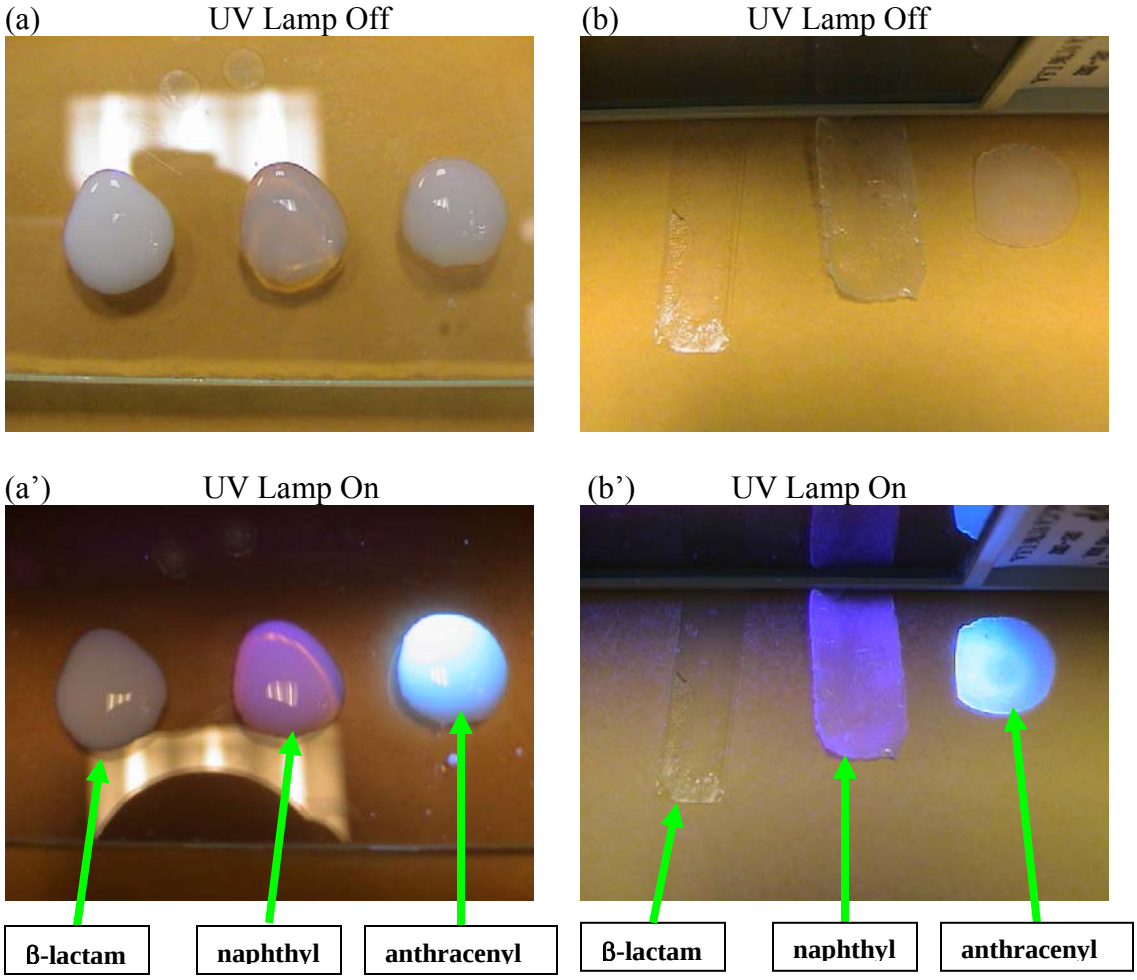

Fig. 4-6 Comparison of the non fluorescence-active β-lactam and the fluorescence-active naphthalyl and anthracenyl emulsified nanoparticles and their corresponding thin films upon UV Irradiation

4.6 Experimental

All reagents were purchased from Sigma-Aldrich Chemical Company and used without further purification. Solvents were obtained from Fisher Scientific Company. Thin layer chromatography (TLC) was carried out using EM Reagent plates with a fluorescence indicator (SiO_2-60, F-254). Products were purified by flash chromatography using J.T. Baker flash chromatography silica gel (40 μm). NMR spectra were recorded in $CDCl_3$ unless otherwise noted. ^{13}C NMR spectra were proton broad-band decoupled.

Procedure for the synthesis of 2-(5-dimethylamino-naphthalene-1-sulfonyloxy)-ethyl acrylate (32).

To a solution of 2-hydroxyethyl acrylate **28** (25.8 mg, 0.2 mmol) in 2 ml of freshly distilled CH_2Cl_2 was added diisopropylethylamine (DIPEA, 0.35 ml, 0.2 mmol) dropwise at 0^oC. Dansyl chloride (50.0 mg, 0.19 mmol) was then added dropwise and the resultant mixture was stirred at room temperature until TLC indicated the disappearance of starting material. The reaction was quenched with a 5% solution of NH_4Cl and extracted (3x20 ml) with CH_2Cl_2. The combined organic layers were dried over anhydrous $MgSO_4$ and purified with column chromatography on silica gel (1:4, EtOAc:hexanes) to give 37.5 mg (56 %) of **32** as a yellow semi solid. ^1H NMR (250 MHz) δ 8.61 (d, J = 8.6 Hz, 1H), 8.26 (t, J = 6.3 Hz, 2H), 7.56 (m, 2H), 7.20 (d, J = 7.7 Hz, 1H), 6.19 (dd, *J* = 16.5, 2.5 Hz, 1H), 5.80 (dd, *J* = 16.5, 10.3 Hz, 1H), 5.71 (dd, *J* = 16.5, 10.3 Hz, 1H), 4.25 (m, 4H), 2.88 (s, 6H). ^{13}C NMR (63 MHz) δ 158.0, 151.7, 131.8, 131.5, 130.9, 130.6, 129.8, 128.8, 127.3, 123.0, 119.4, 115.6, 67.8, 61.5, 45.4.

Procedure for the synthesis of naphthalene-1-carbonyloxy-2-ethyl acrylate (33).

To a solution of 2-hydroxyethyl acrylate **28** (1.01 g, 8.7 mmol) and 1-naphthoic acid **30** (1.00 g, 5.8 mmol) in 10 ml of freshly distilled CH_2Cl_2 was added EDC (1.60 g, 8.7 mmol) and DMAP (cat. amount) at room temperature. The resultant mixture was stirred at room temperature until TLC indicated the disappearance of starting material. The reaction was quenched with a 5% solution of NH_4Cl and the mixture was washed with water. After extraction with EtOAc (3x20 ml), the organic layers were dried over anhydrous $MgSO_4$ and purified with column chromatography on silica gel (1:4, EtOAc:hexanes) to give 1.29 g (82 %) of **33** as a colorless oil. ^{1}H NMR (250 MHz) δ 8.91 (d, J = 8.4 Hz, 1H), 8.21 (d, J = 7.1 Hz, 1H), 8.04 (d, J = 8.2 Hz, 1H), 7.90 (d, J = 8.0 Hz, 1H), 7.57 (m, 3H), 6.49 (d, J = 17.3 Hz, 1H), 6.19 (dd, J = 17.3, 10.4 Hz, 1H), 5.71 (d, *J* = 10.4 Hz, 1H), 4.66 (m, 2H), 4.58 (m, 2H). ^{13}C NMR (63 MHz) δ 167.2, 165.9, 133.8, 133.6, 131.5, 131.3, 130.5, 128.6, 128.0, 127.8, 126.6, 126.2, 125.7, 124.5, 62.7, 62.3.

Procedure for the synthesis of anthracene-9-carbonyloxy-2-ethyl acrylate (34).

To a solution of 2-hydroxyethyl acrylate **28** (0.78 g, 6.8 mmol) and 1-naphthoic acid **30** (1.00 g, 5.8 mmol) in 10 ml of freshly distilled CH_2Cl_2 was added EDC (0.86 g, 4.5 mmol) and DMAP (cat. amount) at room temperature. The resultant mixture was stirred at room temperature until TLC indicated the disappearance of starting material. The reaction was quenched with a 5% solution of NH_4Cl and the mixture was washed with water. After extraction with EtOAc (3x20 ml), the organic layers were dried over

anhydrous $MgSO_4$ and purified with column chromatography on silica gel (1:4, EtOAc:hexanes) to give 0.30 g (21 %) of **34** as a yellow solid, mp 66-68 ^oC. ^1H NMR (250 MHz) δ 8.54 (s, 1H), 8.06 (dd, J = 14.7, 8.0 Hz, 4H), 7.52 (m, 4H), 6.21 (d, J = 17.2 Hz, 1H), 6.21 (dd, J = 17.2, 10.5 Hz, 1H), 5.91 (d, J = 10.5 Hz, 1H), 4.89 (m, 2H), 4.62 (m, 2H). ^{13}C NMR (63 MHz) δ 169.3, 165.3, 131.7, 130.9, 129.7, 128.7, 127.9, 127.1, 125.5, 124.9, 63.2, 62.3.

Procedure for the synthesis of fluorescence-active emulsified nanoparticles.

The mixture of 3-acryloyl *N*-methylthio β-lactam **27** (100 mg, white solid, mp 92-93 ^oC), naphthyl acrylate **33** (50 mg), and ethyl acrylate (170 mg) was warmed to 70 ^oC with slow stirring under a nitrogen atmosphere. Stirring was continued until the mixture was completely mixed to give a homogeneous liquid phase. Deionized water (1.7 ml) containing dodecyl sulfate, sodium salt (Acros, 7 mg) was added with vigorous stirring and the mixture was stirred for one hour to give a milky pre-emulsion state. A solution of potassium persulfate (Sigma, 1.8 mg) dissolved in deionized water (0.3 ml) was added under a nitrogen atmosphere and the mixture was stirred rapidly at 70 ^oC for 6 hr. A solution of potassium persulfate (0.5 mg) dissolved in deionized water (0.1 ml) was added to the emulsion and rapid stirring was continued for 1hr, to give the N-methylthio β-lactam containing fluorescence-active emulsified nanoparticles as a milky emulsion.

Other analogs were prepared similarly based on the formulation described in Table IV-2 and Table IV-3 respectively.

Process for the preparation of thin film on the glass.

Samples of the nanoparticle emulsions were converted to thin films by coalescence as described in previous chapter. A rectangular cardboard frame was fixed on glass and the emulsion was poured into the frame. The emulsion was left to dry for 48 hours to give a transparent thin film.

References

1. Du, H.; Fuh, R. A.; Li, J.; Corkan, A.; Lindsey, J. S. PhotochemCAD: A computer-aided design and research tool in photochemistry. *Photochemistry and Photobiology* **1998**, *68*, 141.
2. Rhys Williams, A. T. Clinical Chemistry Using Fluorescence Spectroscopy- a Review of Current Techniques. Perkin-Elmer Ltd (1976).
3. Rhys Williams, A. T. Fluorescence Derivatisation in Liquid Chromatography. Perkin-Elmer Ltd. (1984).

Chapter Five

Conclusions and Future Directions

Methicillin-resistant *Staphylococcus Aureus* (MRSA) is now the most challenging bacterial pathogen affecting patients in hospitals and in care centers. Infections caused by this bacterium has become a serious national and global problem. The need to develop new drugs for MRSA is the force driving this research project.

N-Thiolated β-lactams are a new family of potent antibacterial compounds that selectively inhibit the growth of *Staphylococcus* species including methicillin-resistant *Staphylococcus aureus* (MRSA), over other common bacterial genera. Recent efforts within this laboratory have been on understanding possible structure-activity profiles of this previously unstudied family of antibiotics.

In chapter 2 of this thesis, results were discussed on the effect of a fatty ester group (CO_2R) on the C_4-phenyl ring of *N*-methylthio β-lactams. The initial expectation was that attachment of long chain ester moieties might increase the hydrophobicity, and thus enhance the drug's ability to penetrate through the cell membrane. However, the result indicate that there is an optimal chain length for the fatty ester groups, with antibacterial activity dropping off rapidly when more than seven carbon atoms are in the chain. These results led to the idea about examining a β-lactam conjugated polymer as a possible drug

delivery method, with the polymer essentially serving as a surrogate for an extremely large, lipophilic ester side chain on the lactam ring. The question being asked is whether this would enhance, or destroy, biological activity.

To synthesize the initial drug-polymer candidate, microemulsion polymerization of an acrylate-substituted lactam was done in aqueous solution to form hydrophilic polymeric nanoparticles containing the highly water-insoluble solid antibiotic, *N*-methylthio β-lactam. This method has advantages over the conventional emulsion polymerization methods because a solid co-monomer (β-lactam drug) can be utilized.

SEM studies show that these polymeric nanoparticles have a microspherical morphology with nano-sizes of 40-150 nm. The *N*-thiolated β-lactam containing nanoparticles display potent anti-MRSA activity at much lower drug amounts compared with free lactam drug, penicillin G or vancomycin. Although at this time the relationship between particle size and activity is not clear and the mode of action is unknown, the *N*-thiolated β-lactam containing nanoparticles dramatically enhance bioactivity, possibly due to increased bioavailability of the antibiotic via endocytosis.

Therefore, the preparation and the biological testing of *N*-thiolated β-lactam containing nanoparticles of different particle size distributions have to be performed to ascertain the relationship between particle size and activity. In vivo and cytotoxicity testing are also necessary for further progress towards commercialization.

Fluorescence-active emulsified nanoparticles containing naphthyl or anthracenyl side chains were also successfully prepared by microemulsion polymerization for possible use in fluorescence studies to determine if the drug enters the cell of MRSA through endocytosis.

It will be necessary to further develop these and possibly other related fluorescence-active emulsified nanoparticles into more intelligent forms which are able to selectively bind to certain biological targets. The emulsified nanoparticles can be converted to dry films that are readily soluble in organic solvents, but which do not retain biological activity. Future work in this laboratory is likely to focus on development of drug-containing thin film polymers for a variety of biomedical and research related applications.

ABOUT THE AUTHOR

Jeung-Yeop Shim currently serves as the Founder and Principle Investigator of the NanoDDS Biotechnology Corporation. Dr. Shim has focused the past 10 years on creating drug discovery as well as a novel drug delivery system by using nonotechnology. He has successfully patented innovative drug delivery system and diagnostic products for marketplaces. He has demonstrated leadership in new business formation having created and managed new ventures, NanoDDS Biotechnology Corporation. He served as a group leader and an executive manager in R&D center at the DPI Co. in Korea and developed several new concepts of polymer coating systems such as waterborne type-thin layer coating system by using nanotechnology. Dr. Shim received his Honors BS and MS from Kangwon National University in Korea, and Ph.D. from University of South Florida.

End Page